4-18-2019 11:00 AM

Synthesis and Characterization of American Ginseng Polysaccharides Nanoparticles

Vincent Lee, *The University of Western Ontario*

Supervisor: Lui, Edmund M.K., *The University of Western Ontario*
Co-Supervisor: Charpentier, Paul A., *The University of Western Ontario*
A thesis submitted in partial fulfillment of the requirements for the Master of Science degree in Physiology and Pharmacology

Abstract

This project was concerned with the synthesis of nanoparticles (NPs) by microfluidics from bulk ginseng polysaccharides (PS) isolated from American ginseng to design a new delivery system to improve the bioavailability of PS. Physicochemical analyses showed products of nanosizing as unimodal spheres with a diameter of ~19 nm. Pharmacological characterization studies *in vitro* of these nanoparticles of PS (NPPS) have demonstrated heightened immunostimulatory activity, and enhanced penetration across skin cell monolayer, which could be considered as evidence of increased bioavailability. Studies using PS sub-fractions with different molecular weights for NPPS synthesis showed that molecular weights is one of the parameters that influence the quality of NPPS. Mechanistic study revealed that NPPS acted like PS in targeting the Toll-like receptor-signalling pathway in mediating the immune-stimulatory effect. This nanotechnology may be applied to produce innovative ginseng polysaccharide-based nutraceuticals with improved bioavailability.

Keywords: American ginseng, *Panax quinquefolius*, ginseng polysaccharides, nanoparticles, microfluidics, nanoprecipitation, macrophages, physicochemical characterization, monolayer model, transport, immunostimulation, molecular weight, TLR signalling

Co-Authorship Statement

Dr. Edmund M.K. Lui and Dr. Paul A. Charpentier supervised and contributed to the design of all the experiments. Farida Akhter greatly helped with the synthesis and characterization of ginseng polysaccharide nanoparticles.

Acknowledgements

I would like to extend my deepest gratitude to my supervisors Dr. Edmund M.K. Lui and Dr. Paul A. Charpentier for providing me the opportunity to work on this project. The amount of aid and knowledge I have received during this project is immeasurable and will prove to be useful in all walks of life.

I would also like to acknowledge the members of my advisory committee Dr. Lina Dagnino, Dr. Thomas Drysdale and Dr. Qingping Feng for their priceless guidance and continuous support throughout the course of my MSc research.

This project would not have been possible if not for the help from Dr. Paul A. Charpentier's lab, their guidance in the synthesis and operation of the experiments and sharing of resources.

Special thanks to Dr. Dixon's lab from whom some of our cells were obtained from, their sharing of their equipment, and the helpful advice and knowledge.

I would also like to thank the staff of the Department of Physiology and Pharmacology at the University of Western Ontario for their help and time. This thesis would not have been made possible if not for the support of family and friends. I would like to express my appreciation to Virginia Lee and Gina Zhu for their boundless aid, care, and support.

I would also like to acknowledge the funding support received from Mitacs Accelerate and Western Phytoceutica. This project would have not been possible without their support.

Table of Contents

List of Figures

List of Abbreviations

A	uronic acid
Ara*f*	arabinofuranose
AUC	area under the curve
BMBM	bone-marrow-derived macrophages
BPI	bactericidal/permeability increasing protein
C2H/HeJ	TLR4 deficient mice
CD14	cluster of differentiation 14
CR3	complement receptor-3
COX-2	cyclooxygenase-2
DAMPs	damage-associated molecular patterns
DLS	dynamic light scattering
DMEM	Dulbecco's Modified Eagle's Medium
EDTA	ethylenediaminetetraacetic acid
ELISA	enzyme-linked immunosorbent assay
ELSD	evaporative light scattering detector
FBS	fetal bovine serum
FTIR	Fourier-transform infrared spectroscopy
Gal	galactose
GBE	ginseng berry extract
Glc	glucose
H_2O_2	hydrogen peroxide
HaCaT	spontaneously transformed aneuploid immortal keratinocyte cell line
hCMEC/D3	human cerebral microvascular endothelial cells
HPLC	high-performance liquid chromatography
IFNγ	interferon gamma
IgM	immunoglobulin M
IKK	inhibitor of nuclear factor kappa-B kinase
IκBα	inhibitor of kappa B
IL	interleukin
iNOS	inducible nitric oxide synthase

IRAK	IL-1R-associated kinase
IRF	interferon regulatory transcription factor
ITAM	immunoreceptor tyrosine-based activation motif
LBP	lipid binding protein
LPS	lipopolysaccharides
LRR	leucine-rich repeat domain
Man	mannose
MAPK	mitogen-activated protein kinases
mCD14	Membrane-bound CD14
MD-2	myeloid differentiation factor-2
MyD88	myeloid differentiation primary response 88
NF-κB	nuclear factor-kappa-light-chain-enhancer of activated B cells
NHPs	natural health products
NK	natural killer
NMWL	nominal molecular weight limit
NO	nitric oxide
NPPS	nanoparticle of ginseng polysaccharides
PAMPs	pattern-associated molecular pattern
PET	polyethylene terephthalate
PGE_2	prostaglandin E2
PI3K	phosphatidylinositol 3-kinase
PRR	pattern recognition receptor
PS	polysaccharides
RANKL	receptor activator of nuclear kappa-B ligand
RAW 264.7	macrophage; Abelson murine leukemia virus transformed
Rha	rhamnose
RI	refractive index
sCD14	soluble CD14
SR	scavenger receptor
SsnB	Sparstolonin B
TCM	Traditional Chinese Medicine

TEER	transepithelial electrical resistance
TEM	transmission electron microscopy
TiO_2	titanium dioxide
TIR	toll-interleukin 1 receptor
TIRAP	TIR-domain-containing adaptor protein
TLR	toll-like receptor
TNFα	tumor necrosis factor alpha
TRAF6	TNF receptor-associated factor 6
TRAM	TRIF-related adaptor molecule
TRIF	TIR-domain-containing adaptor-inducing interferon-β
UV	ultraviolet
UV/Vis	Ultraviolet/Visible
WHO	World Health Organization
XRD	X-ray diffraction
ZnO	zinc oxide

Chapter 1

General Introduction, Literature Review and Research Hypotheses

1.1 Relevance of medicinal plants in modern medicine

Throughout history, medicinal plants have been used to treat common ailments, alleviate discomfort, prevent infection, maintain wellness and restore health[1–3]. A medicinal plant is defined as a plant which contains one or more bioactive compounds in any part(s) of the plant that can be used for therapeutic purposes or as precursors for the development of drugs. These bioactive compounds (i.e., phytochemicals) include alkaloids, flavonoids, tannins, saponins, phenolics, terpenoids, and carbohydrates, to name a few[4]. The discovery of a plant's medicinal value was often accidental, through observation or trial and error. The development of herbalism relied heavily on oral tradition to pass down centuries of knowledge until the advent of writing and record keeping. Herbal knowledge differs geographically due to regional ecozones. In some cultures, herbal medicine has developed into relatively more advanced systems referred to as traditional medicines. Traditional Chinese, Native American, African, and East Indian Ayurvedic medicine are such examples.

Within North America, it is estimated that ~70% of Canadians regularly take natural health products (NHPs) in the management of their health[5]. Under the *Natural Health Products Regulations* (Canada), NHPs include: "vitamins and minerals, herbal remedies, homeopathic medicines, traditional medicines such as Traditional Chinese Medicines, probiotics and other products like amino acids and essential fatty acids"[6]. These NHPs are regulated under the Natural and Non-prescription Health Products Directorate. In Canada, a 2011 Functional Foods and Natural Health Products survey reported revenues of $11.3 billion, with exports of $1.7 billion and $238 million going into research and development[7].

It is a common misconception that the entirety of a traditional medicine system is a pseudo-medicine or placebo-medicine. Although there are such cases, including homeopathy, traditional medicine systems contain many medicinal plants which have been identified to contain bioactive compound(s)[1]. The bark of the Pacific Yew is one Native American example which has been researched and developed into Taxol - a chemotherapeutic[8]. Traditionally, it was used to treat several complaints ranging from gastrointestinal to respiratory ailments. In the 1960s, Taxol was isolated from the Pacific Yew and reported

to exhibit anti-tumor properties[8]. Further research validated its potential as an anti-tumor compound and by 1979, it was reported by Schiff et al. that the compound was an anti-mitotic agent that promotes microtubule stability, thereby inhibiting cell growth by halting cell division and ultimately resulting in cell death[9]. Recently, artemisinin from sweet wormwood (*Artemisia annua*) and its derivatives have been used to treat malaria[10]. It has been traditionally used for dyspepsia, appetite loss and biliary dyskinesia[11]. Artemisinin combination therapy has been estimated to have averted ~146 million clinical cases during 2000 – 2015[10]. Other well-known examples include acetylsalicylic acid from *Salix* spp., atropine from cocaine from *Erythroxylim coca*, digitoxin from *Digitalis purpurea,* ephedrine from *Ephedra sinica*, galanthamine from *Leucojum aestivum,* morphine from *Papaver somniferum*, quinine from *Cinchona ledgeriana*, and, vincristrine or vinblastine from *Catharantus roseus*[1].

Application of ethnobotany to pharmacology has classically been utilized to bridge naturally occurring substances to treat various diseases and conditions[12]. Medicinal plants that have been traditionally used for the treatment of certain illnesses can be screened for potential bioactive compounds[12]. However, some medicinal plants contain multiple bioactive components that act synergistically on different targets[13]. Thus, making it difficult to screen for a specific compound.

1.2 Ginseng

1.2.1 Historical background

Ginseng is a deciduous perennial herb part of the Araliaceae family within genus *Panax* and is found in Asia (*Panax ginseng*) and North America (*Panax quinquefolius*)[14]. Various other species of ginseng have also been identified in around 11 other regions such as *Panax notoginseng, Panax trifolius or Panax vietnamensis*, to name a few[14]. The genus *Panax* originates from the Greek word "panaxos' which literally translates into "cure all" or "all-healing"[14]. The species *ginseng* originates from the Chinese characters "rénshēn", meaning "person-herb" since the shape of the root is similar to the shape of a human[2]. Ginseng-

derived products are often referred to as adaptogens, which are non-toxic and non-specific (i.e., global/ broad effects) substances thought to increase physiological resistance to biological stress. The term 'adaptogen' was first introduced in the late 1940s; however, adaptogenic effects are not well received by the public due to the lack of research behind its non-specific benefits.

Ginseng has been historically used in Traditional Chinese Medicine (TCM). In TCM, normal body function is described to be controlled by a balance of Yin and Yang, the two opposite but complementary forces. Moreover, foods and medicinal plants are classified according to their natural properties, such as temperature characteristics (hot, warm, neutral, cool and cold); and these properties could impact on the Yin –Yang balance. It is believed that unwellness or illness occurs when there is a Yin – Yang imbalance of Yin and Yang, and that sickness can be resolved through rebalancing. Historically, *Panax ginseng* (Asian ginseng) is described to have 'warm' properties, whereas *Panax quinquefolius* (American ginseng) is described as having 'cool' properties. Prior to its introduction and trade to Asia, American ginseng was used in Traditional Native American medicine to relieve cold sore, fever, and gastrointestinal distress[15].

1.2.2 Bioactive constituents of ginseng

Ginseng contains many bioactive compounds include ginsenosides, polysaccharides, peptides, triterpenoids, flavonoids, polyacetylenic alcohols, essential oils, fatty acids and antioxidants[16,17]. These compounds are present in all ginseng species with a degree of variation[18,19]. The diverse range of bioactive compounds present in ginseng could explain why it has been traditionally utilized to treat or alleviate the symptoms of a broad range of illnesses and ailments[2,15,19]. Recent research has reported that ginseng exhibits immunostimulatory, immunosuppressive, anti-mutagenic, anti-tumor, anti-oxidative, and hypoglycemic effects[20–23]. In particular, the pro-inflammatory effects of ginseng have been mainly attributed to polysaccharides[20]. Beneficial effects on halting or slowing the progression of atherosclerosis, osteoporosis, arthritis, depression or diabetic complications have also been reported in the literature[24–28].

1.3 Plant Polysaccharides

Plant polysaccharides (PS) are macromolecules made up of long chains of monosaccharides linked together by glycosidic bonds (Fig 1.1)[29]. In general, plant cells contain mainly starches, pectins, cellulose and hemicellulose. Starches are glucans composed of α-(1,4)-glycosidic linkages (i.e., amylose) and may contain α-(1,6)-glycosidic linked branches along the main chain (i.e., amylopectin)[30]. These PS are found in the amyloplasts of plant cells and are the main glucose storage component of plants. Pectins are also composed of α-(1,4)-glycosidic bonds and maybe branched[30]. Pectic polysaccharides are high in galacturonans and may exist as homopolysaccharides or heteropolysaccharides[30]. They are found in the middle lamella and within the plant cell wall, and function as a structural component. Cellulose is composed of unbranched glucans with β-(1,4)-glycosidic bonds[30]. In contrast, hemicellulose is branched heteropolysaccharides composed of α- and β-glycosidic linkages[31]. Cellulose and hemicellulose are located in the plant cell wall and function as a structural component.

Polysaccharides are recognized as biological polymers due to the high degree of variation in the number and type of repeating monomers, conformation, functional groups and degree of branching. PS are heterogeneous with wide molecular weight distribution because of the broad differences in structure between individual PS[30]. The differences in structure also lead to variation in solublity[30]. Aside from the type of glycosidic bonds present in PS, the main repeating monosaccharide unit(s) determines the subtype of PS (e.g., pectin: type II rhamnogalacturonan). In general, plant PS are hydrophilic due to the presence of multiple hydroxyl groups[30]. However, they become more hydrophobic with an increasing number of internal hydrogen bonds[30]. PS with more intramolecular hydrogen bonding interact less with water decreasing its hydration[30].

1.3.1 Chemical structure of ginseng polysaccharides

Plant PS isolated from ginseng are structural and soluble PS that originate from the plant cell walls. They mainly consist of starch-like PS, pectin PS and hemicellulose[31]. As aforementioned, the structure of the PS differs greatly between individual PS. Starch-like

PS mainly contains branched α-(1,6)-glucans, α-(1,2)-glucans and α-(1,3)-glucans[32]. Pectic PS are primarily rich in homogalacturonans with a molar ratio of up to 70% and a small degree of branching[33]. They are composed of rhamnose (Rha), arabinose (Ara*f*), galactose (Gal), glucose (Glc) and uronic acid (A) (1:4:8:8:50)[33]. A minority of ginseng pectic PS has been identified as type 1 rhamnogalacturonans[33]. Guo et al. demonstrated that these pectic PS exhibit similarity to several citrus pectins[33]. The main sugar residue of these pectins is 4-α-D-GalA and other residues like 2-α-L-Rha, 2-4-α-L-Rha, α-L-Ara*f*, β-D-Gal and 4-β-D-Gal[33]. Recently, ginseng hemicellulose has been shown to predominantly consist of β-glycosylic-linked xylans, xyloglucans and glucomannans[31]. In addition to the different types of ginseng PS, individual PS may have a different number of monomeric repeats. The diversity and complexity of PS result in the heterogeneity of ginseng PS. In particular, the molecular weight of ginseng PS can range from as low as 3.1 kDa to as high as 2,000 kDa[34,35].

Ginseng PS are also broadly separated into two categories: acidic and neutral PS[31]. Acidic PS contains Gal, Rha, Ara, Glc and mannose (Man) that are high in GalA and GlcA[31,36]. These acidic PS are generally pectins[30]. Neutral PS includes starch-like glucans that are high in Ara and Gal and lack carboxyl functional groups[31,32].

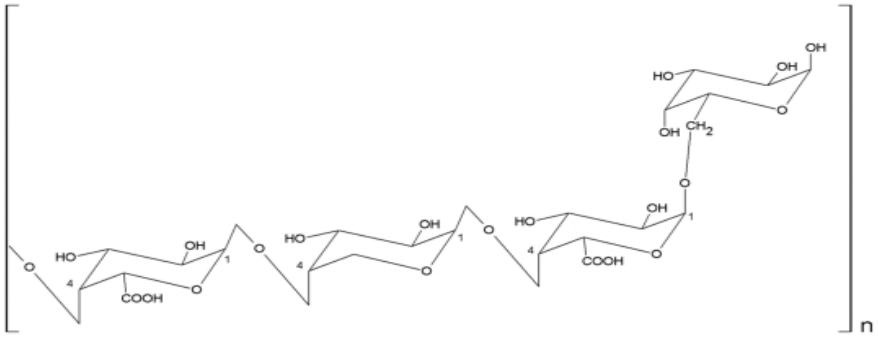

Figure 1.1. Partial chemical structure of ginseng polysaccharides[29].

1.3.2 Chromatography, detection and quantitative analysis of PS

The analysis of plant polysaccharides is a challenge due to low UV/Vis (Ultraviolet/Visible) absorbance and high complexity. As such, quantitation based on UV/Vis absorbance such as High Performance Liquid Chromatography (HPLC) using a UV/Vis detector is unsuitable[37]. HPLC using a Refractive Index (RI) detector is also unsuitable to analyze PS due to problems with sensitivity[37]. HPLC-RI is often performed on homogenous solutions; however, PS are highly complex and heterogeneous which would result in a broad range of RI values. Baseline stability is also a concern when using HPLC-RI for PS because any changes to the eluent composition would require re-equilibration of the detector. Evaporative Light Scattering Detector (ELSD) has been previously used to analyze PS composition because it can detect compounds which are less volatile than the mobile phase rather than detecting optical properties[37]. Despite the benefits of this analytical technique, the quantification of PS concentration is still a problem. Plant PS lack chromophoric moieties, therefore, labelling PS with a fluorescent tag would allow for the detection of PS molecules[38]. Concentration can be quantified with the use of a fluorometer, but this technique is limited by the selectivity of labelling, which has yet to be addressed. Alternatively, it is possible to quantify plant PS by conducting a biological assay and calculating concentration from a preconstructed standard curve. A sensitive assay, such as Griess' assay to detect nitric oxide (NO) or enzyme-linked immunosorbent assay (ELISA) to detect interleukin (IL)-6 or tumor necrosis factor alpha (TNFα) could be used to build this standard curve.

1.3.3 Extraction and isolation of plant polysaccharides

Ginseng PS are typically extracted and isolated from the plant biomass through hot-water extraction followed by precipitation of PS with alcohol. The precipitate can be further purified to yield deproteinated PS (i.e., bulk PS). Briefly, a methodology to extract PS from North American ginseng roots was developed by Professor Lui and Charpentier's group at Western University, Canada. First, ground-up ginseng roots were soaked in water at 40 °C for 5 hours to yield a water-soluble extract. The extract was then concentrated to remove excess solvent and lyophilized to obtain a dry aqueous extract. To isolate PS, the dried aqueous extract was dissolved in distilled water at a known concentration and four

equivalent volumes of 95% ethanol were added to the aqueous solution and lyophilized to obtain the powdered PS extract. The water-soluble PS extract was be furthered processed to remove proteins and yield the deproteinated water-soluble PS extract.

1.3.4 Immunomodulatory and antioxidant effects of plant polysaccharides

The effects of PS vary depending on their origin and composition. Generally, plant PS are immunostimulatory and act primarily on macrophages and circulating monocytes. Other effects including immunosuppressive, antimicrobial and antioxidant activities have also been reported[20,39]. Various plant PS have been recently demonstrated to elicit these effects *in vitro* and *in vivo*. For example, PS isolated from *Sargassum fusiforme*, a brown sea vegetable, have been reported to stimulate peritoneal macrophages through toll-like-receptor (TLR) 2 or TLR4 pathway via P38 mitogen-activated protein kinases (MAPK)[40]. The proliferation of splenic lymphocytes and immunoglobulin M (IgM) expression were both enhanced in cells treated with these PS. In another study, *Sargassum fusiform* PS stimulated TNFα, IL-1 and IL-6 production in RAW 264.7 (Abelson mouse leukemia virus transformed) macrophages[41]. This was mediated by NF-κB signalling via the cluster of differentiation 14 (CD14)/ inhibitor of nuclear factor kappa-B kinase (IKK) and p38 MAPK pathway[41]. Similarly, PS isolated from a heart-leaved moonseed, *Tinospora cordifolia,* have been shown to upregulate TNFα, IL-1β, IL-6, IL-12 and interferon-gamma (IFNγ) in RAW 264.7 macrophages and peritoneal macrophages[42]. Non-starch PS high in galacturonic acid has also been shown to increase NO, TNF-α and IL-6 production in macrophages (RAW 264.7) through the TLR4 pathway[43]. These non-starch PS were isolated from *Dioscorea polystachya* (Chinese Yam). PS isolated from fungi such as *Grifola frondosa* (Hen-of-the-wood) have demonstrated similar effects[44]. Murine macrophages (RAW 264.7) treated with these PS-induced morphological changes, increased IL-1β, IL-10 and NO production[44].

Ma et al. recently reported dose-dependent antioxidant effects exhibited by red onion (*Allium cepa*) PS that were sequentially extracted using hot buffer, chelating agent, dilute alkali and concentrated alkali[39]. The authors demonstrated that the degree of radical scavenging, iron chelating, lipid peroxidation inhibition and reducing power was

influenced by the PS composition[39]. The monosaccharide composition of these four PS fractions was previously shown to be different from each other[45]. Using the same extraction methodology, PS extracted from mulberry leaves (*Morus alba*) also exhibited dose-dependent antioxidant effects. Likewise, the degree of antioxidant activity was dependent on monosaccharide composition[46]. Interestingly, the antioxidant activity of plant PS can be enhanced through hydroxyl modifications. Li et al. showed the antioxidant activity of PS extracted from peony seed dreg (sediments) can be positively altered by sulfation, phosphorylation or carboxyl methylation[47].

1.3.4.1 Biological effects of ginseng polysaccharides.

Ginseng PS exhibit a broad range of biological effects and have been widely reported for their immunomodulatory and antioxidant properties. In a study investigating the immunomodulatory effects of ginseng PS in murine peritoneal macrophages, PS isolated from a ginseng extraction by-product enhanced hydrogen peroxide (H_2O_2) and NO production[48]. Lim et al. reported that PS-treated macrophages had stimulated lysosomal phosphatase and phagocytic activities[48]. Sun et al. recently found enhanced natural killer (NK) cell cytotoxicity in PS-treated immunosuppressed mice, specifically via the upregulation of perforin and granzyme[49]. Similarly, Azike et al. reported that PS treatments exerted immunostimulatory effects on macrophages[20]. IL-6, TNFα and NO were upregulated in a dose-dependent manner[20]. The authors also showed that pre-treating murine macrophages with PS-induced attenuation of immune response[20]. Azike et al. also found that the potency of PS was positively correlated to its molecular weight range[50].

The immunostimulatory activity of the PS is also related to their type, such as acidic or neutral PS. It was previously shown that the bioactive species of PS were mainly acidic and not neutral PS[37]. In one study, rat alveolar macrophages did not respond significantly to treatment with neutral PS but responded to acidic PS[37]. Pretreatment of macrophages with neutral PS resulted in minimal immunosuppressive effects in LPS-stimulated macrophages[37]. In a recent study, a novel neutral PS (3.1 kDa) isolated from North American ginseng and was reported to have significant anti-inflammatory activity[35]. Yu et al. demonstrated that acidic PS were more immunostimulatory compared to neutral PS[51].

In addition, neutral PS were found to be less immunostimulatory than crude PS isolate[51]. Shin et al. showed that acidic ginseng PS stimulated immune cells and upregulated the production of TNFα, IL-6, IL-1β and IFNγ[52]. Similarly, Park et al. investigated the immunomodulatory effects of acidic PS extracted from *Panax ginseng*[53]. Their study revealed that acidic PS-treated mice had higher levels of inducible nitric oxide synthase (iNOS) production compared to the control mice[53]. Moreover, the addition of an iNOS inhibitor (i.e., aminoguanidine) along with acidic PS attenuated the PS-mediated- immune suppression in sheep red blood cells[53]. The authors also showed that macrophages treated with acidic PS have increased cytotoxic activity[53]. In particular, elevated NO and H_2O_2 production and increased phagocytic activity were measured[53].

Pectin-like PS exhibited similar immunostimulatory effects as glucans. For example, increased proliferation of splenocytes and activation of peritoneal exudate macrophages and NK cells were reported in pectin-treated mice[54]. Recently, a novel pectin-like PS extracted in the presence of ethylenediaminetetraacetic acid (EDTA) was demonstrated to stimulate T and B lymphocyte proliferation[55].

1.3.4.2 Ginseng-polysaccharides-derived natural health products.

Several products containing ginseng PS have been marketed and approved by Health Canada; however, many do not have substantial research on their efficacy and safety for consumption. Of note, CVT-E002 (i.e., COLD-FX®) claims to help reduce the frequency, severity and duration of cold and flu symptoms by boosting the immune system[56]. CVT-E002 is a North American Ginseng PS extract which has been demonstrated to reduce eosinophilic airway inflammation in asthma-induced mice[57]. Adamko et al. also found that CVT-E002 reduced airway reactivity[57]. Moreover, CVT-E002 stimulated proliferation of murine B lymphocytes and production of NO, TNFα, IL-1 and IL-6 in peritoneal exudate macrophages[58]. In addition, an elevation in immunoglobulin G (IgG) production was observed in mice treated with CVT-E002[58]. These results have been recently replicated by Song et al. who reported that immunosuppressed mice treated with CVT-E002 increased T and B lymphocyte proliferation and, NK cell activity[59]. Another recent publication reported

that CVT-E002 stimulated the proliferation of T and B cells and production of IL-10 and IL-6 in mice[60].

1.4 Innate immunity

The non-specific immune response of the host to foreign substances (i.e., antigens) and microorganisms such as viruses, bacteria, protozoa and fungi are the initial line of defense against infection. The first aspect of innate immunity is physical and chemical barriers (e.g., epidermis, intestinal epithelium, saliva, bile, stomach acid, etc.) which prevent or limit exposure to foreign materials and cells. Cellular and molecular components present in the tissues and circulatory system such as dendritic cells, NK cells, mast cells and phagocytes, as well as complements or inflammatory mediators are another aspect of innate immunity[61,62]. The former is involved in the capture and elimination of pathogens, particles, cellular debris or infected cells[61]. Complements and inflammatory mediators are responsible for the enhancement of phagocytic activity via opsonization and the recruitment and activation of phagocytes, respectively[62]. Other components of the innate immune system include neutrophils, granulocytes (basophils and eosinophils), and cytokines. Granulocytes produce bactericidal proteins, reactive oxygen species, histamine, as well as cytokines that help regulate cells involved in the innate immune response. A crucial function of the innate immune system involves downstream activation of adaptive immunity[61,63]. The adaptive or acquired immune response involves the activation of T and B lymphocytes via antigen presentation by innate immune cells and the production of memory cells and antibodies targeting specific antigens[63].

1.4.1 Immunomodulation

Immunomodulation refers to the regulation of the immune system by exogenous or endogenous compounds including those that originate from biological stress. Immunomodulatory compounds (i.e., immunomodulators or biological response modifiers) might act to elicit proinflammatory or anti-inflammatory responses through the innate immune system. Some compounds, such as plant PS, can both stimulate and inhibit various immune responses[35,58]. In general, plant PS are known to stimulate immune cells

via TLR signalling[40,43]. Such compounds that can stimulate specific aspects of innate immunity are known as immune-stimulants. On the other hand, compounds capable of inhibiting specific aspects of the host immune response are referred to as immuno-inhibitors. Immuno-suppressors are compounds that can attenuate host immune response which may occur through a variety of pathways, such as receptor desensitization or via inhibition of responses[64,65]. The goal of desensitization is the attenuation of subsequent innate immune responses. For example, desensitization of TLRs in macrophages following stimulation by a TLR agonist leads to the reduced presence of cell-surface TLRs. This attenuates immunostimulatory responsiveness to subsequent treatment with TLR agonists.

1.4.2 Macrophage-mediated innate immunity

Macrophages are mononuclear phagocytic leukocytes that are present in tissues and in the circulatory system. Those in the blood are referred to as monocytes and are differentiated from tissue macrophages. Overall, the functions of macrophages include both the direct phagocytosis of foreign material or cellular debris as well as the indirect secretion of inflammatory mediators such as TNFα and IL-6[66]. Macrophages also play a role in presenting antigens to helper T-cells and are essential in promoting wound closure and tissue repair[63,66]. Macrophages within different tissues exhibit varying morphologies and functions which are niche-specific and tissue-specific. For instance, skin-resident macrophages (i.e. Langerhans cells) are very heterogeneous in morphology and are widely distributed throughout the tissue to act as first responders to potential pathogen invasions[67]. Other examples of tissue-specific macrophages are Kupffer cells in the liver, microglia in the central nervous system, dust cells in the lung, osteoclasts in the bone, sinus histiocytes in the lymph nodes and adipose tissue macrophages in body fat.

It was long-believed that macrophages were classically activated by cytokines IFNγ and TNFα produced by helper T-cells or alternatively activated by regulatory T cell-released IL-10[66]. While it remains true that macrophages polarize toward one phenotype in response to specific signals and are associated with different functions, research in the past decade has led to a paradigm shift in our understanding of the activation of macrophages and the

requirement of T-cells. In light of this, macrophages are classified into two general groups, M1 and M2 macrophages, based on their response or activation/polarization by specific stimuli[66,68,69]. The two groups represent two sides on a linear scale. M1 macrophages lean towards the 'inhibit' or 'kill' function, whereas M2 macrophages lean towards the 'healing' or 'repair' function[69,70]. M1 macrophages that were previously known as the classically activated macrophages are activated by pathogen associated molecular patterns (PAMPs), damage-associated molecular patterns (DAMPs), TNFα or IFNγ[70,71]. These macrophages are mainly pro-inflammatory and phagocytic which produce high levels of IL-12 and low levels of IL-10[68]. On the other hand, M2 macrophages, previously known as alternatively activated macrophages, are activated by inflammatory mediators such as glucocorticoids, IL-4, IL-10, IL-13 or prostaglandins[66,72,73]. Collectively, these stimuli are referred to as M2 stimuli and the response is mainly anti-inflammatory. M2 is further sub-grouped into M2a, M2b, M2c and M2d depending on the stimuli or response. In general, M2 macrophages are involved in wound healing, allergy regulation and Th2 responses, and produce higher levels of IL-10 compared to M1 macrophages[68,69,74]. In addition, M2 macrophages are thought to be the basal phenotype of tissue-resident macrophages[70]. They are not activated into M2 macrophages, but rather present as M2-like or M2-deactivated macrophages under basal conditions. Alternatively, these macrophages are referred to as unprimed or naïve macrophages (M_0)[75]. In the absence of external physical stress, resident macrophages remove cellular debris and senescent cells. Resident macrophages can quickly develop into the M1 phenotype or stay as M2 depending on the stimuli; however, the response of resident macrophages is tissue-specific and niche-specific[69,70]. During wound-healing, the less inflammatory M2 macrophages are the predominant phenotype, and M2-type responses are modulated[69,70]. They promote tissue formation and inflammation resolution through the release of growth factors and phagocytosis of apoptotic neutrophils[69,76].

Macrophage cell lines such as RAW 264.7 or bone-marrow derived macrophages (BMDM) are naïve or unprimed (i.e., M_0) macrophages and can be polarized to M1 or M2 phenotype[75]. RAW 264.7 cell line – which was used in this study – are monocyte/macrophage-like cells established from ascites of a tumor induced by Abselon Leukaemia Virus in BALB/c mice. They have been described as an appropriate model of

macrophages and can be polarized to M1 or M2 via IFNγ or IL-4, respectively[77,78]. In addition, RAW 264.7 cells can be differentiated into osteoclasts with RANKL (receptor activated NF-kappa B ligand)[79]. Compared to other cell lines, RAW 264.7 cells are morphologically unique (elongated; projections). Although its phenotypic and functional stability was initially described by ATCC to lose stability after passage 18, a recent paper recommends the use of up to passage 30[77].

1.4.3 Lipopolysaccharides (LPS)

M1 macrophages are activated in response to PAMPs which are derived from bacteria and other foreign microorganisms[68,70]. PAMPs are recognized by pattern recognition receptors (PRR) on the macrophages[70]. Endotoxin or bacterial lipopolysaccharide (LPS) is a well-reported PAMP originating from the outer monolayer of the outer membrane of gram-negative bacteria[80]. LPS binds to cell-surface TLRs which are a class of pattern recognition receptors (PRRs) found in phagocytes such as neutrophils, macrophages and dendritic cells[80]. LPS are made up of a lipid A and polysaccharide portion[80]. The polysaccharide portion has three regions: O-antigen, outer core and inner core[80]. Lipid A is a glucosamine-based phospholipid and its main function is to enhance the outer membrane stability[80]. The toxicity level of LPS is mainly attributed to its lipid A region. The O-antigen region is not essential for TLR4 binding; however, LPS that lack an O-antigen region (i.e., rough LPS) does not require the help of lipid binding protein (LBP) and CD14[81,82]. Both forms of LPS are highly toxic and can elicit a response from macrophages and monocytes even at a concentration as low as 10 – 500 pg/mL for LPS[83]. Overall, excessive TLR signalling by LPS binding results in fever, hypotension and eventually septic shock that leads to widespread organ failure.

The binding of LPS to TLRs is enhanced by LBP, a soluble protein. LBP non-covalently binds LPS and delivers LPS to cluster of differentiation 14 (CD14) or TLRs[82]. The interaction of LBP and CD14 with LPS forms a ternary complex[82]. The ternary complex facilitates the transfer of monomeric LPS to TLR4/myeloid differentiation factor-2 (MD-2) complex[82]. MD-2 is co-expressed with TLR4, which is vital for the TLR4 response to

LPS as well as the recognition of lipoteichoic acid from gram-positive bacteria[84]. Aside from presenting LPS to the TLR4 complex, CD14 mediates translocation of the TLR4 complex to an endosome[85]. Therefore, CD14 is essential for early and late phase (i.e., endosomal) TLR4-signalling.

1.4.3.1 Toll-like receptor (TLR) 4 signaling

TLR4 signalling is activated upon ligand recognition by the leucine-rich repeat domain (LRR) of the TLR4 and dimerization of the TLR4/MD-2/ligand complex via the LRR domain[86]. Dimerization of the TLR4/MD-2/ligand complex enables dimerization of the intracellular toll-interleukin 1 receptor (TIR)-domain of TLR4[86]. Subsequently, intracellular TLR4 adaptor proteins, which contain TIR-domains, are recruited to the TIR-domain of TLR4[87]. These adaptor proteins include TIR-domain-containing adaptor protein (TIRAP), TRIF (TIR-domain-containing adaptor-inducing interferon-β), TRAM (TRIF-related adaptor molecule) and MyD88 (myeloid differentiation primary response 88). There are two pathways in TLR4 signalling: MyD88-dependent and TRIF-dependent pathway.

1.4.3.2 MyD88-dependent signalling.

In the MyD88-dependent signalling, TIRAP is recruited to TLR4 and binds to the TIR domain of TLR4 through its TIR domain[88]. Upon recruitment, TIRAP facilitates MyD88 recruitment to TLR4 via indirect binding (i.e., bridging)[88]. Recruitment of MyD88 results in downstream activation of TNF receptor-associated factor 6 (TRAF6) via IL-1R-associated kinase (IRAK)1/2[89]. This leads to the downstream activation of IKK complex, which in turn phosphorylates inhibitor of kappa B (IκBα) and targets it for degradation[90]. Subsequently, NF-κB (nuclear factor-kappa-light-chain-enhancer of activated B cells) translocates to the nucleus and binds to promoters target genes including *iNOS/NOS2*, *Cyclooxygenase-2* (*PTGS2*/*COX-2*), *TNFα* and *IL-6*, to name a few[91,92]. COX-2 and iNOS mediate the production of prostaglandin E2 (PGE_2) and NO, respectively.

1.4.3.3 TRIF-dependent signalling.

Following LPS binding, TLR4 complex is internalized into an endosome in a dynamin-dependent-manner[65]. The translocation of TLR4 to endosomes is a prerequisite for TRIF-dependent signalling[93]. The internalization of the TLR4 complex prevents subsequent activation of the MyD88-dependent pathway by TLR4 agonists[94]. TRIF-dependent signalling begins with the recruitment of TRAM to the TIR-domain of TLR4[95]. Similar to TIRAP and MyD88, TRAM recruits and bridges TRIF to TLR4 at the TIR-domain[95]. Following association, TRIF binds to TRAF6 which in turn downstream activates NF-κB resulting in late-phase NF-κB pathway[93,95].

1.4.4 Ginseng PS-mediated activation of TLR signalling

Ginseng exhibits both immunostimulatory and anti-inflammatory effects. The opposing immunological effects have been attributed to the constituent PS and ginsenosides, respectively[20]. However, ginseng PS has also been reported to have anti-inflammatory and immunosuppressive effects[35,96]. Ginseng PS upregulated NO, IL-1β, IL-6, IFN-γ, and TNFα production in macrophages through TLR4 signalling[52]. Studies revealed that ginseng PS modulate immune response through NF-κB, p38 MAPK, MAPK1/3 and PI3K (phosphatidylinositol 3-kinase) cascades[97]. In addition, the expression of CD14 proteins in macrophages was increased after treatment with acidic PS from Asian ginseng[52]. LPS has been known to act through TLR4 signalling and it was reported that macrophages stimulated with LPS exhibited enhanced CD14 expression[98]. Thus, the upregulation of CD14 expression by acidic PS may suggest its involvement in the activation of TLR signalling by PS. Moreover, the production of TNFα, IL-1β, IL-6, IFNγ were impaired in TLR4 deficient mice (C2H/HeJ) treated with ginseng radix extract[99].

Ginseng PS exhibited immunosuppressive effects in LPS-induced models[100]. McElhaney et al. reported that CVT-E002™ suppressed activation of neutrophils and production of inflammatory cytokines (i.e., IL-2, IFNγ) in spleen cells induced by LPS stimulation[100]. Similarly, Zhao et al. reported that ginseng PS reduced the expression of TNFα and IFNγ in intraepithelial lymphocytes and lamina propria lymphocytes in collagen-induced

arthritis rats[101]. Acidic PS isolated from Asian ginseng exhibited suppressive effects in a model of demyelinating disease, experimental autoimmune encephalomyelitis[102]. The extract inhibited autoreactive T-cell proliferation and proinflammatory cytokine (i.e., IFNγ, IL1β and IL-17) production, thereby reducing the progression of autoimmune encephalomyelitis[102]. Furthermore, the extract activated FoxP3 transcription factor which is a regulator of regulatory T-cells[102].

The immunosuppressive or protective effects observed with ginseng PS are likely due to endotoxin-tolerance and negative regulation of downstream pro-inflammatory responses[96,103]. Internalization of TLR4 is characteristic of endotoxin-tolerant immune cells[94,98]. The translocation of TLR4 into endosomes has been reported to be regulated by CD14 mediated by immunoreceptor tyrosine-based activation motif (ITAM)[85]. Subsequent stimulation of endotoxin-tolerant immune cells with PAMPs (e.g., LPS) may result in a reduced immunostimulatory response. Compared to LPS, ginseng PS are non-toxic, lacks the lipid A moiety and is markedly less potent[29,50]. Therefore, the activation of TLR4 signalling by ginseng PS via CD14 is likely to result in the internalization of TLR4 mediated by ITAM[52,85]. This might explain one aspect of the protective effects of ginseng PS found in the literature.

1.5 Nanomaterials

Nanoparticles are defined as particles with at least one dimension less than 1000 nm but greater than 1 nm in diameter; however, they are commonly less than 100 nm. They exhibit different physicochemical properties than the substrate (i.e., bulk material) used to synthesize them such as solubility, permeability or particle size. In particular, the decrease in particle size from its corresponding bulk compound has been shown to enhance its uptake by cells (e.g., epithelial cells within the gastrointestinal tract)[104]. The application of nanotechnology to pharmacological agents has provided many benefits, removed various pre-existing inconveniences or minimized side-effects; however, the toxicity of nanomaterials remains highly controversial. This is because the fate of nanoparticles differs depending on its physicochemical characteristics and some of which have not been clearly identified[105,106].

There are many characteristics of nanoparticles that are desirable in pharmaceutical compounds such as smaller particle size, improved solubility and dissolution or different release characteristics (e.g., pH), to name a few[104,107–109]. Moreover, substrate toxicity can be mitigated by encapsulation or surface modifications[106,110]. In general, the larger surface-area-to-volume ratio promotes greater molecular interactions and ultimately greater cellular uptake[111]. Change in surface chemistry and enhancement of drug solubility can also increase the drug bioavailability[109,112,113]. Common examples include enhancing the lipophilicity of a drug or encapsulating a drug to protect it from degradation and metabolism prior to reaching its site of action. Targeted drug delivery via surface functionalization is another approach used to address some of the predominant issues in the field[114]. For example, albumin can reversibly bind to a drug (e.g., Paclitaxel) to facilitate its transport across the endothelium via glycoprotein 60-mediated transcytosis[115]. Drugs could also be modified with marker-attached polymers (e.g., conjugated antibodies) to target its delivery to specific organs/tissues[116]. The nanoparticle itself can also function as a therapeutic agent (e.g., nanocrystals, PS NPs) with enhanced transport and reduced crystalline/hydrodynamic size[38,104].

1.5.1 Nanomedicine for topical administration

The majority of nanotechnology applications to drugs have been directed to orally administered drugs with low bioavailability or widespread toxic side effects. Thus far, relatively few compounds have been synthesized into nanoparticles for topically administered compounds. Many of these are skin care products such as pain relief, antiseptics, first-aid compounds, scar treatments, acne creams, anti-aging treatments and hydration products. For example, nanoparticles of zinc oxide (ZnO) and titanium dioxide (TiO_2) offer a broader range of UV protection than their microparticle counterparts[117,118]. For physical agents like sunscreens, nanoparticles offer greater transparency as opacity is aesthetically unappealing. Nanotechnology has also been applied in the design of skin cancer drugs for enhanced accumulation in tumor tissue and improved potency[119].

1.5.2 Epidermal drug transport

Most topically administered drugs require penetration into or across the epidermal layer to elicit their pharmacological effect. Thus, the epidermis is present as a physical barrier to these drugs. The epidermis consists of keratinocytes that are differentiated and organized into the stratum corneum at the superficial layer, followed by the stratum granulosum, stratum spinosum and stratum basale. The stratum corneum functions as the main barrier against physical trauma, chemical and pathogenic attack, as well as ultraviolet (UV) irradiation. In addition, a non-polar lipid barrier formed by lamellar bodies in keratinocytes is present at the level of the stratum granulosum[67]. In the stratum spinosum, keratinocytes are connected together by a large number of desmosomes[67]. Macrophages (i.e., Langerhans cells) are also resident to the stratum spinosum[67]. The stratum basale consists of both quiescent and actively proliferating basal keratinocytes that form a monolayer where individual cells are connected through tight junctions and are attached to the basement membrane[67,120].

Transport of drugs across the skin can occur via the paracellular or transcellular, or trans-appendageal pathway. The polarity and size of molecules are important for bypassing the lipid matrix or plasma membrane of keratinocytes and ultimately affects its route of transport[121]. The transport across other cell barriers such as the intestinal epithelium may occur by paracellular or transcellular pathways. For skin, paracellular transport involves movement through the lipid matrix in intercellular spaces of keratinocytes. Sufficiently small particles (< 500 Da) can also be transported paracellularly across tight junctions of keratinocytes[120,121]. Particles which typically undergo this passive process are hydrophilic[122]. In general, particulates that are < 500 nm are transported transcellularly through clathrin-mediated, caveolae-mediated or non-specific endocytosis whereas large particulates are phagocytosed[123]. In addition, molecules with a large surface area to volume ratio have higher uptake into cells due to greater interaction with membrane receptors[124,125].

1.5.3 Synthesis of nanoparticles

In general, there are two approaches to synthesizing nanomaterials: top-down (i.e. bulk material/ substrate to nanoparticles) and bottom-up (i.e. nanomaterial from atomic or

molecular species through chemical reactions)[104,126]. There are various methodologies to synthesize nanomaterials such as nanoprecipitation, microemulsion, nanocrystallization, nano-lithography, and milling with their own associated advantages and disadvantages. There are also more specialized derivatives of the aforementioned approaches. For example, variations of nanoprecipitation include open-microfluidics, continuous-flow microfluidics and digital microfluidics[38,127,128].

The microfluidic methodology involves using a solvent to first dissolve the bulk material/compound, after which an anti-solvent would be added to the dissolved solution to decrease the drug solubility and ultimately induce substrate precipitation. The benefits of using nanoprecipitation include high efficiency and low-costs. Nanoprecipitation does not require high temperatures, ultrasonication, chemical reactions, additional surfactants or toxic solvents which can affect the chemical structure of the substrate. The characteristics of the nanoparticle can also be controlled by altering the substrate concentration, solvent type, ratio of solvents, polymer type and temperature[129]. One nanoprecipitation method involves using water as the solvent and acetone as the anti-solvent. The interaction between acetone and water in contact with the substrate precipitates the substrate polymer. The precipitate exhibits change in hydrodynamic volume and surface chemistry[38]. Lamer et al. proposed that the formation of the nanoparticle occurs through two steps[130]. First, nucleation of small aggregates of polymer in a supersaturated solution corresponds to a reduction in drug solubility by the addition of an anti-solvent. In the second step, the nanoparticle nuclei grow until the stability of the colloidal particle has been reached. Stabilizers can also be added to prevent the dissolution of particles and redeposition into larger particles. The preferential shape of these nanoparticles is spherical because the polymer chains are homogeneously distributed in the solution during nanoprecipition[131,132].

As mentioned before, microfluidics is a variation of nanoprecipitation. The benefits of this technique variant are that the flow rate and/or ratio of the solvent and anti-solvent can be controlled. In continuous-flow microfluidics, the solvents are manipulated through microfabricated channels connected at a junction. There are two types of microchannel geometry: T-junction and cross-junction or flow focusing channels (Fig. 1.2). The

interaction between the solvents at the junction promotes the formation of monodispersed nanoparticles[133]. Nanoparticles synthesized by this method are more uniform in size and morphology compared to the batch process[38].

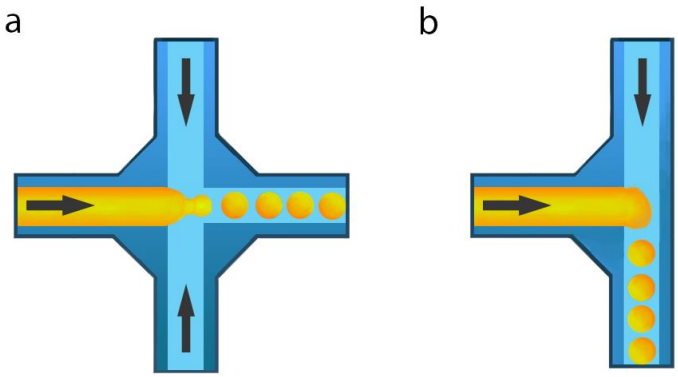

Figure 1.2. Droplet formation using different microfluidic junction geometry (a) cross-junction and (b) T-junction.

1.6 Summary and Rationale

Polysaccharides such as pectins and starch-like glucans are key bioactive phytochemicals in North American ginseng root. It was recently previously reported that the immunostimulatory properties of North American ginseng are chiefly due to this PS component. Contemporary studies have also demonstrated that these PS have antioxidant, immunomodulatory and immuno-protective properties[29,59,134]. The potency of ginseng PS was shown to be related to its molecular weight – higher molecular weight PS were more potent[50,97]. Evidence indicates that PS elicits an immune response through TLR signalling via the NF-kb pathway[52]. Specifically, TLR4 and CD14 have been implicated in the activation of macrophages by ginseng PS[52,99]. Although ginseng PS are pharmacologically active, the effects are limited by its large molecular size which inhibits its absorption in the gastrointestinal tract. The bioavailability of PS is also limited by its hydrophilic nature. However, the transport of PS has not been comprehensively studied because of the lack of chromophores in ginseng PS. Moreover, the limited UV activity of PS poses a challenge for the quantification of PS.

Application of nanotechnology to ginseng PS to control and modify molecular size potentially allows for greater bioavailability. Akhter et al. demonstrated that nanosizing ginseng PS by nanoprecipitation using microfluidics reduces the particle size of PS while increasing its crystallinity[38]. These nanoparticles exhibits marked accumulation in the dermis, increased cellular uptake and enhanced immunostimulatory activity compared to its bulk form[38]. Their results suggest that these observations are likely to be primarily attributed to the physicochemical changes rather than changes to the chemical structure following microfluidic processing of the bulk PS[38]. Various factors may have also contributed to the observation of enhanced biological effect such as potential selectivity of PS molecules by the microfluidic procedure, change in PS mechanism of action or alteration of PS binding kinetics to TLR or CD14. Thus, the basis for the apparent increase in PS biological effect and the transport of PS and its nanoparticle needs to be elucidated. This study focuses on the characterization of NPPS physicochemical properties and investigates if NPPS acts similar to bulk PS. The size and morphology of NPPS and the influence of PS molecular weight on the nanomorphology are studied. Furthermore, the penetration of NPPS across a monolayer is investigated using a novel bioassay to characterize the enhancement of PS transport across a monolayer model. The immunostimulatory activity and mechanism of activation of NPPS are studied to determine the effects of nanosizing on the pharmacodynamics of bulk PS.

1.7 Hypothesis and Aims

Hypothesis:

1. Nanosizing ginseng PS using microfluidic processing reduces their particle size and improves their permeability across the membrane barrier.
2. Nanosizing selectively incorporates higher molecular weight and more bioactive polysaccharides into nanoparticles rendering higher immunostimulatory activity.
3. NPPS possess different cellular mechanism of action as compared to bulk PS, and this contributes to their enhanced immunostimulatory activity.

Aim 1: Synthesize nanoparticles from ginseng PS using microfluidic processing and characterize physicochemical properties and immunostimulatory activity *in vitro.* Nanoparticle synthesis was conducted to ascertain success in replicating the methodology reported by Akhter et al. and for further refinement. Modification of the methodology was performed to address the limitations of the aforementioned procedure and determine parameters which were previously not investigated by Akhter et al. The physicochemical properties – size and morphology – of the NPPS were examined as part of the modification and characterization process.

Aim 2: Compare the penetration of bulk PS and NPPS across a membrane barrier to establish the influence of particle size on its permeability. The transport of NPPS and PS across cell/membrane barriers was investigated *in vitro* using a HaCaT keratinocyte monolayer. Quantification of the passage of bulk PS and NPPS across the monolayer was performed using a macrophage-stimulation-based biological assay.

Aim 3: To determine whether the molecular weight of bulk PS influences the nanosizing process and immunostimulatory activity of NPPS. Size and morphology were examined as potential physicochemical properties influenced by the molecular weight of the substrate – PS. *In vitro* stimulation of RAW 264.7 macrophages was used as an experimental model to study immunostimulatory effect.

Aim 4: To determine whether nanosizing bulk PS changes the mechanism underlying the immunostimulatory action. *In vitro* stimulation of RAW 264.7 macrophages was used as an experimental model. To determine whether TLR-mediated pathway was involved, two experimental designs were used: LPS-induced desensitized macrophages and use of a selective TLR2/TLR4 antagonist.

1.8 References

1. Fowler, M. W. Plants, medicines and man. *J. Sci. Food Agric.* **86**, 1797–1804 (2006).

2. Park, H. J., Kim, D. H., Park, S. J., Kim, J. M. & Ryu, J. H. Ginseng in Traditional Herbal Prescriptions. *J. Ginseng Res.* **36**, 225–241 (2012).

3. Petrovska, B. B. Historical review of medicinal plants' usage. *Pharmacogn. Rev.* **6**, 1–5 (2012).

4. Saxena, M., Saxena, J., Nema, R., Singh, D. & Gupta, A. Phytochemistry of Medicinal Plant. **1**, 15 (2013).

5. Health Canada. Natural health products program summative evaluation. (2010).

6. Health Canada. A Framework for Consumer Health Products. *aem* (2018). Available at: https://www.canada.ca/en/health-canada/services/drugs-health-products/public-involvement-consultations/natural-health-products/framework-consumer-health-products.html. (Accessed: 16th December 2018)

7. Canada, A. and A.-F. C. of. Results from the Functional Foods and Natural Health Products Survey (2011). Available at: http://www.agr.gc.ca/eng/industry-markets-and-trade/canadian-agri-food-sector-intelligence/functional-foods-and-natural-health-products/trends-and-market-opportunities-for-the-functional-foods-and-natural-health-products-sector/results-from-the-functional-foods-and-natural-health-products-survey-2011/?id=1387481727299. (Accessed: 9th August 2018)

8. Singla, A. K., Garg, A. & Aggarwal, D. Paclitaxel and its formulations. *Int. J. Pharm.* **235**, 179–192 (2002).

9. Schiff, P. B., Fant, J. & Horwitz, S. B. Promotion of microtubule assembly in vitro by taxol. *Nature* **277**, 665–667 (1979).

10. Bhatt, S. *et al.* The effect of malaria control on *Plasmodium falciparum* in Africa between 2000 and 2015. *Nature* **526**, 207–211 (2015).

11. Wormwood (Absinthii herba). Available at: https://buecher.heilpflanzen-welt.de/BGA-Commission-E-Monographs/0379.htm. (Accessed: 20th April 2019)

12. Heinrich, M. & Gibbons, S. Ethnopharmacology in drug discovery: an analysis of its role and potential contribution. *J. Pharm. Pharmacol.* **53**, 425–432 (2001).

13. Efferth, T. & Koch, E. Complex interactions between phytochemicals. The multi-target therapeutic concept of phytotherapy. *Curr. Drug Targets* **12**, 122–132 (2011).

14. Yun, T. K. Brief introduction of Panax ginseng C.A. Meyer. *J. Korean Med. Sci.* **16 (Suppl)**, S3-5 (2001).

15. Arnason, T., Hebda, R. J. & Johns, T. Use of plants for food and medicine by Native Peoples of eastern Canada. *Can. J. Bot.* **59**, 2189–2325 (1981).

16. Wang, H., Peng, D. & Xie, J. Ginseng leaf-stem: bioactive constituents and pharmacological functions. *Chin. Med.* **4**, 20 (2009).

17. Assinewe, V. A., Amason, J. T., Aubry, A., Mullin, J. & Lemaire, I. Extractable polysaccharides of Panax quinquefolius L. (North American ginseng) root stimulate TNFalpha production by alveolar macrophages. *Phytomedicine Int. J. Phytother. Phytopharm.* **9**, 398–404 (2002).

18. Qi, L.-W., Wang, C.-Z. & Yuan, C.-S. Ginsenosides from American ginseng: chemical and pharmacological diversity. *Phytochemistry* **72**, 689–699 (2011).

19. Chen, X. *et al.* Phytochemistry, Metabolism, and Metabolomics of Ginseng. *Chin. Herb. Med.* **7**, 98–108 (2015).

20. Azike, C. G., Charpentier, P. A., Hou, J., Pei, H. & King Lui, E. M. The Yin and Yang actions of North American ginseng root in modulating the immune function of macrophages. *Chin. Med.* **6**, 21 (2011).

21. Baek, K.-S. *et al.* Comparison of anticancer activities of Korean Red Ginseng-derived fractions. *J. Ginseng Res.* **41**, 386–391 (2017).

22. Kitts, D. D., Wijewickreme, A. N. & Hu, C. Antioxidant properties of a North American ginseng extract. *Mol. Cell. Biochem.* **203**, 1–10 (2000).

23. Yoo, K. M., Lee, C., Lo, Y. M. & Moon, B. The hypoglycemic effects of American red ginseng (Panax quinquefolius L.) on a diabetic mouse model. *J. Food Sci.* **77**, H147-152 (2012).

24. Lee, J., Cho, J.-Y. & Kim, W.-K. Anti-inflammation effect of Exercise and Korean red ginseng in aging model rats with diet-induced atherosclerosis. *Nutr. Res. Pract.* **8**, 284–291 (2014).

25. Lee, H.-Y. *et al.* Aqueous ginseng extract has a preventive role in RANKL-induced osteoclast differentiation and estrogen deficiency-induced osteoporosis. *J. Funct. Foods* **13**, 192–203 (2015).

26. Jhun, J. *et al.* Red ginseng extract ameliorates autoimmune arthritis via regulation of STAT3 pathway, Th17/Treg balance, and osteoclastogenesis in mice and human. *Mediators Inflamm.* **2014**, 351856 (2014).

27. Dang, H. *et al.* Antidepressant effects of ginseng total saponins in the forced swimming test and chronic mild stress models of depression. *Prog. Neuropsychopharmacol. Biol. Psychiatry* **33**, 1417–1424 (2009).

28. Sen, S. *et al.* Preventive effects of North American ginseng (Panax quinquefolius) on diabetic retinopathy and cardiomyopathy. *Phytother. Res. PTR* **27**, 290–298 (2013).

29. Yoo, D.-G. *et al.* Protective Effect of Ginseng Polysaccharides on Influenza Viral Infection. *PLOS ONE* **7**, e33678 (2012).

30. Guo, M. Q., Hu, X., Wang, C. & Ai, L. Polysaccharides: Structure and Solubility. *Solubility Polysacch.* (2017). doi:10.5772/intechopen.71570

31. Ji, L. *et al.* Structural characterization of alkali-soluble polysaccharides from Panax ginseng C. A. Meyer. *R. Soc. Open Sci.* **5**, 171644 (2018).

32. Luo, D. & Fang, B. Structural identification of ginseng polysaccharides and testing of their antioxidant activities. *Carbohydr. Polym.* **72**, 376–381 (2008).

33. Guo, Q. *et al.* Non-starch polysaccharides from American ginseng: physicochemical investigation and structural characterization. *Food Hydrocoll.* **44**, 320–327 (2015).

34. Ivanova, T., Han, Y., Son, H.-J., Yun, Y.-S. & Song, J.-Y. Antimutagenic effect of polysaccharide ginsan extracted from Panax ginseng. *Food Chem. Toxicol.* **44**, 517–521 (2006).

35. Wang, L. *et al.* Structural and anti-inflammatory characterization of a novel neutral polysaccharide from North American ginseng (Panax quinquefolius). *Int. J. Biol. Macromol.* **74**, 12–17 (2015).

36. Zhang, X. *et al.* Total fractionation and characterization of the water-soluble polysaccharides isolated from Panax ginseng C. A. Meyer. *Carbohydr. Polym.* **77**, 544–552 (2009).

37. Lui, E. M. K. *et al.* Bioactive Polysaccharides of American Ginseng Panax quinquefolius L. in Modulation of Immune Function: Phytochemical and Pharmacological Characterization. *Complex World Polysacch.* (2012). doi:10.5772/50741

38. Akhter, K. F., Mumin, M. A., Lui, E. K. & Charpentier, P. A. Microfluidic Synthesis of Ginseng Polysaccharide Nanoparticles for Immunostimulating Action on Macrophage Cell Lines. *ACS Biomater. Sci. Eng.* **2**, 96–103 (2016).

39. Ma, Y.-L. *et al.* Antioxidant and antibacterial evaluation of polysaccharides sequentially extracted from onion (Allium cepa L.). *Int. J. Biol. Macromol.* **111**, 92–101 (2018).

40. Fan, S. *et al.* Antitumor activity and underlying mechanism of Sargassum fusiforme polysaccharides in CNE-bearing mice. *Int. J. Biol. Macromol.* **112**, 516–522 (2018).

41. Chen, L. *et al.* Sargassum Fusiforme Polysaccharide SFP-F2 Activates the NF-κB Signaling Pathway via CD14/IKK and P38 Axes in RAW264.7 Cells. *Mar. Drugs* **16**, (2018).

42. Gupta, P. K., Rajan, M. G. R. & Kulkarni, S. Activation of murine macrophages by G1-4A, a polysaccharide from Tinospora cordifolia, in TLR4/MyD88 dependent manner. *Int. Immunopharmacol.* **50**, 168–177 (2017).

43. Li, M. *et al.* Non-starch polysaccharide from Chinese yam activated RAW 264.7 macrophages through the Toll-like receptor 4 (TLR4)-NF-κB signaling pathway. *J. Funct. Foods* **37**, 491–500 (2017).

44. Hou, L., Meng, M., Chen, Y. & Wang, C. A water-soluble polysaccharide from Grifola frondosa induced macrophages activation via TLR4-MyD88-IKKβ-NF-κB p65 pathways. *Oncotarget* **8**, 86604–86614 (2017).

45. Zhu, D.-Y. *et al.* Insights into physicochemical and functional properties of polysaccharides sequentially extracted from onion (Allium cepa L.). *Int. J. Biol. Macromol.* **105**, 1192–1201 (2017).

46. Liao, B.-Y. *et al.* Thermal and Antioxidant Properties of Polysaccharides Sequentially Extracted from Mulberry Leaves (Morus alba L.). *Mol. Basel Switz.* **22**, (2017).

47. Li, X.-L. *et al.* Effects of different chemical modifications on the antioxidant activities of polysaccharides sequentially extracted from peony seed dreg. *Int. J. Biol. Macromol.* **112**, 675–685 (2018).

48. Lim, T.-S., Na, K., Choi, E.-M., Chung, J.-Y. & Hwang, J.-K. Immunomodulating activities of polysaccharides isolated from Panax ginseng. *J. Med. Food* **7**, 1–6 (2004).

49. Sun, Y. *et al.* Effect of ginseng polysaccharides on NK cell cytotoxicity in immunosuppressed mice. *Exp. Ther. Med.* **12**, 3773–3777 (2016).

50. Azike, C. G. American Ginseng Modulation of Immune Function and Phytochemical Analysis. *Diss. Univ. West. Ont.* (2014).

51. Yu, X.-H. *et al.* Isolation, purification, characterization and immunostimulatory activity of polysaccharides derived from American ginseng. *Carbohydr. Polym.* **156**, 9–18 (2017).

52. Shin, J.-Y. *et al.* Immunostimulating effects of acidic polysaccharides extract of *Panax ginseng* on macrophage function. *Immunopharmacol. Immunotoxicol.* **24**, 469–482 (2002).

53. Park, K. M. *et al.* Nitric Oxide is Involved in the Immunomodulating Activities of Acidic Polysaccharide from Panax ginseng. *Planta Med.* **67**, 122–126 (2001).

54. Shin, M.-S., Hwang, S.-H., Yoon, T.-J., Kim, S. H. & Shin, K.-S. Polysaccharides from ginseng leaves inhibit tumor metastasis via macrophage and NK cell activation. *Int. J. Biol. Macromol.* **103**, 1327–1333 (2017).

55. Zheng, Y. *et al.* Structural analysis of ginseng polysaccharides extracted by EDTA solution. *RSC Adv.* **6**, 2724–2730 (2016).

56. Products | COLD-FX. Available at: https://cold-fx.ca/products/. (Accessed: 18th December 2018)

57. Adamko, D. J., Ebeling, C. & Wu, Y. Cvt-e002, A Polysaccharide From North American Ginseng (panax Quinquefolium) Reduces Allergic Immune Response And Development Of Airway Reactivity In A Mouse Model Of Asthma. *J. Allergy Clin. Immunol.* **123**, 729 (2009).

58. Wang, M. *et al.* Immunomodulating activity of CVT-E002, a proprietary extract from North American ginseng (Panax quinquefolium). *J. Pharm. Pharmacol.* **53**, 1515–1523 (2001).

59. Song, Y.-R. *et al.* Enzyme-assisted extraction, chemical characteristics, and immunostimulatory activity of polysaccharides from Korean ginseng (Panax ginseng Meyer). *Int. J. Biol. Macromol.* **116**, 1089–1097 (2018).

60. Hong, H.-D. *et al.* Mixing ratio optimization for functional complex extracts of Rhodiola crenulata, Panax quinquefolius, and Astragalus membranaceus using mixture design and verification of immune functional efficacy in animal models. *J. Funct. Foods* **40**, 447–454 (2018).

61. Akira, S., Uematsu, S. & Takeuchi, O. Pathogen recognition and innate immunity. *Cell* **124**, 783–801 (2006).

62. Charles A Janeway, J., Travers, P., Walport, M. & Shlomchik, M. J. The complement system and innate immunity. *Immunobiol. Immune Syst. Health Dis. 5th Ed.* (2001).

63. Iwasaki, A. & Medzhitov, R. Control of adaptive immunity by the innate immune system. *Nat. Immunol.* **16**, 343–353 (2015).

64. Didierlaurent, A. *et al.* Sustained desensitization to bacterial Toll-like receptor ligands after resolution of respiratory influenza infection. *J. Exp. Med.* **205**, 323–329 (2008).

65. Rajaiah, R., Perkins, D. J., Ireland, D. D. C. & Vogel, S. N. CD14 dependence of TLR4 endocytosis and TRIF signaling displays ligand specificity and is dissociable in endotoxin tolerance. *Proc. Natl. Acad. Sci. U. S. A.* **112**, 8391–8396 (2015).

66. Hesketh, M., Sahin, K. B., West, Z. E. & Murray, R. Z. Macrophage Phenotypes Regulate Scar Formation and Chronic Wound Healing. *Int. J. Mol. Sci.* **18**, (2017).

67. Simpson, C. L., Patel, D. M. & Green, K. J. Deconstructing the skin: cytoarchitectural determinants of epidermal morphogenesis. *Nat. Rev. Mol. Cell Biol.* **12**, 565–580 (2011).

68. Gerber, J. S. & Mosser, D. M. Reversing lipopolysaccharide toxicity by ligating the macrophage Fc gamma receptors. *J. Immunol. Baltim. Md 1950* **166**, 6861–6868 (2001).

69. Shook, B., Xiao, E., Kumamoto, Y., Iwasaki, A. & Horsley, V. CD301b+ Macrophages Are Essential for Effective Skin Wound Healing. *J. Invest. Dermatol.* **136**, 1885–1891 (2016).

70. Mills, C. D. & Ley, K. M1 and M2 Macrophages: The Chicken and the Egg of Immunity. *J. Innate Immun.* **6**, 716–726 (2014).

71. Su, Z. *et al.* HMGB1 Facilitated Macrophage Reprogramming towards a Proinflammatory M1-like Phenotype in Experimental Autoimmune Myocarditis Development. *Sci. Rep.* **6**, 21884 (2016).

72. Mosser, D. M. & Edwards, J. P. Exploring the full spectrum of macrophage activation. *Nat. Rev. Immunol.* **8**, 958–969 (2008).

73. Jetten, N. *et al.* Wound administration of M2-polarized macrophages does not improve murine cutaneous healing responses. *PloS One* **9**, e102994 (2014).

74. Müller, U. *et al.* IL-13 induces disease-promoting type 2 cytokines, alternatively activated macrophages and allergic inflammation during pulmonary infection of mice with Cryptococcus neoformans. *J. Immunol. Baltim. Md 1950* **179**, 5367–5377 (2007).

75. Freemerman, A. J. *et al.* Metabolic reprogramming of macrophages: glucose transporter 1 (GLUT1)-mediated glucose metabolism drives a proinflammatory phenotype. *J. Biol. Chem.* **289**, 7884–7896 (2014).

76. Greenlee-Wacker, M. C. Clearance of apoptotic neutrophils and resolution of inflammation. *Immunol. Rev.* **273**, 357–370 (2016).

77. Taciak, B. *et al.* Evaluation of phenotypic and functional stability of RAW 264.7 cell line through serial passages. *PLOS ONE* **13**, e0198943 (2018).

78. Lam, R. S. *et al.* Unprimed, M1 and M2 Macrophages Differentially Interact with Porphyromonas gingivalis. *PLOS ONE* **11**, e0158629 (2016).

79. Vincent, C., Kogawa, M., Findlay, D. M. & Atkins, G. J. The generation of osteoclasts from RAW 264.7 precursors in defined, serum-free conditions. *J. Bone Miner. Metab.* **27**, 114–119 (2009).

80. Raetz, C. R. H. & Whitfield, C. Lipopolysaccharide endotoxins. *Annu. Rev. Biochem.* **71**, 635–700 (2002).

81. Huber, M. *et al.* R-form LPS, the master key to the activation ofTLR4/MD-2-positive cells. *Eur. J. Immunol.* **36**, 701–711 (2006).

82. Ryu, J.-K. *et al.* Reconstruction of LPS Transfer Cascade Reveals Structural Determinants within LBP, CD14, and TLR4-MD2 for Efficient LPS Recognition and Transfer. *Immunity* **46**, 38–50 (2017).

83. Hamann, L., Alexander, C., Stamme, C., Zähringer, U. & Schumann, R. R. Acute-Phase Concentrations of Lipopolysaccharide (LPS)-Binding Protein Inhibit Innate Immune Cell Activation by Different LPS Chemotypes via Different Mechanisms. *Infect. Immun.* **73**, 193–200 (2005).

84. Dziarski, R. & Gupta, D. Role of MD-2 in TLR2- and TLR4-mediated recognition of Gram-negative and Gram-positive bacteria and activation of chemokine genes. *J. Endotoxin Res.* **6**, 401–405 (2000).

85. Zanoni, I. *et al.* CD14 controls the LPS-induced endocytosis of Toll-like receptor 4. *Cell* **147**, 868–880 (2011).

86. Park, B. S. *et al.* The structural basis of lipopolysaccharide recognition by the TLR4-MD-2 complex. *Nature* **458**, 1191–1195 (2009).

87. Park, B. S. & Lee, J.-O. Recognition of lipopolysaccharide pattern by TLR4 complexes. *Exp. Mol. Med.* **45**, e66 (2013).

88. Valkov, E. *et al.* Crystal structure of Toll-like receptor adaptor MAL/TIRAP reveals the molecular basis for signal transduction and disease protection. *Proc. Natl. Acad. Sci. U. S. A.* **108**, 14879–14884 (2011).

89. Kawagoe, T. *et al.* Sequential control of Toll-like receptor-dependent responses by IRAK1 and IRAK2. *Nat. Immunol.* **9**, 684–691 (2008).

90. Zhang, J., Clark, K., Lawrence, T., Peggie, M. W. & Cohen, P. An unexpected twist to the activation of IKKβ: TAK1 primes IKKβ for activation by autophosphorylation. *Biochem. J.* **461**, 531–537 (2014).

91. Xie, Q. W., Kashiwabara, Y. & Nathan, C. Role of transcription factor NF-kappa B/Rel in induction of nitric oxide synthase. *J. Biol. Chem.* **269**, 4705–4708 (1994).

92. Liu, T., Zhang, L., Joo, D. & Sun, S.-C. NF-κB signaling in inflammation. *Signal Transduct. Target. Ther.* **2**, 17023 (2017).

93. Kagan, J. C. *et al.* TRAM couples endocytosis of Toll-like receptor 4 to the induction of interferon-beta. *Nat. Immunol.* **9**, 361–368 (2008).

94. Balachandran, Y. Role of Endocytosis in TLR Signaling: An Effective Negative Regulation to Control Inflammation. *MOJ Immunol.* **3**, (2016).

95. Verstak, B. *et al.* The TLR signaling adaptor TRAM interacts with TRAF6 to mediate activation of the inflammatory response by TLR4. *J. Leukoc. Biol.* **96**, 427–436 (2014).

96. Ahn, J.-Y. *et al.* The immunomodulator ginsan induces resistance to experimental sepsis by inhibiting Toll-like receptor-mediated inflammatory signals. *Eur. J. Immunol.* **36**, 37–45 (2006).

97. Lemmon, H. R., Sham, J., Chau, L. A. & Madrenas, J. High molecular weight polysaccharides are key immunomodulators in North American ginseng extracts: characterization of the ginseng genetic signature in primary human immune cells. *J. Ethnopharmacol.* **142**, 1–13 (2012).

98. Tan, Y., Zanoni, I., Cullen, T. W., Goodman, A. L. & Kagan, J. C. Mechanisms of Toll-like receptor 4 endocytosis reveal a common immune-evasion strategy used by pathogenic and commensal bacteria. *Immunity* **43**, 909–922 (2015).

99. Nakaya, T.-A., Kita, M., Kuriyama, H., Iwakura, Y. & Imanishi, J. Panax ginseng induces production of proinflammatory cytokines via toll-like receptor. *J. Interferon Cytokine Res. Off. J. Int. Soc. Interferon Cytokine Res.* **24**, 93–100 (2004).

100. McElhaney, J. E., Goel, V., Toane, B., Hooten, J. & Shan, J. J. Efficacy of COLD-fX in the prevention of respiratory symptoms in community-dwelling adults: a randomized, double-blinded, placebo controlled trial. *J. Altern. Complement. Med. N. Y. N* **12**, 153–157 (2006).

101. Zhao, H. *et al.* Effect of ginseng polysaccharide on TNF- and IFN- produced by enteric mucosal lymphocytes in collagen induced arthritic rats. *J. Med. Plants Res.* **5**, 1536–1542 (2011).

102. Hwang, I. *et al.* An acidic polysaccharide of Panax ginseng ameliorates experimental autoimmune encephalomyelitis and induces regulatory T cells. *Immunol. Lett.* **138**, 169–178 (2011).

103. Peng, Q., O'Loughlin, J. L. & Humphrey, M. B. DOK3 Negatively Regulates LPS Responses and Endotoxin Tolerance. *PLOS ONE* **7**, e39967 (2012).

104. Soisuwan, S., Teeranachaideekul, V., Wongrakpanich, A., Langguth, P. & Junyaprasert, V. B. In vitro performances and cellular uptake of clarithromycin nanocrystals produced by media milling technique. *Powder Technol.* **338**, 471–480 (2018).

105. Zhao, F. *et al.* Cellular Uptake, Intracellular Trafficking, and Cytotoxicity of Nanomaterials. *Small* **7**, 1322–1337 (2011).

106. Sukhanova, A. *et al.* Dependence of Nanoparticle Toxicity on Their Physical and Chemical Properties. *Nanoscale Res. Lett.* **13**, (2018).

107. Juère, E. *et al.* In Vitro Dissolution, Cellular Membrane Permeability, and Anti-Inflammatory Response of Resveratrol-Encapsulated Mesoporous Silica Nanoparticles. *Mol. Pharm.* **14**, 4431–4441 (2017).

108. Akhter, F. Ginseng Polysaccharides Nanoparticles-Synthesis, Characterization, and Biological Activity. *Diss. Univ. West. Ont.* (2016).

109. Zhang, W. *et al.* Effect of Shape on Mesoporous Silica Nanoparticles for Oral Delivery of Indomethacin. *Pharmaceutics* **11**, 4 (2019).

110. Balmuri, S. R. *et al.* Effect of surfactant in mitigating cadmium oxide nanoparticle toxicity: Implications for mitigating cadmium toxicity in environment. *Environ. Res.* **152**, 141–149 (2017).

111. Shang, L., Nienhaus, K. & Nienhaus, G. U. Engineered nanoparticles interacting with cells: size matters. *J. Nanobiotechnology* **12**, 5 (2014).

112. Hu, J., Johnston, K. P. & Williams, R. O. Spray freezing into liquid (SFL) particle engineering technology to enhance dissolution of poorly water soluble drugs: organic solvent versus organic/aqueous co-solvent systems. *Eur. J. Pharm. Sci. Off. J. Eur. Fed. Pharm. Sci.* **20**, 295–303 (2003).

113. Chen, X., Young, T. J., Sarkari, M., Williams, R. O. & Johnston, K. P. Preparation of cyclosporine A nanoparticles by evaporative precipitation into aqueous solution. *Int. J. Pharm.* **242**, 3–14 (2002).

114. Mitra, S. *et al.* Targeted Drug Delivery in Covalent Organic Nanosheets (CONs) via Sequential Postsynthetic Modification. *J. Am. Chem. Soc.* **139**, 4513–4520 (2017).

115. Miele, E., Spinelli, G. P., Miele, E., Tomao, F. & Tomao, S. Albumin-bound formulation of paclitaxel (Abraxane® ABI-007) in the treatment of breast cancer. *Int. J. Nanomedicine* **4**, 99–105 (2009).

116. Ulbrich, K., Hekmatara, T., Herbert, E. & Kreuter, J. Transferrin- and transferrin-receptor-antibody-modified nanoparticles enable drug delivery across the blood–brain barrier (BBB). *Eur. J. Pharm. Biopharm.* **71**, 251–256 (2009).

117. Zvyagin, A. V. *et al.* Imaging of zinc oxide nanoparticle penetration in human skin in vitro and in vivo. *J. Biomed. Opt.* **13**, 064031 (2008).

118. Popov, A. P., Lademann, J., Priezzhev, A. V. & Myllylä, R. Effect of size of TiO2 nanoparticles embedded into stratum corneum on ultraviolet-A and ultraviolet-B sun-blocking properties of the skin. *J. Biomed. Opt.* **10**, 064037 (2005).

119. Dianzani, C. *et al.* Drug Delivery Nanoparticles in Skin Cancers. *BioMed Research International* (2014). doi:10.1155/2014/895986

120. Yuki, T. *et al.* Tight junction proteins in keratinocytes: localization and contribution to barrier function. *Exp. Dermatol.* **16**, 324–330 (2007).

121. Bos, J. D. & Meinardi, M. M. The 500 Dalton rule for the skin penetration of chemical compounds and drugs. *Exp. Dermatol.* **9**, 165–169 (2000).

122. Laksitorini, M., Prasasty, V. D., Kiptoo, P. K. & Siahaan, T. J. Pathways and Progress in Improving Drug Delivery through the Intestinal Mucosa and Blood-Brain Barriers. *Ther. Deliv.* **5**, 1143–1163 (2014).

123. Oh, N. & Park, J.-H. Endocytosis and exocytosis of nanoparticles in mammalian cells. *Int. J. Nanomedicine* **9**, 51–63 (2014).

124. Elias, D. R., Poloukhtine, A., Popik, V. & Tsourkas, A. Effect of ligand density, receptor density, and nanoparticle size on cell targeting. *Nanomedicine Nanotechnol. Biol. Med.* **9**, 194–201 (2013).

125. Hoshyar, N., Gray, S., Han, H. & Bao, G. The effect of nanoparticle size on in vivo pharmacokinetics and cellular interaction. *Nanomed.* **11**, 673–692 (2016).

126. Sinha, B., Müller, R. H. & Möschwitzer, J. P. Bottom-up approaches for preparing drug nanocrystals: Formulations and factors affecting particle size. *Int. J. Pharm.* **453**, 126–141 (2013).

127. Oliveira, N. M., Neto, A. I., Song, W. & Mano, J. F. Two-Dimensional Open Microfluidic Devices by Tuning the Wettability on Patterned Superhydrophobic Polymeric Surface. *Appl. Phys. Express* **3**, 085205 (2010).

128. Paul Urbanski, J., Thies, W., Rhodes, C., Amarasinghe, S. & Thorsen, T. Digital microfluidics using soft lithography. *Lab. Chip* **6**, 96–104 (2006).

129. Miladi, K., Sfar, S., Fessi, H. & Elaissari, A. Nanoprecipitation Process: From Particle Preparation to In Vivo Applications. in *Polymer Nanoparticles for Nanomedicines: A Guide for their Design, Preparation and Development* (eds. Vauthier, C. & Ponchel, G.) 17–53 (Springer International Publishing, 2016). doi:10.1007/978-3-319-41421-8_2

130. LaMer, V. K. & Dinegar, R. H. Theory, Production and Mechanism of Formation of Monodispersed Hydrosols. *J. Am. Chem. Soc.* **72**, 4847–4854 (1950).

131. Schubert, S., Joseph T. Delaney, J. & Schubert, U. S. Nanoprecipitation and nanoformulation of polymers: from history to powerful possibilities beyond poly(lactic acid). *Soft Matter* **7**, 1581–1588 (2011).

132. Aubry, J., Ganachaud, F., Cohen Addad, J.-P. & Cabane, B. Nanoprecipitation of Polymethylmethacrylate by Solvent Shifting:1. Boundaries. *Langmuir* **25**, 1970–1979 (2009).

133. Karnik, R. *et al.* Microfluidic Platform for Controlled Synthesis of Polymeric Nanoparticles. *Nano Lett.* **8**, 2906–2912 (2008).

134. Saba, E. *et al.* A comparative study on immune-stimulatory and antioxidant activities of various types of ginseng extracts in murine and rodent models. *J. Ginseng Res.* **42**, 577–584 (2018).

Chapter 2

Synthesis and characterization of physicochemical and biological properties of nanoparticles prepared from American ginseng polysaccharides

2.1 Introduction

North American ginseng has been widely reported to be immunomodulatory *in vivo* with both immunostimulatory and immunosuppressive effects[1–3]. They have been used to manufacture various nutraceuticals – a standardized dietary product – such as COLD-FX® and Jamieson™ Canadian Ginseng. The immunostimulatory effects are exerted by the ginseng polysaccharides (PS), which are derived from the cell wall of the ginseng root[4]. Ginseng PS are composed of complex chains of monosaccharides high in galactose (Gal), arabinose (Ara), galacturonic acid (GalA), rhamnose (Rha) and glucose (Glc)[5]. Polysaccharides are heterogeneous in nature due to a high degree of variation in the number and type of monosaccharide repeating units. As a result, a wide range of diversity is present in the solubility, hydrophilicity, molecular weight, structure and conformation of PS. Previous studies have shown that the biological effects of ginseng PS are mainly attributed to higher molecular weight PS rather than lower molecular weight PS[6,7].

Although diverse biological effects of PS have been reported, their effects are limited by its bioavailability. The large molecular size of PS and their hydrophilicity are both limiting factors to their absorption in the gastrointestinal tract[6,8]. These limitations to bioavailability can be potentially addressed by the application of nanotechnology to PS to modify particle size/polarity. It has been well-demonstrated that reducing the particle size of large and poorly permeable compounds to the nano-scale range improves its oral bioavailability[9,10]. A nanosizing methodology for ginseng PS has been developed by Prof. Lui and Charpentier's group to synthesize nanoparticles of ginseng PS (NPPS) by nanoprecipitation using continuous-flow microfluidics[11]. The resulting NPPS exhibited uniform and spherical characteristics with a narrow size distribution (20 ± 4 nm)[11]. In addition, the ginseng NPPS were monodispersed (i.e., uniform size and shape) with a higher crystallinity (i.e., higher order of structure) than the bulk material[11].

Similar to nutraceuticals, quality control of ginseng NPPS physicochemical properties is critical for ensuring safety and efficacy. For regular herbal products, phytochemical (i.e., bioactive compounds) profiling is the usual approach. However, to develop high-quality nanoparticles as nutraceuticals, a set of physicochemical parameters are usually used in the

evaluation process. In this study, we evaluated size and morphology, and measured the penetrative ability of the nanoparticles.

Previously, Akhter et al. used fluorescent-labelled NPPS to study its disposition in skin after topical application to hairless mice. It has been shown that following treatment, NPPS passed into the dermis mainly through the transappendageal route (hair follicle, sweat gland) and dispersed throughout the dermis[12]. Furthermore, NPPS accumulated in dermal blood vessels and exhibited greater immunostimulatory activity than PS in samples collected from the skin[12]. Ginseng NPPS also demonstrated greater immunostimulatory activity *in vitro* compared to bulk PS[11]. In particular, ginseng NPPS increased tumor necrosis factor alpha (TNFα), interleukin (IL)-6, IL-1β and nitric oxide (NO) production in RAW 264.7 macrophages[11]. The authors concluded that the enhancement of biological activity of NPPS in macrophages might be related to its greater cellular uptake. NPPS accumulated within macrophages whereas bulk PS accumulated apically of the plasma membrane[12]. This apparent increase in cellular uptake of NPPS was speculated to be secondary to changes in surface chemistry and size rather than skeletal structure[11].

The increase in biological membrane permeability of NPPS is expected to enhance absorption from gastrointestinal tract and increase systemic bioavailability. This should also apply to the penetration of dermal barrier after topical application. The uptake of the nanoparticle depends on its physicochemical properties such as size or charge. Nanomaterials can be transported across the skin through transappendageal (diffusion via follicles/glands), paracellular and/or transcellular transport. Generally, nanoparticles that are transported transcellularly via receptor mediated-endocytosis or non-specific mechanisms[13,14]. The fate of the nanoparticle within a cell also varies depending on the compound, cell type and nanoparticle type[14]. Following endocytosis, the nanoparticles can be incorporated into endosomes, which could then be excreted or participate in the fusion with late endosomes that subsequently fuses with lysosomes[14]. The nanoparticles could also distribute in the cytoplasm or localize in the nucleus, mitochondria, ER or Golgi apparatus[14]. The lack of understanding on the fate of nanomaterials poses a potential issue of toxicity.

The amount of NPPS penetration was not measured by Akhter et al. due to difficulties quantifying the concentration of PS and its nanoparticle. Furthermore, there is a lack of technology for quantitation of PS polymers which do not have chromophoric moieties[3]. To address this, a biological assay was developed to estimate the amount of PS in biological samples. However, this assay is only viable under *in vitro* conditions in the absence of biological influences which could affect the specificity of the assay.

In this study, penetration of NPPS and its bulk substrate (PS) across a cell monolayer was evaluated in order to provide a biological basis to explain the observed difference in deposition profiles between NPPS and bulk PS in dermal tissue *in vivo* following topical adminisration[12]. In order to verify the observed enhanced dermal penetration of NPPS *in vivo*, human keratinocytes (HaCaT) were used as an *in vitro* biological barrier to bulk PS and NPPS. The *in vitro* keratinocyte monolayer model – herein referred to as a monolayer model – was used to determine if NPPS penetrate the dermal barrier better than ginseng PS. The monolayer model is made up of a monolayer of confluent keratinocytes cultured on a trans-well insert with an established membrane integrity. The monolayer model was used to enable the examination of the penetration of a biological membrane in isolation without other biological influences.

Since ginseng PS are known to be heterogeneous in size distribution, it is not certain how this factor influences the nanosizing process. To address this question, bulk PS was separated by ultrafiltration through different membranes of defined pore sizes into sub-fractions of different molecular sizes. The PS sub-fractions were used as substrates for the preparation of NPPS, which was subsequently subjected to physicochemical and biological characterization *in vitro*. In summary, this chapter will address the modification of the microfluidic procedure, physicochemical and biological characterization of NPPS. We hypothesized that microfluidic processing of PS reduces particle size, improves permeability with heightened biological activity and that molecular size of PS is a determinant of resulting NPPS. In addition, we were able to develop an *in vitro*

keratinocyte monolayer model that was coupled with a bioassay for PS quantitation to evaluate the transport of NPPS.

2.2 Experimental Procedure

2.2.1 Materials

Four-year-old *Panax quinquefolius* roots were collected in 2007 from five separate farms (Ontario, Canada) to prepare aqueous extracts which were then combined to produce a composite extract. The composite extract was provided by the Ontario Ginseng Innovation and Research Consortium for further extraction and isolation of ginseng PS.

HaCaT human keratinocytes (CLS 300493) purchased from Cell Lines Services GmbH (CLS; Germany) were used to prepare an *in vitro* monolayer model and RAW 264.7 murine macrophages (ATCC TIB 67) provided by Dr. Jeff Dixon (Department of Physiology and Pharmacology, University of Western Ontario, Canada) were used for pharmacological studies. Dulbecco's Modified Eagle's Medium (DMEM) and Fetal Bovine Serum (FBS) (US origin) were purchased from Gibco Laboratories (USA). Lipopolysaccharides (LPS) from *Escherichia coli* (O111:B4) and Griess' reagent (modified) were purchased from Sigma-Aldrich (Canada).

2.2.2 Preparation of ginseng PS

2.2.2.1 Crude PS ginseng.

Dried ginseng root was grounded and soaked in nano-pure water (1:20) at 40 °C for 4 hrs. The extraction procedure was repeated three times and the extracts were combined, centrifuged and filtered to remove any particulate matters. The extract was concentrated via rotary evaporator (Buchi) under vacuum at 50 °C and lyophilized using a freeze dryer (Labconco). Ginseng PS fraction was precipitated by the addition of 95% ethanol in four sequential volumes, giving a final concentration of ethanol of 40% ethanol (v/v). The

solution was centrifuged at 350 x g for 10 mins to obtain the precipitate (pellet). The pellet was further purified by dissolving the pellet in nano-pure water at approximately 1 g/mL and precipitated again with ethanol to remove remaining water-insoluble materials. The precipitate was lyophilized with a freeze dryer to obtain the crude PS ginseng extract. The crude PS extract was further processed by deproteinization using prepared Sevag reagent made with n-butanol and chloroform (1:4 ratio by volume). Briefly, powdered crude PS (10 g) was dissolved in nano-pure water (300 mL) and partitioned five times with 1000 mL of Sevag reagent. Once again, PS was precipitated from the solution by 95% ethanol and lyophilized via freeze dryer to obtain the bulk PS extract.

2.2.2.2 Sub-fractionation of bulk ginseng PS by ultrafiltration.

Ginseng PS were separated into molecular weight sub-fractions through ultrafiltration using Amicon® Ultra centrifugal filter devices (Millipore Sigma) (Fig. 2.1). Five Amicon® Ultra tubes with different pore sizes for a specified nominal molecular weight limit (NMWL) were used: 100,000, 50,000, 30,000, 10,000 and 3,000. Herein, NWML will be referred to in kilodaltons (e.g., 100 kDa) and Amicon® Ultra tubes as UF tubes. Briefly, PS were dissolved at a concentration of 1 mg/mL and sonicated for 1 hr. Five millilitres of the PS solution were placed into the 100 kDa UF tube and centrifuged at 4000 x g in a swinging bucket rotor at 25°C for 30 mins. Subsequently, the precipitate was removed and labelled as the ≥ 100 kDa fraction while the filtrate was diluted to a final volume of 5 mL and transferred into the 50 kDa UF tube. The precipitate after centrifugation was labelled as the 50-100 kDa fraction. Once again, the filtrate was diluted to 5 mL and transferred into the 30 kDa UF tube. The precipitate was labelled as the 30-50 kDa fraction. This was performed for a total of 10 times.

After ultracentrifugation, the precipitates were combined and concentrated to 10 mL and transferred into a 15 mL centrifuge tube. Samples were frozen overnight and then lyophilized for 3-4 days to obtain ≥ 100 kDa, 50 - 100 kDa and 30 – 50 kDa PS. Herein, the fractions will be referred to as large (L-PS), medium(M-PS), small (S-PS), respectively. Samples were then weighed, and the final yield was calculated.

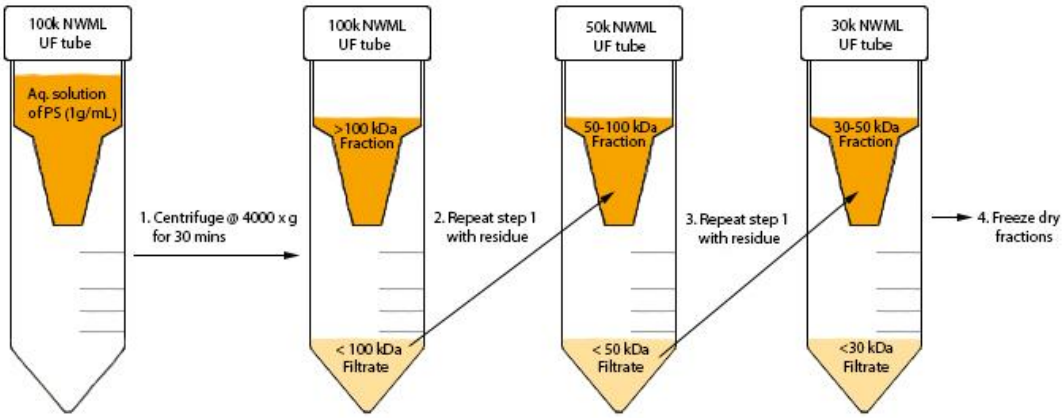

Figure 2.1. Schematic illustration of ultrafiltration procedure for separation of ginseng polysaccharides by nominal molecular weight limit (NWML).

2.2.2.3 Synthesis of ginseng PS nanoparticles by microfluidic nanoprecipitation.

NPPS and sub-fractionated NPPS were prepared from bulk PS and sub-fractionated PS respectively by a continuous microfluidic system using T-junction geometry (Fig. 2.2). Stainless steel T-junction or Micro-TEE (Upchurch Scientific) was used, with an inner diameter of 1500 µM. The microfluidic setup consisted of two infusion syringe pumps, Legato 1100 and Legato 2200 (KD Scientific) attached to the arms of the T-junction. The first pump attached to Arm 1 was used to infuse the solvent which was an aqueous solution of deproteinated ginseng PS. This PS solution was prepared using nano-pure water at a concentration of 0.55 g/mL followed by ultrasonication. The second pump attached to Arm 2 was used to pump the anti-solvent (acetone; 100%; HPLC grade). The solvent and anti-solvent were infused at a ratio of 1:20. Specifically, the solvent was infused at 0.01 mL/min and the anti-solvent at 0.2 mL/min. Attached to Arm 3 is PEEK tubing with an outer diameter of 1500 µM and an inner diameter of 75 µM (Upchurch Scientific). Arm 3 was directed towards a reservoir containing 15 mL of acetone, which is continuously mixed with a magnetic stirrer at room temperature to prevent sedimentation. The dispersion containing synthesized NPPS was collected from the reservoir and concentrated to remove excess acetone and centrifuged at 350 x g for 15 mins to sediment the precipitate. The

precipitate was recovered by removing the supernatant by vacuum suction. The precipitate was resuspended and then combined into a composite batch. The batch was concentrated and centrifuged again prior to lyophilization by freeze drying. The lyophilized powdered ginseng NPPS was stored at 4 °C before ready for experimentation.

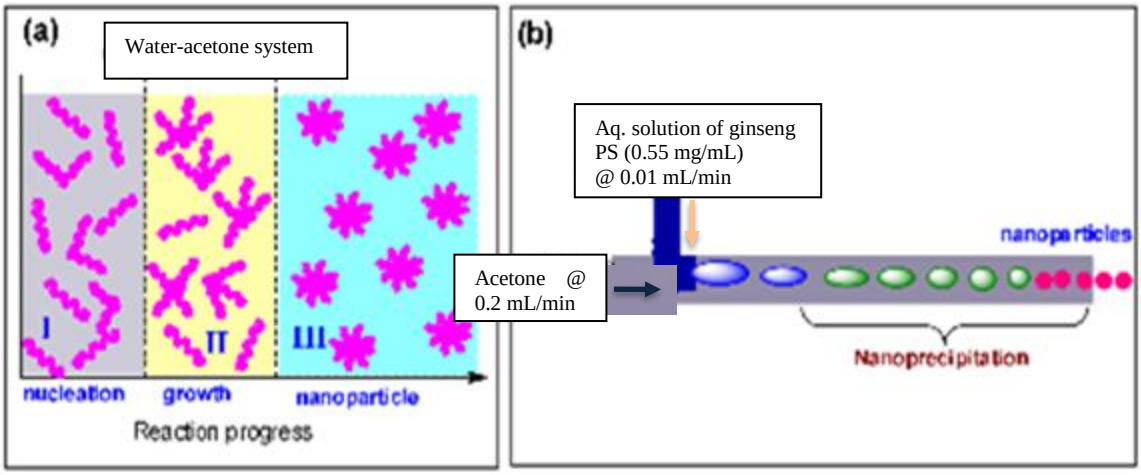

Figure 2.2. Experimental setup of continuous microfluidics system for the preparation of ginseng polysaccharide nanoparticles. Pump 1: Solvent phase (H_2O) containing ginseng polysaccharide. Pump 2: Anti-solvent (acetone). Adapted from Akhter et al.[12].

2.2.3 Physicochemical characterization of ginseng PS nanoparticles

The size and morphology of nanomaterial samples were examined using transmission electron microscopy (TEM) (Philips CM10). No stain was used for the samples. Nanoparticles for TEM imaging were prepared by dispersing samples in acetone. The dispersion products were deposited onto formvar-coated copper grids. TEM images were also measured by 'ImageJ' software to assess the size distribution of the sample. The contrast of TEM images was adjusted to assist visualization and measurement of particles.

The size distribution of the nanomaterials was measured by dynamic light scattering (DLS) (Malvern Zetasizer Nano ZS(R)) instrument; Nano S model ZEN 1600, Malvern, Orsay,

France). Briefly, the PS samples were dispersed in water and then ultrasonicated for 5 mins to assist in the dispersion. Dispersed samples were loaded into a disposable polystyrene sizing cuvette (DSTS0012) and backscattering measurements (173°) was collected at room temperature (25°C) at a measurement position of 4.65 mm. The sizing cuvette containing the sample was allowed to equilibrate for 30 sec before 3 consecutive acquisitions that were averaged over 2 sec were recorded.

2.2.4 Biological analyses

2.2.4.1 Cell culture.

Spontaneously transformed aneuploid immortal human keratinocytes (HaCaT) and Abelson murine leukemia virus transformed macrophages (RAW 264.7) were cultured in DMEM supplemented with 10% FBS and 1% penicillin/streptomycin. Cell cultures were maintained at 37℃ in a humidified incubator with 10% CO_2. The concentration of CO_2 was used in accordance with the concentration of sodium bicarbonate (3.7 g/L) contained in the media to maintain a physiological pH of ~ 7-7.4. HaCaT cells were passaged every 8-10 days at approximately 80% confluency. Cell culture media were changed biweekly. RAW 264.7 cells were passaged every 3-4 days at approximately 80% confluency. Cell culture media was changed one day prior to passage. Cell viability was determined by trypan blue dye exclusion test, which is based on the permeability of non-viable cells to the dye. Cell cultures were tested for mycoplasma contamination using the MycoAlert® Mycoplasma Detection Kit (Lonza). None of the cell cultures used were tested positive.

2.2.4.2 Stimulation of macrophage function *in vitro.*

Immunostimulatory activity of PS and NPPS was investigated using RAW 264.7 murine macrophage cells. Macrophage cells were seeded during the logarithmic phase (~80% confluency) into 96-well tissue culture plates at a density of 1.5 x 10^5 cells per well and incubated at 37 ℃ and 10% CO_2. RAW 264.7 cells were treated with PS and NPPS for 24 hrs. Treatment concentrations of PS and NPPS were at 50, 100, 200 and 300 µg/mL. At 24 hrs the cell culture supernatant was removed to measure NO production by the macrophages. Data was subsequently used to construct bioassay standard curves for PS and NPPS.

To study the effects of substrate molecular weight on the immunostimulatory effects of sub-fractionated NPPS samples (i.e., L-NPPS, M-NPPS, S-NPPS), RAW 264.7 macrophages were treated with 0 – 200 µg/mL of sub-fractionated NPPS. In addition, cells were treated with 0 – 200 µg/mL of sub-fractionated ginseng PS (i.e., L-PS, M-PS, S-PS) and compared with ginseng NPPS to investigate the effects of nanosizing on its immunostimulatory activity. At 24 hrs the cell culture supernatant was removed to measure NO production by the macrophages.

2.2.4.3 *In vitro* model for measurement of penetration of PS and NPPS across monolayer.

The purpose of this model was to measure the penetration of ginseng PS and NPPS across a viable cellular membrane with biological integrity, which may provide an estimation of bioavailability. A keratinocyte monolayer was used to simulate a dermal barrier. The *in vitro* skin model consists of keratinocytes cultured on polyethylene terephthalate (PET) trans-well inserts (1 µM pore) placed within a 24-well plate (Fig. 2.3). HaCaT cells were seeded at a density of 5.0×10^4 cells/ insert. Inserts were immersed in cell culture media and incubated until confluency. Cell culture media in the apical and basolateral compartment were changed biweekly. Three days post-confluency, transepithelial electrical resistance (TEER) of the keratinocyte monolayer was measured with EVOM^2 STX2 electrodes and monitored to ensure membrane integrity. Monolayers with a TEER less than 50 Ω*cm^2 attributed to low membrane integrity were discarded. The threshold was determined based on the study conducted by Ferreira et al., and data from preliminary studies (i.e., TEER values at non-confluence)[15].

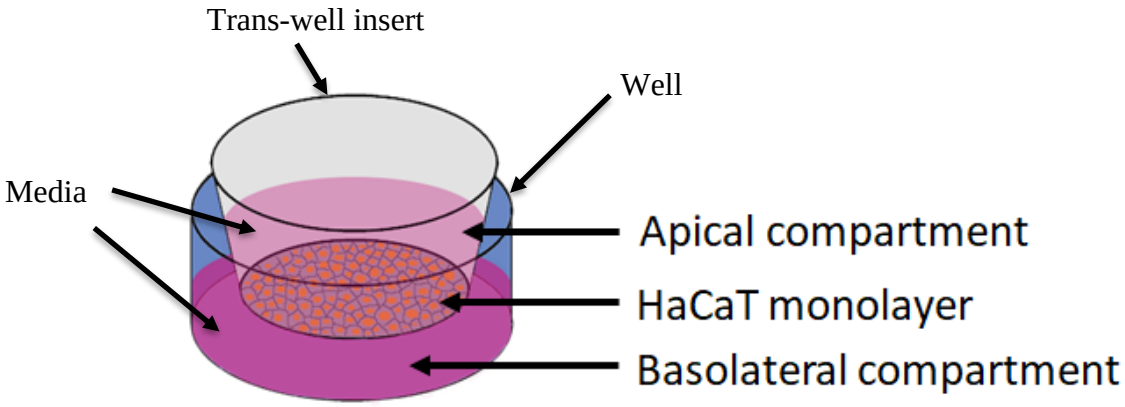

Figure 2.3. Schematic of penetration model. HaCaT keratinocyte monolayers were cultured on 1 µM transwell inserts (polyethylene terephthalate). Transwell inserts were immersed in cell culture media inside wells of a 24-well plate.

Both the apical and basolateral compartments were filled with 1000 µL of culture media. Experiment to evaluate sample penetration over time across the keratinocyte monolayer into the basolateral compartment was performed by replacing the media in the apical compartment with 1000 µL of ginseng NPPS or PS (300 µg/ mL). 1000 µL of conditioned media was removed from the basolateral compartment at 6, 12 and 18 hrs for quantitation of PS and NPPS. At each time point of sampling, an equal volume of fresh media was added for replacement. Herein, samples obtained from the basolateral compartment will be referred to as conditioned media.

To evaluate the influence of concentration on the penetration of samples across the keratinocyte monolayer, the apical compartment was treated with media (1000 µL) containing 0, 50, 100, 200 or 300 µg/mL of ginseng NPPS or PS for 24 hrs. Thereafter, conditioned media were removed from the basolateral compartment and stored until quantification via bioassay.

2.2.4.4 Bioassay for quantitation of PS and NPPS

In the absence of a chemically-based methodology to quantify PS and NPPS, a bioassay that was based on the stimulation of NO production by RAW 264.7 macrophage was developed to quantify the presence of PS and NPPS in the basolateral compartment (Appendix A1). A standard curve based on stimulation of plated macrophages NO production 24 hrs following treatment with 0, 50, 100, 200 and 300 µg/mL of ginseng PS or NPPS was prepared. Nitric oxide was estimated indirectly by measuring nitrite concentration by the Griess' assay. The standard curve was constructed as a semi-log plot from nitrite concentration (dependant) and treatment concentration (independent) (Fig. A.1). The standard curve was subsequently used to calculate the unknown sample concentrations.

To determine the concentration of PS or NPPS found in the conditioned media collected from the bio-membrane penetration study, experimental samples (200 µL) were added to the macrophage cultured in 96-well plates. The accumulation of NO in the culture media over 24 hrs was determined by the Griess' reagent test. The concentration of PS or NPPS in the samples was estimated from the PS or NPPS standard curve, respectively.

2.2.4.5 Quantification of NO production

Nitric oxide production was measured by colorimetric detection of the presence of nitrite ion in the media. Nitrite is a final product of the NO oxidation pathway. Nitric oxide in culture supernatants was determined using modified Griess' reagent containing 0.5% sulfanilic acid, 0.002% N-1-naphthyl-ethylenediamine dihydrochloride and 14% glacial acetic acid (Sigma-Aldrich, USA). Briefly, 50 µL of Griess reagent was added to 50 µL of culture supernatant and incubated away from light at room temperature for 15 mins. Absorbance at 540 nm wavelength was measured using *uQuant* microplate reader (Biotek Inc.). Wells containing air bubbles which distort measurements were excluded. Nitrite concentrations in samples were estimated from the standard curve prepared by dilutions of sodium nitrite.

2.2.5 Statistical analysis

Data are presented as mean ± standard error of the mean (SEM). The two-way analysis of variance (ANOVA) followed by Bonferroni's post hoc test was used for the comparison of means between treatment groups. The one-way analysis of variance (ANOVA) followed by Dunnett's post-hoc was used for the comparison of means with the untreated control (vehicle). Statistical analysis was performed using GraphPad Prism 6 software (San Diego, CA). Values $P < 0.05$ compared between treatment groups were considered statistically significant.

2.3 Results and discussion

In this study, crude ginseng PS was isolated from a water extract of 4-year-old Ontario-grown American ginseng roots by precipitation with 40% ethanol with a yield of **~ 9 ±** 1 % by dry-weight of root sample. This is consistent with what was reported in other studies[6]. Ginseng NPPS were prepared from bulk PS based on the microfluidic methodology designed by Akhter et al.[11] (see Fig. 2.1.). This procedure was modified successfully (i.e., substrate concentration) to address susceptibility for sample build-up in the T-junction and PEEK tubing. Nanosizing ginseng PS from 15 batches provided a yield of ~ 95% by weight relative to the substrate (i.e., bulk PS) weight. Subsequently, the resulting nanoparticles were characterized physicochemically and compared with the ginseng NPPS characteristics reported by Akhter et al.[11]. Penetration of ginseng NPPS across the dermal barrier was investigated to provide a biological basis for the apparent increase in deposition of ginseng PS into the dermis *in vivo*[12]. The influence of PS characteristics – namely its molecular weight – on the characteristics of the nanoparticles and its potency were also studied. The results of these studies were presented below.

2.3.1 Morphology and size distribution of ginseng PS and NPPS

Transmission electron microscopy (TEM) was performed on a NPPS composite sample prepared from 15 batches and a comparable bulk PS sample was used as a reference. As shown in Fig. 2.1a, bulk PS has an indistinct and unresolved structure with no regular nanomorphology. The unclear TEM micrograph is expected as one of the challenges

associated with the characterization of PS structures is that they have poor electron density, making it difficult to obtain high-resolution TEM images[16]. Furthermore, no stains were used during TEM preparation of PS samples. PS macromolecules and supramolecules (higher-leveled structures of macromolecules) are present as indicated within the micrographs by the arrows. Furthermore, agglomerates of PS were observed in the TEM micrograph. The TEM micrograph indicates that the PS supramolecules were amorphous and irregular in shape. Preliminary studies (data not shown) investigating the effect of aggregation has shown that the bulk PS would aggregate at concentrations past the solubility threshold (i.e., ~ 0.75 mg/mL) and rapidly sediment. The TEM micrograph of the nanosized ginseng PS (Fig 2.4b) showed that the prepared nanoparticles were much more uniform and within the nano-size range (< 100 nm). Particle size analysis of the TEM micrograph using "ImageJ" software of Fig. 2.4b gave a molecular distribution of approximately 12 – 26 nm in diameter with an average size of 19 nm (Fig. 2.5). The nanoparticles were also distinctly separated from one another and did not agglomerate. From these images, it is apparent that the morphology of ginseng NPPS was much more regular in size compared to PS, with spherical and smooth surfaces. The nanomorphology of these ginseng NPPS was similar to the characteristics of the ginseng NPPS reported by Akhter et al. Briefly, the authors also reported monodispersed nanoparticles that were unimodal and spherical in shape. These nanoparticles synthesized by Akhter et al. were characterized to be on average 20 ± 4 nm in diameter[11].

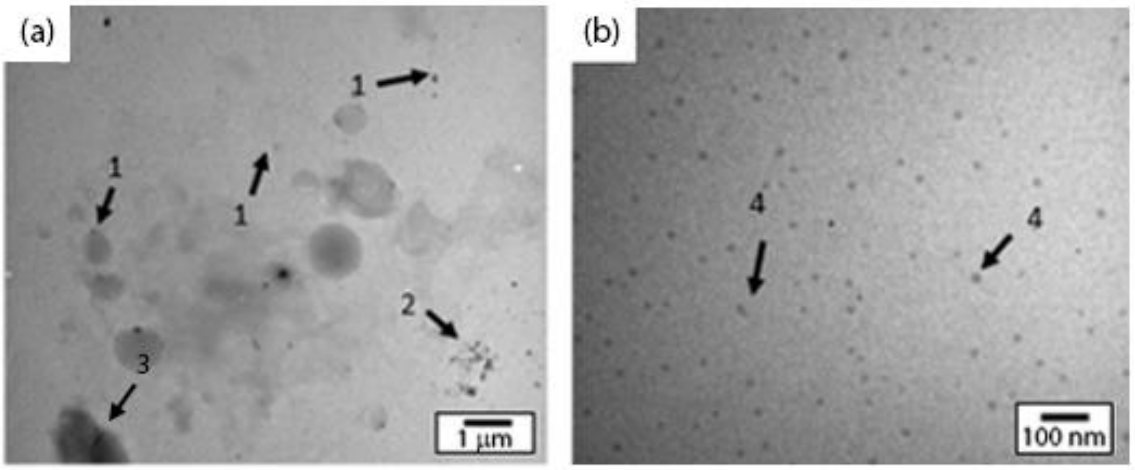

Figure 2.4. Transmission electron microscopy (TEM) micrograph of (a) bulk PS and (b) NPPS. Ginseng NPPS were synthesized by nanoprecipitation using microfluidics with a 1:20 flow rate ratio and 75 µm (inner diameter) PEEK tubing. Samples were dispersed in acetone and TEM was performed using Philips CM10 without using any stains. Arrow 1: PS macromolecule. Arrow 2: PS supramolecules. Arrow 3: PS agglomerates. Arrow 4: NPPS.

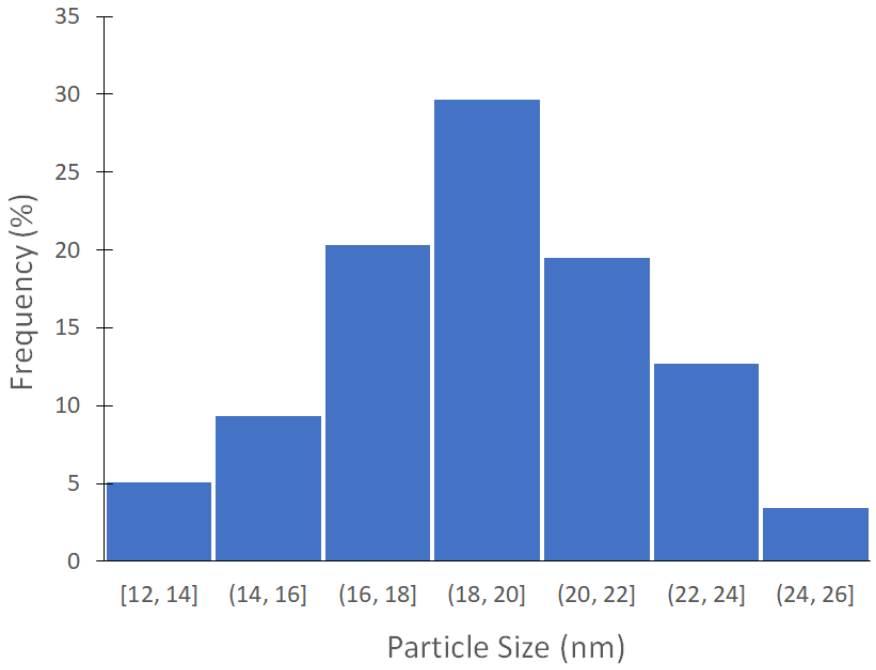

Figure 2.5. Size distribution of ginseng NPPS prepared by nanoprecipitation using microfluidics. Particle size is in diameter and was measured by ImageJ Software. Data presented was from a representative experiment.

In addition to TEM, the size distribution of the prepared NPPS was characterized using dynamic light scattering (DLS). As a comparison, bulk PS was also analyzed via DLS. Two separate size distributions were observed with bulk PS at approximately 90 – 140 nm and 820 – 1800 nm in diameter, with a mean peak of 110 nm and 1200 nm, respectively (Fig. 2.6a). The small and large size components had an area under the curve (AUC) of 14% and 86%, respectively. In contrast, NPPS had a single mean particle size of ~34 nm in diameter was measured (Fig. 2.6b). The measured particle size range of 28 – 44 nm corroborates with the TEM results. Results from the DLS indicate the hydrodynamic diameter of these particles in water based on a large number of molecules using light scattering. In comparison, TEM measurements from ImageJ (Fig. 2.5) use only a small number of measurements (i.e., ~ 100). Both results (Fig. 2.5 and Fig. 2.6) indicate successful nanoparticle formation (i.e., < 100 nm in diameter). TEM samples are dispersed and subsequently dried on a copper grid whereas DLS samples are dissolved in a solvent.

With this consideration, the difference in size distributions indicates NPPS interact to a small degree non-covalently when in solution.

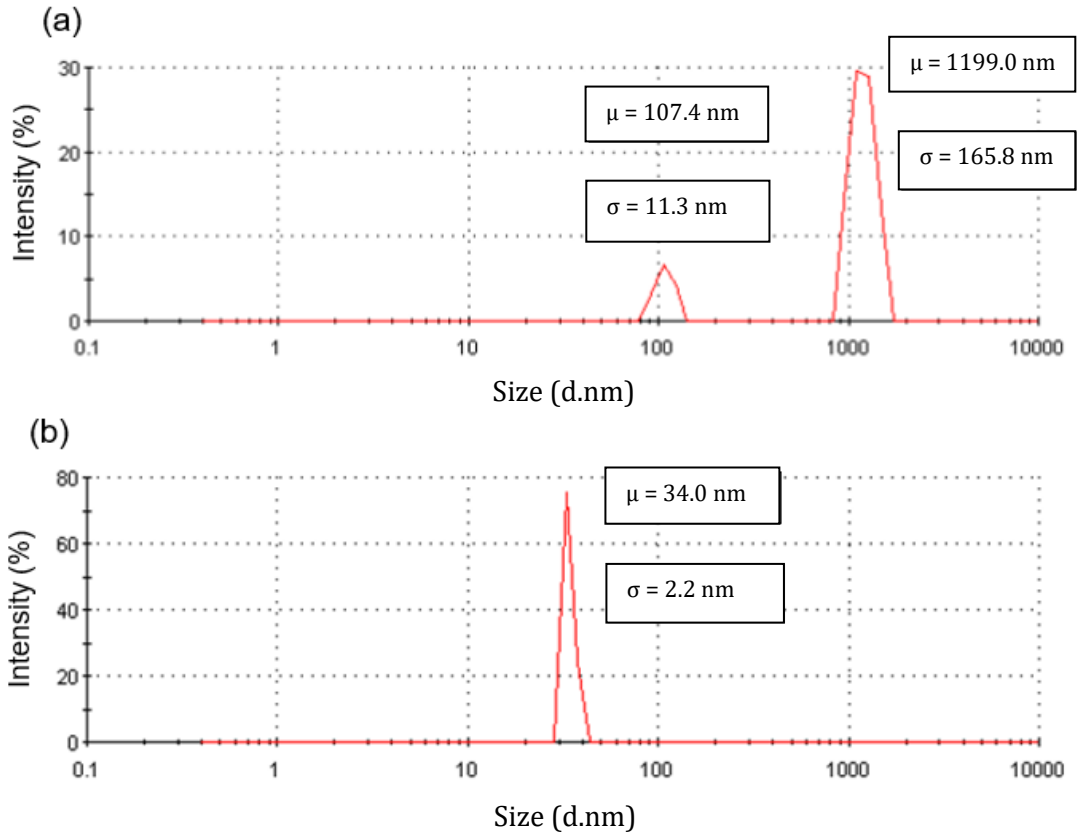

Figure 2.6. Dynamic Light Scattering of (a) ginseng PS and (b) NPPS using Zetasizer Nanosizer. Size distribution is presented as the diameter of the particles in nm and displayed as a function of intensity. Analysis was performed three times. Data presented was from a representative experiment. μ = mean; σ = standard deviation.

The parameters used for microfluidic processing of ginseng PS in the study conducted by Akhter et al. was similar to the parameters used in this current study, namely the anti-solvent to solvent ratio, flow rate, MicroTEE thru-hole, and PEEK tubing size. The main difference between these two procedures was the concentration of substrate used (0.55 mg/mL) and the technique to recover the product. The concentration of the substrate was not reported in the reference procedure. The concentration of the substrate used in the

procedure was also modified to allow for higher success rates (i.e., no clogging/ system errors) and greater yields. Based on the results (Fig 2.5), these alterations to the microfluidic procedure did not seem to greatly affect the average size (± 1 nm) or morphology of the nanoparticle compared to those reported by Akhter et al. Thus, the ginseng NPPS (15 batches) synthesized for our study demonstrated reproducibility (i.e. size and morphology) of the aforementioned nanoparticles in the study conducted by Akhter et al.[11].

Nanoprecipitation of bulk PS was demonstrated by Akhter et al. to not affect its chemical structure but increases its crystallinity[11]. Although there is higher structural order, the NPPS are still amorphous. Furthermore, the nanoparticles were formed due to interactions between the solvent and anti-solvent at the channel junction rather than through reactions with the acetone[17,18]. The chemical structure of a substrate is not typically altered following nanoprecipitation unless compounds, markers or tags are conjugated to the substrate and if the substrate reacts with the solvents. In a study conducted using nanoparticles prepared by bottom-up nanocrystallization (i.e., probe-sonication controlled precipitation), the chemical structure of the substrate compound did not change following size reduction[19]. This was attributed to changes in the crystalline structure and no functional changes were observed[19]. In another study, Zhou et al. reported that hydroxycamptothecin (HCPT: $C_{20}H_{16}N_2O_5$) nanorods and nanoparticles prepared by nanoprecipitation did not exhibit differences in its chemical structure compared to bulk HCPT[20]. These functionality changes could be attributed to physicochemical changes.

2.3.2 Biological characterization of NPPS

2.3.2.1 Stimulation of macrophage function.

To investigate the pharmacodynamics of the ginseng NPPS with reference to bulk PS, 24-hr response in cultured murine macrophages was examined. Ginseng PS and NPPS treatment showed dose-dependent stimulation of NO production up to 200 µg/ml and no further increase was observed with a higher dose (Fig. 2.7). The stimulatory response was

significantly higher with NPPS treatment by approximately 35% at all concentrations. It should be noted that the maximum response to NPPS was similar in magnitude to that induced by the positive control (1 µg/ml LPS) (data not shown). Based on the dose-response data, the respective EC_{50} values of 73.84 µg/mL and 93.12 µg/mL for NPPS and PS have been estimated. This provides further evidence of elevated potency with NPPS.

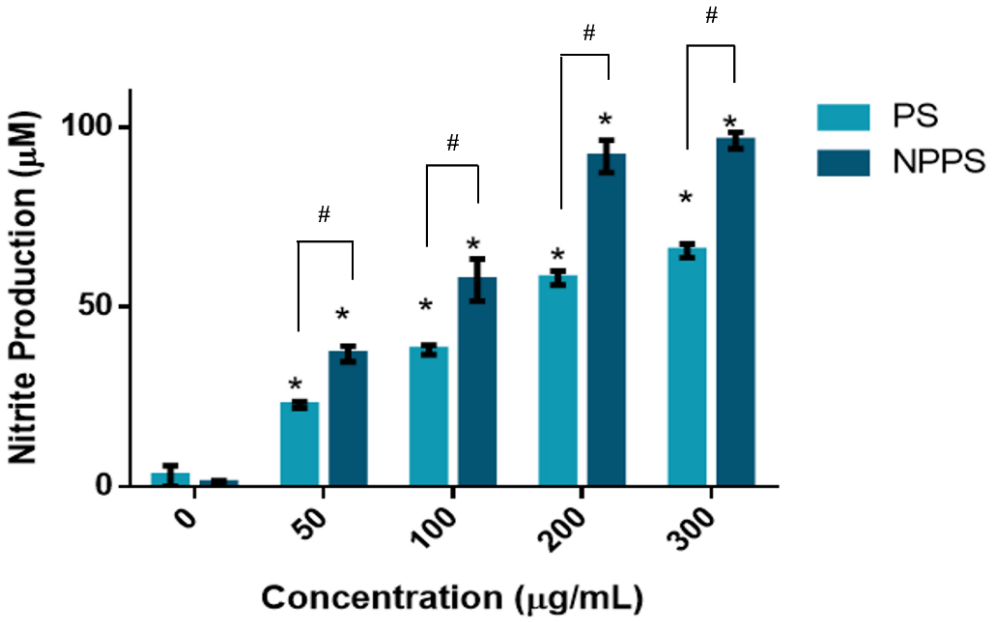

Figure 2.7. Immunostimulatory effects of ginseng PS and NPPS on macrophage NO production. Macrophages were treated with 0-300 µg/mL of NPPS and PS for 24 hrs. Three independent experiments were performed in triplicates. Data are presented as mean ± SEM. Datasets were statistically analysed by two-way ANOVA followed by Bonferroni's post hoc test. * Values $P < 0.05$ compared to the control were statistically significant. # Values < 0.05 compared between treatment groups were statistically significant.

Nitric oxide as an inflammatory mediator has been widely reported to be involved in the immunomodulatory activity of plant PS[21–23]. The up-regulation of NO production observed with ginseng PS treatment was consistent with the results reported previously in the literature[4,24]. The increase in NO production by NPPS was also consistent with the study conducted by Akhter et al.[11]. Both studies show that NPPS are more effective

immunostimulating agents compared to ginseng PS. The authors also reported enhanced TNFα, IL-1β and IL-6 production induced by NPPS[11]. This suggests that the apparent enhancement is not limited to stimulation of NO production but possibly related to the NF-κB pathway[12]. Perez et al. recently synthesized another type of ginseng nanoparticle and studied their pharmacological effects[25]. In this case, gold/silver salts and whole ginseng berry extract (GBE) instead of pure PS were used. The main phytochemicals present in ginseng berry extract are PS, phenolics, flavonoids, tannins, and ginsenosides. Characterization of the resulting nanoparticles suggested that ginsenosides, acidic polysaccharides, polyphenols and reducing sugars were capped onto the gold or silver nanoparticles[25]. These gold or silver core GBE nanoparticles were non-toxic and had enhanced pharmacological effects (e.g. free radical scavenging activity) compared to bulk GBE[25]. Although the nanoparticles from both studies are different, both indicated enhanced bioactivity following reduction of hydrodynamic volume[25].

Various other nanoparticles have similarly demonstrated enhanced biological effects compared to its corresponding substrate, which includes enhanced immunological, bactericidal or toxic effects. Morones et al. reported that the bactericidal effects of silver nanoparticles were improved with decreasing size due to the increased surface area interaction[26]. In a different study, zinc oxide (ZnO) nanoparticles exhibited enhanced antimicrobial effects compared to bulk ZnO[27]. Padmavathy et al. also reported that the enhancement of effect was inversely related to its size[27]. Although in each case different methodology and materials were used, the enhancement was consistently attributed to the change in size and surface chemistry because of the absence of functional changes to the molecules.

2.3.2.2 Penetration of NPPS across keratinocyte monolayer model *in vitro.*

2.3.2.2.1 Validation of the monolayer system.

Monolayer models have been regularly used in the pharmaceutical industry and in academic research institutions to estimate and predict intestinal drug absorption *in vitro* and study the mechanisms underlying drug transport. These models are often used to

identify relevant drug transporters, potential drug absorption complications, and if the drug is actively or passively transported. In these models, cell monolayers (e.g., Caco-2 or HT29 intestinal epithelial cells) are cultured on permeable inserts to simulate a cellular barrier[28,29]. Various models have also been developed to study drug transport across other barriers, such as the blood-brain barrier or dermal barrier. Examples of these models include human cerebral microvascular endothelial cells (hCMEC/D3) or immortalized human keratinocytes (HaCaT), respectively[30,31]. In this current study, we used a HaCaT monolayer model to study the transport of ginseng PS and NPPS across cultured keratinocyte monolayer. Transepithelial Electrical Resistance (TEER) was used to ascertain the functional integrity of monolayers in this study[30]. Typically, higher resistance is measured when the monolayer has high membrane integrity (i.e., tight junctions) due to the interference of the monolayer between electrical probes. A lower TEER threshold (> 50 Ohms*cm^2) was used to select intact keratinocyte monolayers. The lower threshold represents the baseline TEER to determine membrane integrity. Moreover, as shown in the data presented below, bulk PS, which are known to have limited systemic bioavailability also showed limited, if any, penetration. This provides further evidence of a functional monolayer system.

To determine the penetration of a test compound across a monolayer, the change in its concentration in the compartment(s) as a function of time has to be measured. The quantification of a test compound is typically performed using chemical detection technology. However, quantification of plant PS is difficult because of its lack of chromophoric moieties. There is also a lack of effective chromatographic techniques to provide resolution to ginseng PS which are known to be heterogeneous in molecular size. Akhter et al. has developed a methodology to label PS with a fluorescent tag (5-FTSC) for bioimaging but has many limitations for quantitative analysis[12]. A bioassay was used in this study to measure PS concentration (Fig. A.1). This bioassay was developed based on the initial characterization study of the immunostimulation of macrophages by ginseng PS and NPPS as described earlier (Fig. 2.7). A standard curve was prepared by measuring 24-hrs NO production by RAW 264.7 macrophages with 50 – 300 μg/mL concentrations of ginseng PS and NPPS (Fig. A.1). The PS and NPPS standard curves are sensitive to sample

concentrations between the stimulation conditions (50 – 300 μg/mL). Although the bioassay can estimate sample concentration based on its degree of macrophage stimulation, other stimulatory factors may be present in the sample which may have been released by the keratinocytes that could interact with the sample. If that is the case, there may be an overestimation of the result, affecting the specificity of the assay. Despite the limitations, this monolayer model has allowed us to compare the penetrations of PS and NPPS and test our hypothesis. In view of our failure to monitor changes in membrane integrity at the end of the penetration experiment, we could not rule out the induction of monolayer toxicity (dysfunction) rendering a false-positive-evidence for penetration.

2.3.2.2.2 Penetration of ginseng PS and NPPS across monolayer.

To determine whether the keratinocyte monolayer is a barrier to PS and NPPS, a solution of PS or NPPS (300 μg/mL) was added to the apical compartment and their accumulation in the basolateral compartment over the course of 18 hrs was determined by a bioassay. As shown in Fig 2.8, no PS was detectable in the basolateral compartment over the 18-hr period (PS detection limit: 50 μg/mL). In contrast, significant levels of NPPS were detected at the 18-hr sampling time-point but not at earlier time-points. This apparent abrupt increase in penetration may be attributed to the low degree of sensitivity of detection. The sensitive concentration for NPPS was 50 μg/ml; as compared to ~ 110 μg/ml recorded for NPPS at 18 hrs. The accumulation at 12 hrs may have been near but below the minimum sensitive concentration. If so, the increase observed would be comparably small but still significant. Despite the low sensitivity, results show that it is likely that the keratinocyte monolayer was a barrier for PS, but not NPPS. The marked increase in penetration at 18 hrs and lack of prior detectable penetration could potentially be attributed to a loss of membrane integrity over time induced by NPPS. Moreover, the loss of membrane integrity would have been small enough to maintain the barrier function to PS.

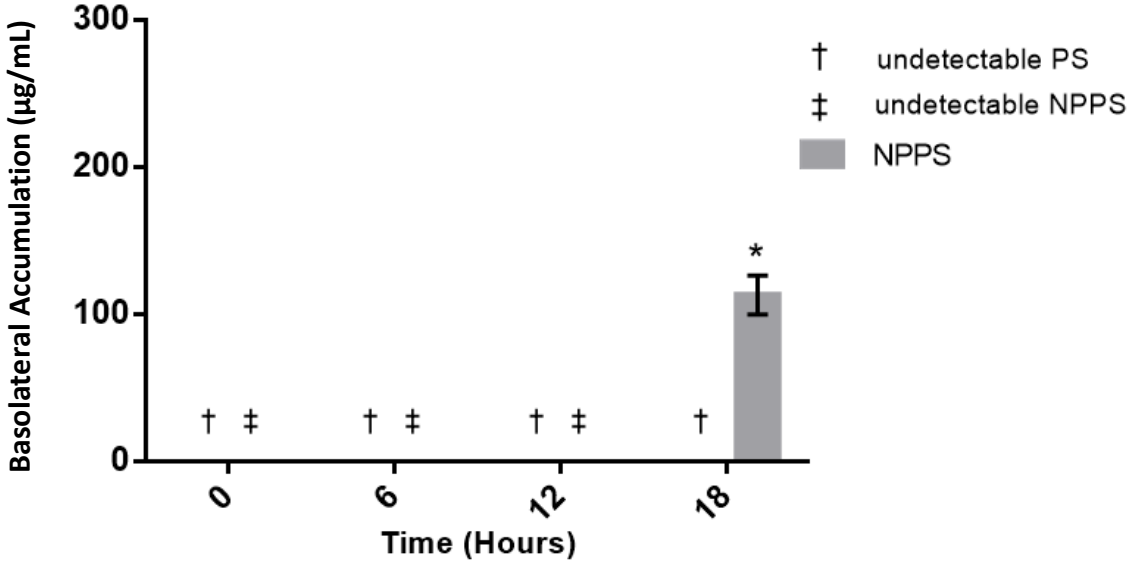

Figure 2.8. Accumulation of ginseng PS and NPPS in the basolateral compartment over periodic 6-hr intervals. RAW 264.7 cells were treated with conditioned media (300 µg/mL PS or NPPS treatment) collected from the basolateral compartment at 6, 12 and 18 hrs for PS or NPPS quantitation. Concentration was estimated from 24-hr macrophage NO production using respective standard curves. The sensitivity of bioassay was 50 - 300 µg/mL; therefore, concentrations below 50 µg/mL were undetectable. Experiments were performed in triplicates and the data are presented as mean ± SEM, n =3. * indicated time-dependent differences in accumulation; $P < 0.05$; two-way ANOVA).

In view of the observed accumulation of NPPS (300 µg/mL) over time across the keratinocyte monolayer, an additional experiment was conducted to determine whether the penetration was dependent on the concentration. This may provide additional information regarding the nature and mechanism of penetration. Four concentrations of ginseng PS and NPPS were used (50, 100, 200, 300 µg/mL) and the result was expressed based on the resulting basolateral concentrations (Fig. 2.9).

As shown in Fig. 2.5, the 24-hr accumulation of PS was insignificant even at the highest concentration tested (values being below the detection limit of 50 μg/mL). Significant accumulation of NPPS was detected at treatment concentrations of 200 and 300 μg/mL, but not at lower concentrations (Fig. 2.9). It was estimated that at 200 μg/mL of NPPS, approximately 65% of the NPPS load penetrated the monolayer into the basolateral compartment over the 24-hr period. However, the accumulation was not dose-dependent between 200 and 300 μg/mL. This may suggest that the penetration of NPPS across the monolayer was reaching saturation at higher concentrations.

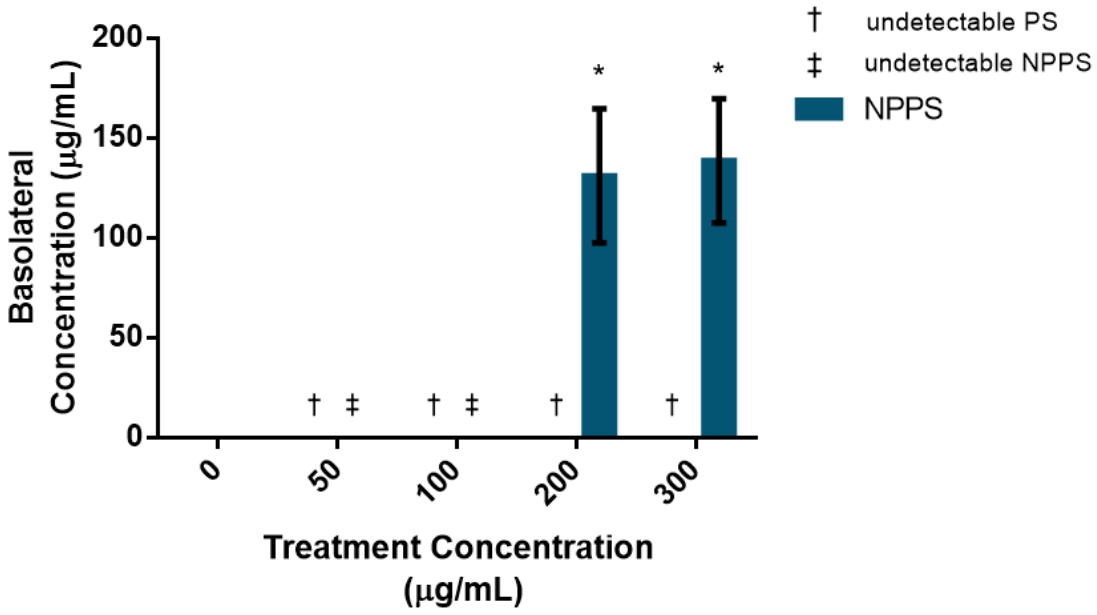

Figure 2.9. Basolateral concentration of PS and NPPS after 24-hr treatment. Conditioned sample was obtained from the basolateral compartment after 24-hr treatment to the keratinocyte monolayer model. The model was treated with 0-300 μg/mL of NPPS or PS. Three independent experiments were performed in triplicates and the data were presented as mean ± SEM. Datasets were statistically analysed by two-way ANOVA followed by Bonferroni's post hoc test. * Values $P < 0.05$ compared with zero control were statistically significant.

The observed enhancement of ginseng NPPS penetration of the keratinocyte monolayer is consistent with our previous *in vivo* observation following topical application in hairless mice (Akhter et al.)[12]. Furthermore, results are consistent with the poor permeability of other plant PS that has been reported[8]. The apparently limited penetration of PS is likely due to the lack of passive transport pathways which are mainly restricted by its large particle size. Typically, large particles or agglomerates are engulfed by phagocytosis (> 0.5 μm) leading to downstream lysosomal degradation[32]. In addition, PS may also undergo receptor-mediated endocytosis, pinocytosis and macropinocytosis[32]. These pathways target particles to early endosomes and may result in downstream basolateral transcytosis or degradation[14]. If the metabolites of these degradative pathways are not immunologically active, the bioassay would not quantify PS that undergo transport by these mechanism(s), which leads to an underestimation of PS penetration.

We have not studied the basis for the apparent high penetration of NPPS across keratinocyte monolayer. However, NPPS may undergo several modes of transport across membrane/cellular structure: (1) passive diffusion; (2) paracellular transport - nano-scale molecules penetrate basolaterally across the keratinocyte monolayer in between cells due to their extremely small size (< 50 nm); and (3) transcellular pathway (active transport) - endocytotic uptake by keratinocytes followed by basolateral release. This may include pinocytosis (non-adsorptive or adsorptive), macropinocytosis and/or receptor-mediated-endocytosis. (< 0.5 μM)[14,32]. It is likely that more than one of these processes may have occurred concurrently. The relative contributions of these mechanisms may depend on several factors, including nanoparticle size, lipophilicity and concentration. The last factor is dynamic and is expected to change with exposure time. Agglomeration of NPPS in solution can also affect the transport of the nanoparticle.

Our physicochemical analysis showed a reduction in particle size of PS corresponding to a reduction in hydrodynamic volume (Fig 2.5 & 2.6), which is consistent with what is reported in the literature[11]. The reduction of particle size should enable passive transport of PS particles across the monolayer which is limited by the surface charge and size of the particles. In a recent publication, nano-formulations of beta-carotene exhibited greater

kinetic saturation solubility and dissolution compared to bulk beta-carotene[33]. The nano-formulation was also demonstrated to be taken up by HaCaT keratinocytes faster than the poorly-soluble bulk-formulations[33]. In addition, the resorption of the nano-formulations of beta-carotene decreased with increasing crystalline size of beta-carotene[33]. In cases like ginseng NPPS where the nanoparticles consist of the drug itself (i.e., substrate only), smaller particle size was the main factor which increased bioavailability[34,35]. Megace ® ES (Par) and TriCor® (Abbot) are recent nano-pharmaceutical examples of such nanoparticle drugs which exhibited enhanced bioavailability[34,35]. Although different nanomaterials have different characteristics, the size was a common factor which has been shown to increase penetration across barriers[36]. The decrease in particle size of bulk PS following nanosization also increases surface-area-to-volume ratio[37]. A larger surface-area-to-volume ratio exhibits greater solubility, faster dissolution, and allows for greater interaction with the cellular membrane[38–40]. Therefore, passive transports are more likely.

It is evident that the particle size of NPPS also plays a role in active transport. Li et al. showed that the transport of lipid nanoparticles across Caco-2 monolayers was dependent on size[41]. Transport of these nanomaterials was found to occur mainly by endocytosis and smaller lipid nanoparticles exhibited higher permeability[41]. The attainment of high relative basolateral/treatment NPPS concentration (> 65%) and the evidence of apparent saturating transport characteristic at high concentration is suggestive of the involvement of active transport mechanisms. In a paper evaluating the cellular uptake of chitosan nanoparticles in Caco-2 cells, the authors reported change from extracellular interaction of chitosan to cellular internalization via clathrin-mediated endocytosis following nanosization[42]. Chitosan nanoparticles were also reported to be internalized via adsorptive endocytosis, macropinocytosis and caveolae-mediated endocytosis[43,44].

Various factors may have influenced the apparent detection of PS or NPPS accumulation in the basolateral compartment. Firstly, as pointed out earlier in the validation of the model, the bioassay used for measuring PS and NPPS lacks specificity in that it registers all immunostimulatory activity. In this regard, the induction of keratinocyte monolayer by NPPS to produce immunostimulatory factors and the subsequent release into the

basolateral compartment could lead to an apparent increase in NPPS penetration resulting in an over-estimation of penetration. Obviously, this is not true for PS as no penetration was detected. Secondly, the loss of the membrane integrity due to PS or NPPS toxicity could not be ruled out as we did not assess this parameter at the end of the experiment. This could have been measured by evaluating the TEER of the monolayer at the conclusion of the penetration study. As pointed out by Konishi et al., lower integrity of the monolayer may result in higher permeability of the membrane[28]. Therefore, the limitations of the bioassay and experimental design allow for the possibility that nanosizing bulk PS did not enhance its penetration. Instead, potential NPPS toxicity to the monolayer affected the viability and disrupted tight junctions thereby affecting its ability to act as a barrier to NPPS.

Increasing the penetration of a compound across a monolayer clinically translates to increasing its bioavailability[45–47]. The monolayer model used in the present study provides evidence to support the hypothesis that nanosizing PS enhances its penetration across a membrane barrier. This conclusion is based on assumptions that: (1) there was no cellular metabolism of PS; (2) NPPS did not affect the integrity of the monolayer, and; (3) NPPS did not interact with keratinocytes and induce a release of stimulatory factors.

2.3.3 Effect of substrate molecular weight on nanosization

2.3.3.1 Morphology and size distribution of NPPS prepared from ginseng PS of different molecular sizes.

As mentioned earlier, ginseng PS are quite heterogeneous with molecular weights ranging from as high as 2,000 kDa to as low as 3.1 kDa[48,49]. This raises the question of whether this parameter would influence the responsiveness to the nanosizing process as well as the quality and biological activity of the resulting NPPS. The other issue is whether the heterogeneity of the PS sample would be able to facilitate the process. Three different substrates were obtained by ultrafiltration of PS into three molecular weight sub-fractions: ≥ 100 kDa, 50 - 100 kDa or 30 – 50 kDa. Herein, they will be referred to as sub-fraction L, M and S, respectively. This separation was based on the pore size specification of

membranes used in the filtration system (see Fig. 2.3). The average yields for the separation of bulk PS were as follows: 54%, 27% and 14% for fraction L, M and S, respectively. The remaining 5 % fraction (< 30 kDa) was not used in the subsequent study. The yield of the NPPS synthesized from these fractions averaged approximately 94% and similar to the yield of NPPS prepared using bulk PS.

The size and morphology of the L-NPPS, M-NPPS and S-NPPS were characterized by TEM (Fig. 2.10i) and then processed by "ImageJ" software (Fig. 2.10ii). TEM image showed that the nanoparticles obtained from the three sub-fractions were spherical and monodispersed. As shown in Fig. 2.6ii, the NPPS obtained from the sub-fractions S, M and L had a mean diameter of 12 nm, 16 nm and 16 nm, respectively. S-NPPS had a relatively smaller size distribution than other two NPPS – M-NPPS and L-NPPS. In general, the size of these NPPS was smaller than those prepared from bulk PS (19 nm) (Fig. 2.5)

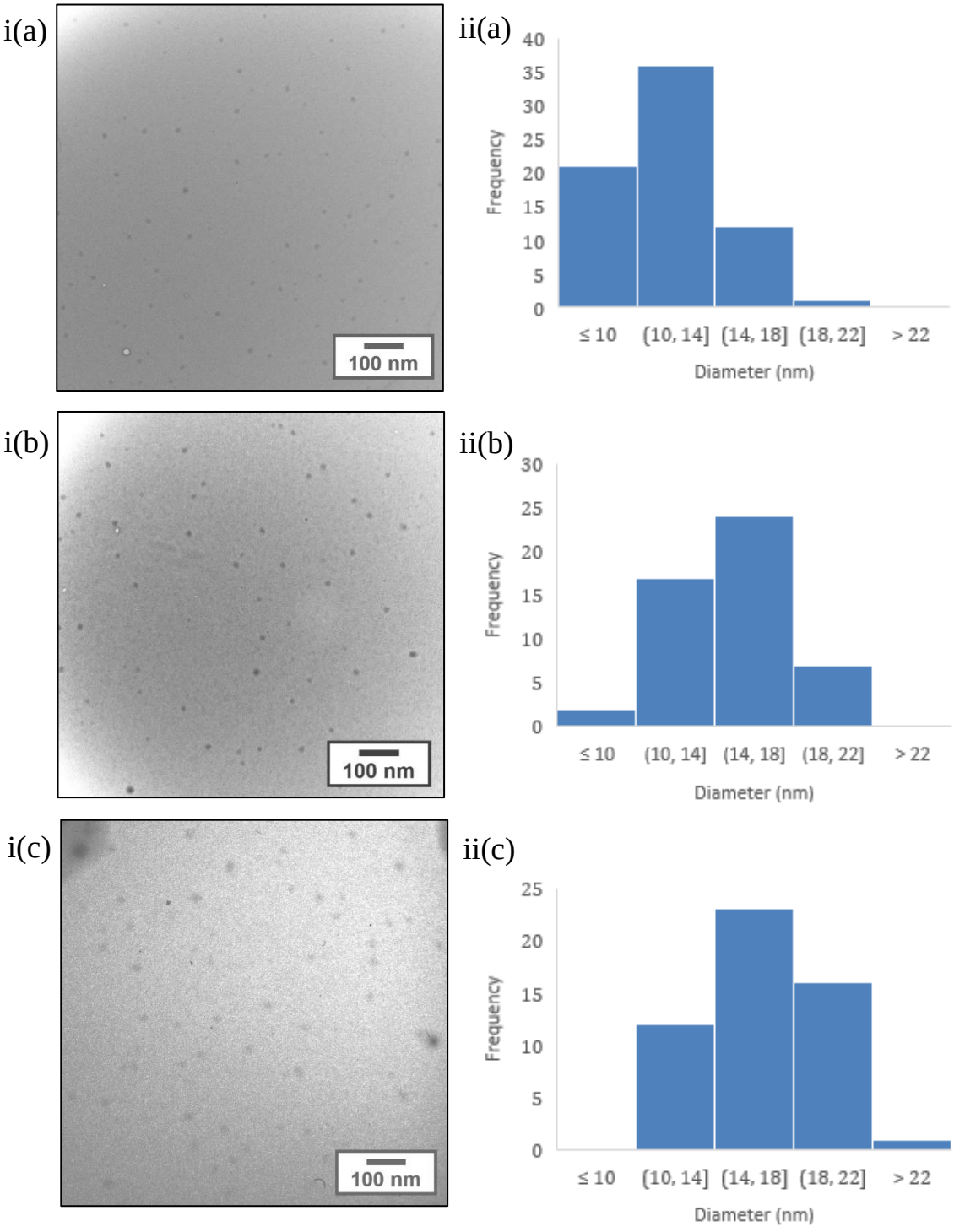

Figure 2.10. (i) Transmission electron microscopy (TEM) and (ii) size distribution of NPPS prepared using (a) 30-50 kDa, (b) 50-100 kDa and (c) >100 kDa ultracentrifuged PS fractions. NPPS were synthesized by nanoprecipitation using microfluidics with a 1:20

flow rate ratio and 0.020-inch PEEK tubing. TEM was performed using Philips CM10 and acetone as a dispersant. The scale is at 100 nm.

Separation of bulk PS into molecular weight sub-fractions reduces its heterogeneity in molecular weight. Compared to conventional polymers, PS polymers are not only heterogeneous due to differences in monomeric repeat number, but also in its composition. Results revealed that using more homogenous substrates (L-PS < M-PS < S-PS) produced NPPS with similar yields but with smaller particle sizes compared to using a bulk heterogeneous PS. Among the NPPS produced from the sub-fractions, the small molecular fraction resulted in smaller NPPS. It is possible that restricting the heterogeneity of the substrate enhances the order during nucleation, thereby increasing crystallinity. If the substrate is more homogenous, it is possible that nucleation of individual PS molecules during nanoprecipitation would be more uniform because there is less variability in molecular weight constrained by separation into molecular weight sub-fractions. Conversely, nucleation of highly heterogeneous PS would result in variable crystallization. To investigate this claim, further analysis such as X-ray diffraction (XRD) would be needed to determine crystallinity between fractionated NPPS. Differences in viscosity and sedimentation velocity between molecular weight fraction of PS may also contribute to the apparent shift in size. These two factors could potentially influence the agglomeration of PS.

The influence of polymeric molecular weight on nanomorphology and size has been reported previously in the literature. Polymeric molecular weight was observed to decrease, increase or have no effect on particle size in different studies[50–52]. Although this has been demonstrated, microfluidic processing of ginseng PS differs in lacking an additional stabilizer or polymer. Using microfluidics, Akhter et al. demonstrated that similar factors compared to conventional nanoprecipitation influenced nanoparticle characteristics[11]. These factors include the flow-rate of solvents and anti-solvents as well as the water-to-acetone ratio[11]. Our preliminary data (not shown) also indicate that solvent concentration affects nanoparticle size above the solubility threshold. Part of this was attributed to

clogging of the pore and build-up in the T-junction by aggregates that form at high concentrations.

2.3.3.2 Effect of substrate molecular weight on the bioactivity of NPPS.

Following the analysis of the physicochemical property of the three NPPS preparations (L-, M- and S-NPPS), we proceeded to examine their immunostimulatory activity to determine if a relationship existed between these two parameters. Data presented in Fig. 2.11. showed the 24-hr stimulation of NO production by macrophages. Both PS and NPPS displayed good dose-dependent effects. As shown in Fig. 2.11, the immunostimulatory potency of PS was related to the molecular size; the smallest sub-fraction – 'S' – was less potent compared to the M and L fraction. This observation was consistent with previous reports from Azike et al. and Lemmon et al.[6,7]. NPPS prepared from these 3 different sub-fractions showed higher potency than L-, M- and S-PS, indicating the potency enhancing effect of nanosization; however, there were no significant differences among them. This is consistent with our previous finding using bulk PS as the substrate which demonstrated enhanced potency with nanosization (Fig. 2.7.). We have also found that nanosization had the greatest effect on the smallest fraction, with the largest increase in potency. This may also suggest that nanosization of a bulk PS sample containing species with a range of molecular sizes may reduce the heterogeneity of the population in reference to individual molecules.

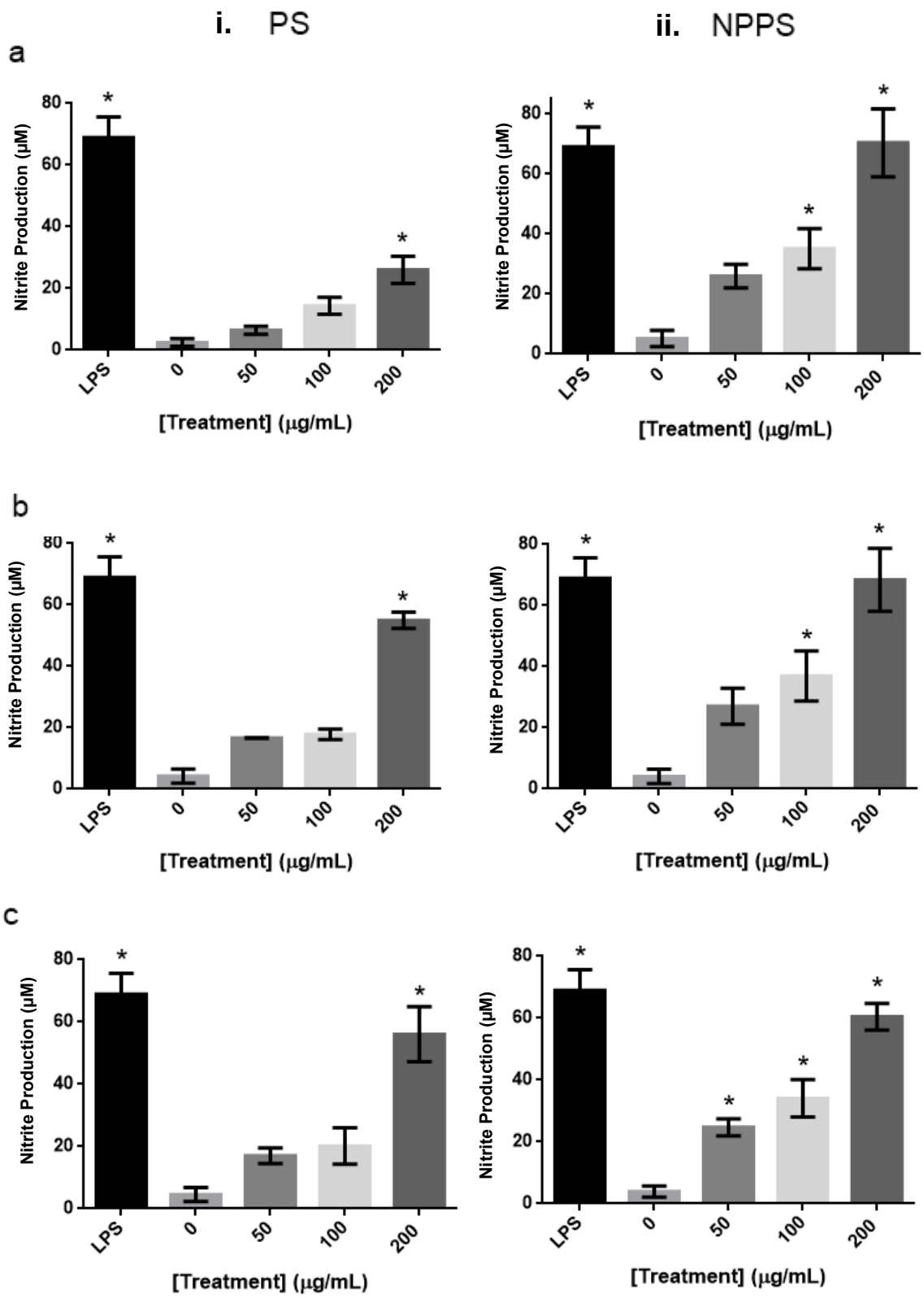
i. PS
ii. NPPS
a
b
c
Nitrite Production (μM)
0
20
40
60
80
*
LPS
0
50
100
200
[Treatment] (μg/mL)

Figure 2.11. Immunostimulatory effects of (i) ginseng PS and (ii) NPPS on the production of NO by macrophages after 24 hrs. Three molecular weight fractions were used: (a) 30-50 kDa (S), (b) 50-100 kDa (M) or (c) >100 kDa fractions (L). RAW 264.7 cells were treated with 0, 50, 100 or 200 µg/mL of sub-fractionated PS or NPPS for 24 hrs. LPS (1 µg/mL) was used as the positive control; LPS control was used in each figure for better comparison. Experiments were performed in triplicates and the data are presented as mean ± SEM, n = 3. Data were statistically analysed by one-way ANOVA followed by Dunnett's post-hoc test. * Values $P < 0.05$ compared to the vehicle (zero) control are statistically significant.

This section focused on the influence of the molecular size of PS on its nanosization into NPPS. Results of this experiment indicated that PS of different molecular sizes could be nanosized by microfluidics into more active immunostimulatory NPPS. These NPPS (S, M and L) exhibited similar bioactivity despite some differences in particle size. Furthermore, it was demonstrated that microfluidic processing could be applied equally well to a heterogeneous mixture of PS (i.e., bulk PS) as compared to more homogeneous sub-fractions (i.e., S-, M- and L-PS). This finding may have implications in designing future protocols for microfluidics-based nanosization of ginseng PS.

2.4 Conclusions

We have been successful in preparing NPPS from bulk PS substrate by a continuous microfluidics methodology as described by Akhter et al. with modifications[11]. This procedure produced nanoparticles with uniform morphology and narrow size distribution of ~10-25 nm. The resulting nanoparticles were unimodal spheres, monodispersed and exhibited low agglomeration compared to the bulk material, ginseng PS.

These NPPS showed enhanced immunostimulatory activity as compared to bulk PS when tested in cultured RAW 264.7 macrophages. NPPS also demonstrated good penetration across the keratinocyte monolayer *in vitro*, while PS showed little, if any, penetration.

These findings provided critical and corroborating evidence supporting our earlier observation of the disposition of NPPS, but not PS, in dermal tissues following topical application in an animal model. Lastly, a study was conducted to investigate the influence of the molecular size of PS substrates on the production of NPPS by the microfluidics-based nanoprecipitation procedure. This was essential, as the crude PS used in our study is known to be heterogeneous, making up of PS of different molecular sizes: ≥ 100 kDa (L), 50 - 100 kDa (M) and 30 – 50 kDa (S), with sub-fraction 'S' showing the lowest immunostimulatory activity. Data showed that all three sub-fractions could be prepared into nanoparticles with similar yield and comparable enhanced immunostimulatory activity.

In conclusion, we have been successful in modifying the microfluidics methodology for the preparation of ginseng NPPS from bulk PS. The characterization study has provided evidence of well-defined and consistent physicochemical and pharmacological properties; this data will support its application in the nutraceutical field. However, its fate in biological tissues and organism is largely unknown. Information is needed to address their potential toxicity. Future studies should investigate the fate of ginseng NPPS and address the potential toxicity associated with nanomaterials.

2.5 Acknowledgments

This work was funded by Western Phytoceutica (WPC) and Mitacs Canada.

2.6 References

1. Lim, T.-S., Na, K., Choi, E.-M., Chung, J.-Y. & Hwang, J.-K. Immunomodulating activities of polysaccharides isolated from Panax ginseng. *J. Med. Food* **7**, 1–6 (2004).

2. Sen, S. *et al.* Preventive effects of North American ginseng (Panax quinquefolius) on diabetic retinopathy and cardiomyopathy. *Phytother. Res. PTR* **27**, 290–298 (2013).

3. Lui, E. M. K. *et al.* Bioactive Polysaccharides of American Ginseng Panax quinquefolius L. in Modulation of Immune Function: Phytochemical and Pharmacological Characterization. *Complex World Polysacch.* (2012). doi:10.5772/50741

4. Azike, C. G., Charpentier, P. A., Hou, J., Pei, H. & King Lui, E. M. The Yin and Yang actions of North American ginseng root in modulating the immune function of macrophages. *Chin. Med.* **6**, 21 (2011).

5. Ji, L. *et al.* Structural characterization of alkali-soluble polysaccharides from Panax ginseng C. A. Meyer. *R. Soc. Open Sci.* **5**, 171644 (2018).

6. Azike, C. G. American Ginseng Modulation of Immune Function and Phytochemical Analysis. *Diss. Univ. West. Ont.* (2014).

7. Lemmon, H. R., Sham, J., Chau, L. A. & Madrenas, J. High molecular weight polysaccharides are key immunomodulators in North American ginseng extracts: characterization of the ginseng genetic signature in primary human immune cells. *J. Ethnopharmacol.* **142**, 1–13 (2012).

8. Lin, X. *et al.* A sensitive and specific HPGPC-FD method for the study of pharmacokinetics and tissue distribution of Radix Ophiopogonis polysaccharide in rats. *Biomed. Chromatogr.* **24**, 820–825 (2010).

9. Junyaprasert, V. B. & Morakul, B. Nanocrystals for enhancement of oral bioavailability of poorly water-soluble drugs. *Asian J. Pharm. Sci.* **10**, 13–23 (2015).

10. Jain, S., Reddy, V. A., Arora, S. & Patel, K. Development of surface stabilized candesartan cilexetil nanocrystals with enhanced dissolution rate, permeation rate across CaCo-2, and oral bioavailability. *Drug Deliv. Transl. Res.* **6**, 498–510 (2016).

11. Akhter, K. F., Mumin, M. A., Lui, E. K. & Charpentier, P. A. Microfluidic Synthesis of Ginseng Polysaccharide Nanoparticles for Immunostimulating Action on Macrophage Cell Lines. *ACS Biomater. Sci. Eng.* **2**, 96–103 (2016).

12. Akhter, F. Ginseng Polysaccharides Nanoparticles-Synthesis, Characterization, and Biological Activity. *Diss. Univ. West. Ont.* (2016).

13. Salatin, S. & Khosroushahi, A. Y. Overviews on the cellular uptake mechanism of polysaccharide colloidal nanoparticles. *J. Cell. Mol. Med.* **21**, 1668–1686 (2017).

14. Behzadi, S. *et al.* Cellular Uptake of Nanoparticles: Journey Inside the Cell. *Chem. Soc. Rev.* **46**, 4218–4244 (2017).

15. Ferreira, M. *et al.* Methotrexate loaded lipid nanoparticles for topical management of skin-related diseases: Design, characterization and skin permeation potential. *Int. J. Pharm.* **512**, 14–21 (2016).

16. Lienemann, C.-P., Mavrocordatos, D. & Perret, D. Enhanced visualization of polysaccharides from aqueous suspensions. *Microchim. Acta* **126**, 123–129 (1997).

17. Karnik, R. *et al.* Microfluidic Platform for Controlled Synthesis of Polymeric Nanoparticles. *Nano Lett.* **8**, 2906–2912 (2008).

18. LaMer, V. K. & Dinegar, R. H. Theory, Production and Mechanism of Formation of Monodispersed Hydrosols. *J. Am. Chem. Soc.* **72**, 4847–4854 (1950).

19. Sohn, J. S., Yoon, D.-S., Sohn, J. Y., Park, J.-S. & Choi, J.-S. Development and evaluation of targeting ligands surface modified paclitaxel nanocrystals. *Mater. Sci. Eng. C Mater. Biol. Appl.* **72**, 228–237 (2017).

20. Zhou, M. *et al.* Shape regulated anticancer activities and systematic toxicities of drug nanocrystals in vivo. *Nanomedicine Nanotechnol. Biol. Med.* **12**, 181–189 (2016).

21. Azike, C. G., Charpentier, P. A. & Lui, E. M. K. Stimulation and suppression of innate immune function by American ginseng polysaccharides: biological relevance and identification of bioactives. *Pharm. Res.* **32**, 876–897 (2015).

22. Li, M. *et al.* Non-starch polysaccharide from Chinese yam activated RAW 264.7 macrophages through the Toll-like receptor 4 (TLR4)-NF-κB signaling pathway. *J. Funct. Foods* **37**, 491–500 (2017).

23. Hou, L., Meng, M., Chen, Y. & Wang, C. A water-soluble polysaccharide from Grifola frondosa induced macrophages activation via TLR4-MyD88-IKKβ-NF-κB p65 pathways. *Oncotarget* **8**, 86604–86614 (2017).

24. Shin, J.-Y. *et al.* Immunostimulating effects of acidic polysaccharides extract of *Panax ginseng* on macrophage function. *Immunopharmacol. Immunotoxicol.* **24**, 469–482 (2002).

25. Jiménez Pérez, Z. E. *et al.* Ginseng-berry-mediated gold and silver nanoparticle synthesis and evaluation of their in vitro antioxidant, antimicrobial, and cytotoxicity effects on human dermal fibroblast and murine melanoma skin cell lines. *Int. J. Nanomedicine* **12**, 709–723 (2017).

26. Morones, J. R. *et al.* The bactericidal effect of silver nanoparticles. *Nanotechnology* **16**, 2346–2353 (2005).

27. Padmavathy, N. & Vijayaraghavan, R. Enhanced bioactivity of ZnO nanoparticles—an antimicrobial study. *Sci. Technol. Adv. Mater.* **9**, 035004 (2008).

28. Konishi, Y. & Kobayashi, S. Transepithelial Transport of Chlorogenic Acid, Caffeic Acid, and Their Colonic Metabolites in Intestinal Caco-2 Cell Monolayers. *J. Agric. Food Chem.* **52**, 2518–2526 (2004).

29. Pan, F., Han, L., Zhang, Y., Yu, Y. & Liu, J. Optimization of Caco-2 and HT29 co-culture in vitro cell models for permeability studies. *Int. J. Food Sci. Nutr*. **66**, 680–685 (2015).

30. Silva, E., Barreiros, L., Segundo, M. A., Costa Lima, S. A. & Reis, S. Cellular interactions of a lipid-based nanocarrier model with human keratinocytes: Unravelling transport mechanisms. *Acta Biomater.* **53**, 439–449 (2017).

31. Urich, E., Lazic, S. E., Molnos, J., Wells, I. & Freskgård, P.-O. Transcriptional profiling of human brain endothelial cells reveals key properties crucial for predictive in vitro blood-brain barrier models. *PloS One* **7**, e38149 (2012).

32. Oh, N. & Park, J.-H. Endocytosis and exocytosis of nanoparticles in mammalian cells. *Int. J. Nanomedicine* **9**, 51–63 (2014).

33. Lohan, S. B., Vitt, K., Scholz, P., Keck, C. M. & Meinke, M. C. ROS production and glutathione response in keratinocytes after application of β-carotene and VIS/NIR irradiation. *Chem. Biol. Interact.* **280**, 1–7 (2018).

34. Jang, K. *et al.* Novel nanocrystal formulation of megestrol acetate has improved bioavailability compared with the conventional micronized formulation in the fasting state. *Drug Des. Devel. Ther.* **8**, 851–858 (2014).

35. Kumar, R. & Siril, P. F. Enhancing the Solubility of Fenofibrate by Nanocrystal Formation and Encapsulation. *AAPS PharmSciTech* **19**, 284–292 (2018).

36. Kumari, A. & Yadav, S. K. Cellular interactions of therapeutically delivered nanoparticles. *Expert Opin. Drug Deliv.* **8**, 141–151 (2011).

37. Shang, L., Nienhaus, K. & Nienhaus, G. U. Engineered nanoparticles interacting with cells: size matters. *J. Nanobiotechnology* **12**, 5 (2014).

38. Hoshyar, N., Gray, S., Han, H. & Bao, G. The effect of nanoparticle size on in vivo pharmacokinetics and cellular interaction. *Nanomed.* **11**, 673–692 (2016).

39. Elias, D. R., Poloukhtine, A., Popik, V. & Tsourkas, A. Effect of ligand density, receptor density, and nanoparticle size on cell targeting. *Nanomedicine Nanotechnol. Biol. Med.* **9**, 194–201 (2013).

40. Zhang, W. *et al.* Effect of Shape on Mesoporous Silica Nanoparticles for Oral Delivery of Indomethacin. *Pharmaceutics* **11**, 4 (2019).

41. Li, H., Chen, M., Su, Z., Sun, M. & Ping, Q. Size-exclusive effect of nanostructured lipid carriers on oral drug delivery. *Int. J. Pharm.* **511**, 524–537 (2016).

42. Ma, Z. & Lim, L.-Y. Uptake of Chitosan and Associated Insulin in Caco-2 Cell Monolayers: A Comparison Between Chitosan Molecules and Chitosan Nanoparticles. *Pharm. Res.* **20**, 1812–1819 (2003).

43. Huang, M., Ma, Z., Khor, E. & Lim, L.-Y. Uptake of FITC-Chitosan Nanoparticles by A549 Cells. *Pharm. Res.* **19**, 1488–1494 (2002).

44. Nam, H. Y. *et al.* Cellular uptake mechanism and intracellular fate of hydrophobically modified glycol chitosan nanoparticles. *J. Control. Release Off. J. Control. Release Soc.* **135**, 259–267 (2009).

45. Sahana, D. K., Mittal, G., Bhardwaj, V. & Kumar, M. N. V. R. PLGA nanoparticles for oral delivery of hydrophobic drugs: influence of organic solvent on nanoparticle formation and release behavior in vitro and in vivo using estradiol as a model drug. *J. Pharm. Sci.* **97**, 1530–1542 (2008).

46. Shofia, S. I., Jayakumar, K., Mukherjee, A. & Chandrasekaran, N. Efficiency of brown seaweed (*Sargassum longifolium*) polysaccharides encapsulated in nanoemulsion and nanostructured lipid carrier against colon cancer cell lines HCT 116. *RSC Adv.* **8**, 15973–15984 (2018).

47. Miele, E., Spinelli, G. P., Miele, E., Tomao, F. & Tomao, S. Albumin-bound formulation of paclitaxel (Abraxane® ABI-007) in the treatment of breast cancer. *Int. J. Nanomedicine* **4**, 99–105 (2009).

48. Ivanova, T., Han, Y., Son, H.-J., Yun, Y.-S. & Song, J.-Y. Antimutagenic effect of polysaccharide ginsan extracted from Panax ginseng. *Food Chem. Toxicol.* **44**, 517–521 (2006).

49. Wang, L. *et al.* Structural and anti-inflammatory characterization of a novel neutral polysaccharide from North American ginseng (Panax quinquefolius). *Int. J. Biol. Macromol.* **74**, 12–17 (2015).

50. Chorny, M., Fishbein, I., Danenberg, H. D. & Golomb, G. Lipophilic drug loaded nanospheres prepared by nanoprecipitation: effect of formulation variables on size, drug recovery and release kinetics. *J. Controlled Release* **83**, 389–400 (2002).

51. Budhian, A., Siegel, S. J. & Winey, K. I. Haloperidol-loaded PLGA nanoparticles: Systematic study of particle size and drug content. *Int. J. Pharm.* **336**, 367–375 (2007).

52. Limayem Blouza, I., Charcosset, C., Sfar, S. & Fessi, H. Preparation and characterization of spironolactone-loaded nanocapsules for paediatric use. *Int. J. Pharm.* **325**, 124–131 (2006).

Chapter 3

Mechanism of macrophage stimulation *in vitro* by American ginseng polysaccharides nanoparticles

3.1 Introduction

Panax ginseng (Asian ginseng) is a perennial plant that has been traditionally used as a herbal remedy for the treatment of general malaise, gastrointestinal distress and diseases of the respiratory system, whereas *Panax quinquefolius* (North American ginseng) was primarily used to relieve cold sores, fevers and gastrointestinal distress[1,2]. The two major phytochemicals in ginseng are ginsenosides and polysaccharides (PS). Ginseng PS are not secondary plant metabolites but are part of the cell wall and are released by hydrolysis during processing. Polysaccharides are large hydrophilic molecules that have diverse composition, conformation and structure. The PS component consists mainly of starch-like PS, pectins and hemicellulose, with starch-like PS being the primary carbohydrate component[3].

Ginseng PS are known as adaptogens, which are substances thought to increase physiological resistance to physical and chemical stress. Adaptogenic effects are non-specific, and; immunomodulation is one of these adaptogenic effects. Ginseng PS have been demonstrated *in vitro* to enhance hydrogen peroxide (H_2O_2) and nitric oxide (NO) production of murine peritoneal macrophages[4]. PS-treated macrophages were also shown to exhibit stimulated lysosomal phosphatase and phagocytic activities[4]. In addition, cytokine production – tumor necrosis factor alpha (TNFα), NO, interleukin (IL)-6 and IL-1β – was upregulated in RAW 264.7 macrophages (Abelson murine leukemia virus transformed macrophages) treated with PS[5]. Similar upregulation of cytokine production was observed in mice treated with orally administered PS[6]. In a recent preclinical study, a ginseng PS extract was reported to increase T and B lymphocyte proliferation and natural killer (NK) cell activity in cyclophosphamide-induced immunosuppressed mice[7].

North American ginseng roots are marketed as teas, beverages and natural health products (NHPs). COLD-FX® (CVT-E002), which is one of the best-known NHPs in Canada, is manufactured from NA ginseng as a PS extract enriched in polyfuranosyl-pyranosyl-saccharides. Clinical trials revealed that COLD-FX® was effective in preventing acute respiratory illness in immunocompetent seniors[8]. In a more recent clinical trial, a

decreasing trend in the incidence of acute respiratory illness in Chronic Lymphocytic Leukemia patients taking COLD-FX® was reported[9].

Ginseng PS act by binding to pathogen recognition receptors (i.e., toll-like receptor (TLR) 2/4) which trigger subsequent intracellular pathways resulting in an immune response[10,11]. Briefly, dimerization of TLR4 mediates the activation of the nuclear factor-kappa-light-chain-enhancer of activated B cells (NF-κB) cascade downstream[12]. Consequently, the production of TNFα, IL-6, IL-1β and NO are upregulated, to name a few[13,14]. In addition to the NF-κB cascade, ERK-1/2, PI3K and p38 pathways have been implicated in the immunomodulatory effects of ginseng PS[15]. Following TLR activation, cell-surface TLRs are internalized, which reduces the responsiveness of immune cells to TLR agonists[16,17]. The TLRs are endocytosed as a complex with the TLR ligand, which may be mediated by cluster of differentiation 14 (CD14)[17,18]. This is commonly known as TLR desensitization or TLR tolerance in macrophages. Animal lectins that can recognize and bind carbohydrates are another potential receptor for ginseng PS[19]. These potential mechanisms of activation of PS may differ following microfluidic processing to synthesize nanoparticles of ginseng PS (NPPS).

Nanoparticles are particles with at least one-dimension that ranges from 1 – 1000 nm. They are surrounded by a surface/interfacial layer, which is the "region intermediate between two bulk phases in contact"[20]. This region may or may not contain other inorganic materials or ions, depending on the methodology used to prepare them. Nanotechnology is often applied to compounds that are poorly soluble and large in size to produce nanoparticles while controlling these properties[21,22]. Nanoparticles typically exhibit size-related properties different from their substrate compound[23,24]. They have been shown to have higher permeability than the drug or substrate that was used to prepare them[25]. The enhanced permeability is generally attributed to the reduction in particle size and alteration of surface chemistry (ex. polarity, solubility, etc.)[22,24,26].

NPPS possess different potencies than its substrate, in addition to different physicochemical properties. Bulk PS are present in solution as large micron-sized particles

and agglomerates whereas NPPS have a uniform and spherical nanomorphology. These NPPS have exhibited greater immunostimulatory activity (NO, TNFα, IL-6) *in vitro* relative to regular ginseng PS (i.e., bulk PS)[6]. Ginseng NPPS have been shown to correlate with greater NO and cytokine (TNF-α) levels in murine blood samples collected by cardiac puncture following oral gavage[6]. In addition, higher levels of IL-1β, TNF-α and NO in blood serum and skin samples have also been reported in hairless mice topically treated with ginseng NPPS[6]. Previous research indicated that ginseng NPPS accumulated within the macrophages with no apparent retention at the cell membrane and showed earlier intracellular uptake[6]. On the other hand, ginseng PS was retained at the cellular membrane[6]. Although NPPS appeared to exhibit higher immunostimulatory activity and showed enhanced cellular uptake; the underlying mechanism is poorly understood. Accordingly, the present study has been conducted to test the hypothesis that NPPS do not share the same cellular mechanism in mediating its immunostimulatory action as compared to PS. In order to do this, we examined the role of TLRs by i) defining the time-course of macrophage activation; ii) assessing the influence of TLR desensitization by LPS; and iii) suppression of activation by selective TLR antagonist. Our data showed that in contrary to our hypothesis, NPPS behaved like PS under these experimental conditions.

3.2 Experimental Procedure

3.2.1 Materials

Ginseng PS were extracted and isolated from aqueous extract of *Panax quinquefolius* which was provided by the Ontario Ginseng Innovation and Research Consortium. Deproteinated PS (i.e., bulk PS) was used to synthesize ginseng NPPS by nanoprecipitation using microfluidics (Fig. 2.1)[27]. Subsequently, the resulting nanomaterials were characterized for its physicochemical properties (Ch. 2.2.) prior to performing pharmacological studies on ginseng NPPS.

Abelson murine leukemia virus transformed macrophages (RAW 264.7) (ATCC TIB 67) provided by Dr. Jeff Dixon (Department of Physiology and Pharmacology, University of

Western Ontario, Canada) were used for pharmacological studies. Dulbecco's Modified Eagle's Medium (DMEM) and Fetal Bovine Serum (FBS) (US origin) were purchased from Gibco laboratories (USA). Lipopolysaccharides from *Escherichia coli* (O111:B4), Sparstolonin B (SsnB) and Griess' reagent (modified) were purchased from Sigma-Aldrich (Canada).

3.2.2 Macrophage cell culture and marker of activation

RAW 264.7 were cultured in DMEM supplemented with 10% Fetal Bovine Serum (FBS) and 1% penicillin/streptomycin. Cell cultures were maintained at 37 ℃ in a humidified incubator with 10% CO_2. The concentration of CO_2 was used in accordance with the concentration of sodium bicarbonate (3.7 g/L) within the media to maintain a pH of ~ 7.4. RAW 264.7 cells were passaged every 3-4 days at approximately 80% confluency. Cell culture media were changed one day prior to passaging. Cell cultures were tested for mycoplasma contamination and were negative for contamination. For experiments, RAW 264.7 cells were seeded in 96-well tissue culture plates at a density of 1.5 x 10^5 cells per well and incubated at 37 ℃ and 10% CO_2.

The marker of macrophage activation was the induction of iNOS, which was assessed by measuring NO production via colorimetric detection of the presence of nitrite ions in the media. Nitrite is a final product of the NO oxidation pathway. Nitrite was quantified using a modified Griess' reagent containing 0.5% sulfanilic acid, 0.002% N-1-naphthyl-ethylenediamine dihydrochloride and 14% glacial acetic acid (Sigma-Aldrich, USA). Briefly, 50 µL of Griess' reagent was added to 50 µL of culture supernatant and incubated away from light at room temperature for 15 mins. Absorbance at 540 nm wavelength was measured using *uQuant* microplate reader (Biotek Inc.). Nitrite concentrations in samples were estimated from the standard curve prepared by dilutions of sodium nitrite.

3.2.3 Time-course of immunostimulation

To determine the onset of action, RAW 264.7 cells were treated with 200 µg/mL of PS or NPPS for 6, 9, 12, 15, 18, 21 or 24 hrs. Macrophage response to PS or NPPS was determined by measuring the NO level in the culture supernatant.

3.2.4 Effect of TLR desensitization by LPS pre-treatment

To determine whether NPPS act via binding to TLRs and followed by internalization (i.e., translocation), a model of LPS-induced desensitization of macrophage responsiveness via treatment-induced internalization of TLRs was used. This model was set-up by pre-treating cultured RAW 264.7 cells with 1 µg/mL of LPS or vehicle control (media) for 24 hrs to induce TLRs internalization. Following pre-treatment, LPS-challenged macrophages were washed three times with PBS to remove the remaining LPS. Cells were subsequently treated with 50 and 200 µg/mL of ginseng PS or NPPS. LPS (1 µg/mL) was used as the positive control. At 24 hrs, cell culture supernatant was removed. The end-point was 24 hrs NO production by macrophages.

3.2.5 Effect of pre-treatment with a selective inhibitor of TLR 2/4 (Sparstolonin B)

To determine the role of cell surface toll-like receptors in the mediation of NPPS activity, SsnB, a selective TLR2/4 antagonist, was used to inhibit downstream TLR signalling in cultured macrophages[28]. For this, cultured RAW 264.7 cells were treated with or without SsnB (10 µg/mL and 100 µg/mL). Cells were treated concurrently with ginseng PS or NPPS (200 µg/mL). At 24 hrs, cell culture supernatant was removed for determination of 24 hrs NO accumulation.

3.2.6 Statistical analysis

Data are present as mean ± standard error of the mean (SEM). The two-way analysis of variance (ANOVA) followed by Bonferroni's post hoc test was used for the comparison of means between treatment groups. Statistical analysis was performed using GraphPad Prism 6 software (San Diego, CA). Values $P<0.05$ compared between treatment groups were considered statistically significant.

3.3 Results and Discussion

3.3.1 Time-course of immunostimulatory effect of PS and NPPS in macrophages *in vitro*

To investigate if NPPS and PS have a different mechanism of action, the onset of immunostimulation *in vitro* was studied. This was studied by treating cultured macrophages with bulk PS or NPPS for 24 hrs and examined the response in 3-hr intervals. Bulk PS treatment induced significant NO production over control values beginning at ~ 15 hrs (Fig. 3.1). Nitric oxide production from PS stimulation reached plateau at ~ 18 hrs. On the other hand, the earliest significant increase in NO production with NPPS was observed at ~ 12 hrs; and maximum stimulation was noted at ~ 15 hr. In summary, compared to bulk PS treatment, NPPS treatment elicited a greater maximal response in macrophages and had an earlier onset.

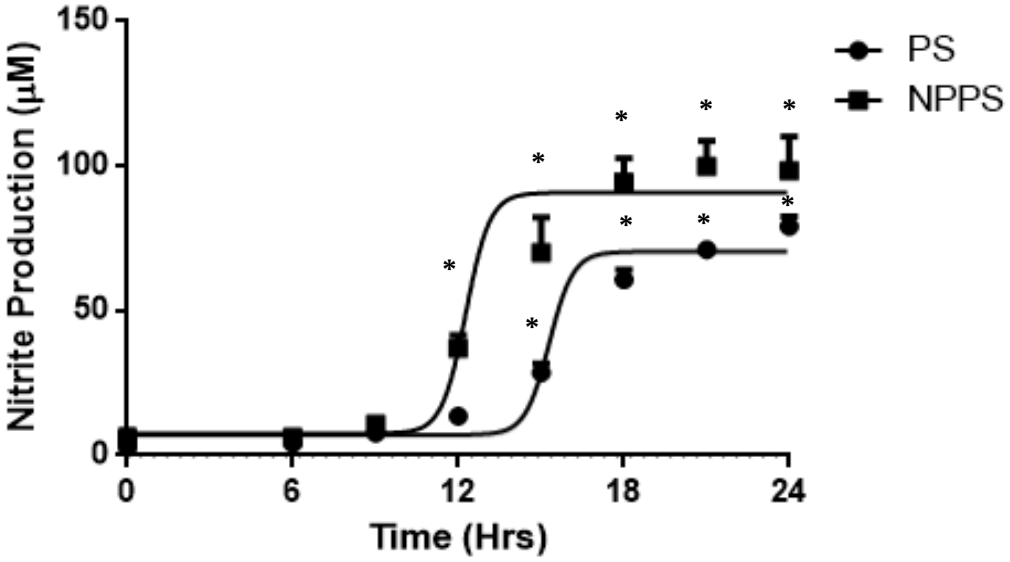

Figure 3.1. Immunostimulatory effects of ginseng PS and NPPS on macrophage nitrite production. Stimulation of RAW 264.7 macrophages by ginseng PS or NPPS. RAW 264.7 cells were treated with 200 µg/mL of PS and NPPS for 6-24 hrs. Three independent experiments were performed in triplicates and the data are presented as mean ± SEM. Datasets were statistically analysed by two-way ANOVA followed by Bonferroni's post hoc test. * Values $P < 0.05$ compared to time zero (i.e., control) are statistically significant.

The observed time-course of action of NO production is consistent with the reported activation of the TLR-dependent NF-κB signalling pathway induced by pathogen associated molecular patterns (PAMPs). Jacobs et al. also reported a similar finding pertaining to LPS induced iNOS protein response in RAW 264.7 cells[29]. In this study, detectable levels of NO with NPPS and PS treatment groups were observed at ~ 9 hrs. Consistent with our results, NO production rate was reported by Jacobs et al. to reach steady-state levels at ~ 9 hrs before reaching maximum plateau[29]. For NPPS-treated macrophages, NO levels increased linearly until a maximum plateau at approximately 15 hrs following treatment, similar to the time taken to reach the plateau phase observed by He et al.[30]. In addition, we have previously determined that ginseng extracts can elicit optimal stimulation at approximately 24 hrs. The significance of the earlier onset of action associated with NPPS treatment (Fig. 3.1.) is not clear; however, this appears to support the earlier cellular uptake of NPPS compared to PS as determined by bioimaging using RAW 246.7 macrophages[6]. The observed difference in time-course of action between NPPS and PS suggests that NPPS may not mediate its cellular activation by the activation of TLR signalling pathway that has been well established for PS. Some nanomaterials have been shown to penetrate the cell which allows for the activation of intracellular mechanisms[31–33].

3.3.2 Immunostimulatory effects of NPPS in LPS-desensitized macrophages *in vitro*

To determine the involvement of the TLR signalling pathway in mediating the action of NPPS, we desensitized macrophages with prior LPS treatment for 24 hrs to induce TLR internalization. These cells were then challenged with 0, 50 or 200 μg/mL of PS or NPPS treatment to assess their responsiveness. LPS were used as the positive control to establish standard cellular responsiveness. NO production was measured as a basis for macrophage responsiveness to LPS, PS or NPPS. As shown in Fig. 3.2, pre-treating macrophages with LPS reduced the macrophage response to subsequent LPS stimulation by ~ 48%. This finding is consistent with our earlier report[5]. The observed reduction in responsiveness is believed to be a result of the reduced presence of cell-surface TLRs and the attenuation of responsiveness to TLR agonists[17,34]. A study by Rajaiah et al. showed that the induction of tolerance by exposure of macrophages to LPS induced TLR4 endocytosis[18]. The apparent

LPS-induced loss of responsiveness was not due to artifacts resulting from additional 24-hr incubation since pretreatment with the vehicle did not alter the macrophage responsiveness. Additionally, the response to PS and NPPS in macrophages pretreated with the vehicle for 24 hr showed good dose-dependency and was comparable to what we reported in Chapter 2 for regular (non-treated) macrophages (Fig. 2.4). Data presented in Fig. 3.2 also showed that LPS-pretreatment reduced the responsiveness to both levels of PS and NPPS challenges by 33 to 50%. This finding suggested that NPPS like PS is an agonist of TLR in view of their sensitivity to LPS-induced desensitization. However, it should be noted that because the LPS-induced desensitization on NPPS and PS was less than 50%, our data could not rule out the participation of other mechanism(s).

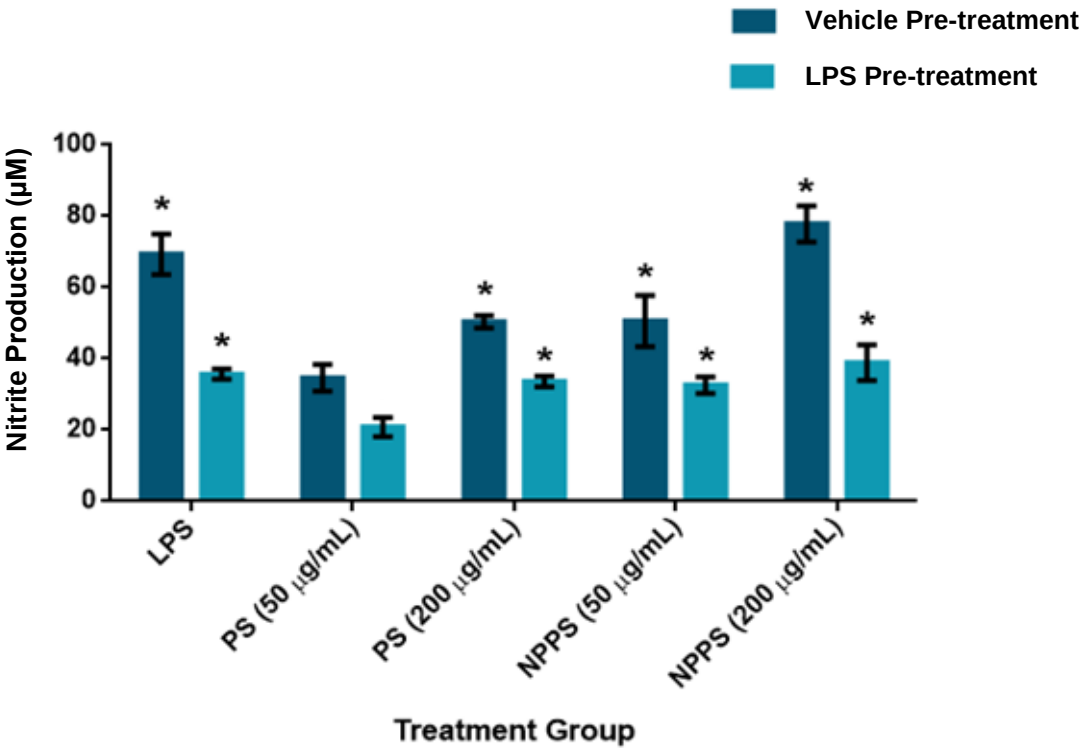

Figure 3.2. Immunostimulatory effects of ginseng PS and NPPS on macrophage NO production. RAW 264.7 cells were pretreated with vehicle or LPS (1 μM) for 24 hrs prior to treatment with 200 μg/mL of NPPS or PS for 24 hrs. LPS was used as a positive control to evaluate cellular responsiveness. Experiments were performed in triplicates and the data are presented as mean ± SEM, n =3. Data were statistically analysed by two-way ANOVA

followed by Bonferroni's post hoc test. *Values $P < 0.05$ compared between pre-treatments are statistically significant.

3.3.3 TLR 2/4 antagonist suppressed NPPS activity

To further ascertain whether TLR2/4 are involved in the mediation of NPPS activity, a selective antagonist (SsnB) was used to inhibit the recruitment of myeloid differentiation primary response 88 (MyD88) to TLR2/4 in macrophages, which is a critical step in the activation process. As expected with PS, the presence of SsnB significantly reduced PS-mediated NO production by macrophages (Fig. 3.3). The degree of inhibition was related to concentration of the antagonist: 10 μg/mL and 100 μg/mL SsnB, induced a ~ 60% and ~ 98% reduction, respectively. A similar concentration-dependent SsnB induced reduction of NPPS-mediated NO production by macrophages was also observed.

Sparstolonin B is a novel compound isolated from *Sparganium stoloniferum* that has been demonstrated to inhibit signalling pathways (i.e., MAPK and NF-κB) downstream of TLR2/4 activation. Considerable evidence suggests the presence of SsnB intracellularly inhibits the ligand-induced association of MyD88 to TIR-domain-containing adaptor protein (TIRAP) and TLR2/4 complex[28]. Therefore, a reduction in the macrophage response to TLR2/4 agonists is expected as a result of the reduced MyD88 association. Together with the purported SsnB antagonistic activity, these lines of evidence suggest that ginseng NPPS, like PS, act on TLR2/4 signalling. Furthermore, the marked suppression of NPPS action in the presence of a selective TLR 2/4 antagonist observed in this experiment strongly implicates the involvement of the TLR pathway in mediating the immunostimulatory action of NPPS. In addition, in light of the known mechanism of action of the antagonist used, the site of action of NPPS and bulk PS could be narrowed down to a site in the TLR4 signalling upstream of ligand-induced MyD88 association.

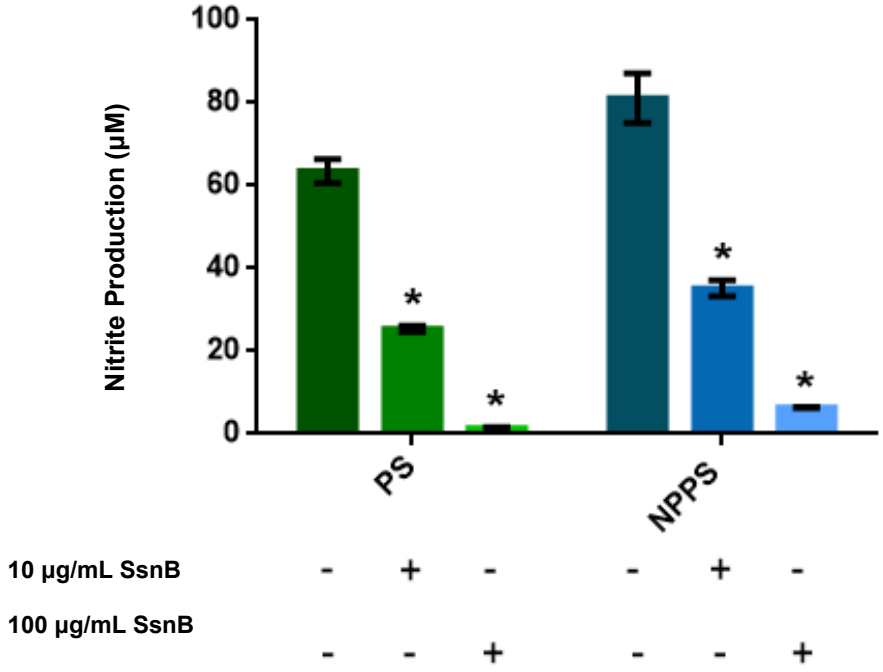

Figure 3.3. Immunostimulatory effects of ginseng PS and NPPS on macrophage NO production over a 24-hr period. RAW 264.7 cells were treated in the presence of 10 or 100 μg/mL SsnB and, with 200 μg/mL of PS or NPPS for 24 hrs. Treatment with PS or NPPS in the absence of SsnB were the negative controls. Experiments were performed in triplicates and the data are present as mean ± SEM, n =3. Data were statistically analysed by two-way ANOVA followed by Bonferroni's post-hoc test. *Values $P < 0.05$ compared with the negative control within the treatment group are statistically significant.

Ginseng and other plant PS have been reported to activate TLR2 or TLR4 signalling. For example, *Agaricus brasiliensis* beta-glucans has recently been shown to enhance phagocytic activity of monocytes via TLR2/4 signalling[35]. In another study, ginseng PS immunostimulation was impaired in TLR4 deficient mice (C2H/HeJ)[36]. TLR2 and TLR4 have also been implicated in the response of mammary glands treated with ginseng extracts[37]. Shin et al. reported that CD14 was upregulated in macrophages treated with a ginseng PS preparation (i.e., ginsan), which implicates CD14 in PS activation of

macrophages[10]. A contemporary study showed that smaller chains of ginseng PS activate TLR2 as opposed to TLR4[11]. Therefore, ginseng PS may be directly binding to CD14 or TLR2/4 to elicit a response. Our data suggest that both NPPS and PS may mediate macrophage response via TLR signalling; however, it is not certain whether the molecular mechanism of PS could be extended to NPPS. This question should be addressed by taking into consideration that microfluidics processing was demonstrated to not functionally alter ginseng PS, but rather alter surface chemistry.

The activation of TLR signalling by NPPS may be through binding to CD14 or directly to TLR2/4. The binding to CD14 has been studied with reference to LPS[38,39]. This usually involves the interaction of LPS aggregates to CD14, which catalyzes its monomerization prior to presentation to TLR4[39,40]. Based on their data, Kitchens et al. proposed that monomeric LPS-CD14 complexes are necessary to elicit a response[38]. Similarly, ginseng PS exists in aqueous solution as aggregates. It is not certain how NPPS, which has a smaller particle size than PS, would behave under this condition. However, it is possible that ginseng PS and NPPS also require monomerization by CD14 and presentation to TLR4. Ginseng NPPS may also be more potent than PS due to the smaller apparent size of its agglomerates. This is supported by the report that aggregates of LPS are less potent when their aggregates sizes were increased[41]. With this consideration, we propose that nanosization enhances binding affinity through the reduction in particle size.

The observation that NPPS stimulated macrophages earlier and to a greater extent than bulk PS suggested the possibility of a different mechanism of activation between NPPS and bulk PS. Alternatively, NPPS may be acting via similar mechanism(s) as bulk PS but act faster and more efficiently to achieve high maximum response. Higher receptor affinity or involvement of accessory proteins are possible explanations for this speculation. Partially reduced responsiveness was observed following LPS-desensitization in both NPPS and PS conditions. This suggested that they may share the same pathway of activation; although, they may still act differently at certain levels (e.g., CD14). The observed reduction could also be the result of non-specific effects of LPS. The hypothesis that NPPS act differently than bulk PS was refuted by the activation of TLR signalling by

the nanoparticles, but the possibility of a different mechanism should not be entirely discarded. It is possible that additional mechanism(s) may exist in conjunction with TLR activation, or other mechanism(s) of activation by PS such as animal lectins have been lost following nanonization. Further studies are needed to determine other potential receptors of NPPS. Despite this, the results of this experiment have enabled us to begin to elucidate the basis behind the enhancement of PS' stimulatory effect following nanonization.

Alternative pathways for NPPS activation of macrophages could be examined in future studies. Other potential receptors for ginseng PS are complement receptor-3 (CR3), scavenger receptor (SR), dectin-1 and mannose receptors, which have been demonstrated to bind to carbohydrates and are implicated in the activation of the NF-kB pathway in macrophages[19,42]. Dectin-1 and mannose receptors are animal lectins (carbohydrate-binding proteins) that have high specificity for sugar moieties[19]. Dectin-2, galectins and immunoglobulin-like lectins are other animal lectins that have been implicated in the immunostimulatory activity of botanical polysaccharides[19].

3.4 Conclusions

The objective of this chapter was to investigate the mechanism of immunostimulation exerted by NPPS that was prepared by microfluidic processing from ginseng PS. The strategy was to define the time-course of action in cultured macrophages and to determine whether NPPS shared a different mechanism as PS and LPS. Our data showed that NPPS has a faster onset of action and a higher maximum response than PS, which corroborated with the bioimaging data from our previous study using macrophages. Using an LPS-induced desensitization model involving increased TLR internalization and downstream negative regulation of TLR signalling, we showed that TLR-dependent pathway was involved – at least in part – in the mediation of action of NPPS and PS. Furthermore, the successful suppression of NPPS and PS-induced immune response with the selective TLR2/4 antagonist, SsnB, has provided evidence to identify a site in the TLR4 signalling upstream of ligand-induced MyD88 association. It is likely that NPPS act similar to ginseng PS in activating TLR-mediated NF-κB signalling; however, it remains to be

determined whether other mechanism(s) may be involved and the basis underlying the more rapid onset and higher potency of NPPS.

3.5 Acknowledgments

This work was funded by Western Phytoceutica (WPC) and Mitacs Canada.

3.6 References

1. Park, H. J., Kim, D. H., Park, S. J., Kim, J. M. & Ryu, J. H. Ginseng in Traditional Herbal Prescriptions. *J. Ginseng Res.* **36**, 225–241 (2012).

2. Arnason, T., Hebda, R. J. & Johns, T. Use of plants for food and medicine by Native Peoples of eastern Canada. *Can. J. Bot.* **59**, 2189–2325 (1981).

3. Ji, L. *et al.* Structural characterization of alkali-soluble polysaccharides from Panax ginseng C. A. Meyer. *R. Soc. Open Sci.* **5**, 171644 (2018).

4. Lim, T.-S., Na, K., Choi, E.-M., Chung, J.-Y. & Hwang, J.-K. Immunomodulating activities of polysaccharides isolated from Panax ginseng. *J. Med. Food* **7**, 1–6 (2004).

5. Azike, C. G., Charpentier, P. A. & Lui, E. M. K. Stimulation and suppression of innate immune function by American ginseng polysaccharides: biological relevance and identification of bioactives. *Pharm. Res.* **32**, 876–897 (2015).

6. Akhter, F. Ginseng Polysaccharides Nanoparticles-Synthesis, Characterization, and Biological Activity. *Diss. Univ. West. Ont.* (2016).

7. Song, Y.-R. *et al.* Enzyme-assisted extraction, chemical characteristics, and immunostimulatory activity of polysaccharides from Korean ginseng (Panax ginseng Meyer). *Int. J. Biol. Macromol.* **116**, 1089–1097 (2018).

8. McElhaney, J. E., Goel, V., Toane, B., Hooten, J. & Shan, J. J. Efficacy of COLD-fX in the prevention of respiratory symptoms in community-dwelling adults: a randomized, double-blinded, placebo controlled trial. *J. Altern. Complement. Med. N. Y. N* **12**, 153–157 (2006).

9. High, K. P. *et al.* A Randomized, Controlled Trial of Panax quinquefolius extract (CVT-E002) to Reduce Respiratory Infection in Patients with Chronic Lymphocytic Leukemia. *J. Support. Oncol.* **10**, 195–201 (2012).

10. Shin, J.-Y. *et al.* Immunostimulating effects of acidic polysaccharides extract of *Panax ginseng* on macrophage function. *Immunopharmacol. Immunotoxicol.* **24**, 469–482 (2002).

11. Seo, J. Y., Choi, J. W., Lee, J. Y., Park, Y. S. & Park, Y. I. Enzyme Hydrolysates of Ginseng Marc Polysaccharides Promote the Phagocytic Activity of Macrophages Via Activation of TLR2 and Mer Tyrosine Kinase. *J. Microbiol. Biotechnol.* **28**, 860–873 (2018).

12. Núñez Miguel, R. *et al.* A Dimer of the Toll-Like Receptor 4 Cytoplasmic Domain Provides a Specific Scaffold for the Recruitment of Signalling Adaptor Proteins. *PLoS ONE* **2**, (2007).

13. Liu, T., Zhang, L., Joo, D. & Sun, S.-C. NF-κB signaling in inflammation. *Signal Transduct. Target. Ther.* **2**, 17023 (2017).

14. Jones, E., Adcock, I. M., Ahmed, B. Y. & Punchard, N. A. Modulation of LPS stimulated NF-kappaB mediated Nitric Oxide production by PKCε and JAK2 in RAW macrophages. *J. Inflamm. Lond. Engl.* **4**, 23 (2007).

15. Lemmon, H. R., Sham, J., Chau, L. A. & Madrenas, J. High molecular weight polysaccharides are key immunomodulators in North American ginseng extracts: characterization of the ginseng genetic signature in primary human immune cells. *J. Ethnopharmacol.* **142**, 1–13 (2012).

16. Tan, Y., Zanoni, I., Cullen, T. W., Goodman, A. L. & Kagan, J. C. Mechanisms of Toll-like receptor 4 endocytosis reveal a common immune-evasion strategy used by pathogenic and commensal bacteria. *Immunity* **43**, 909–922 (2015).

17. Balachandran, Y. Role of Endocytosis in TLR Signaling: An Effective Negative Regulation to Control Inflammation. *MOJ Immunol.* **3**, (2016).

18. Rajaiah, R., Perkins, D. J., Ireland, D. D. C. & Vogel, S. N. CD14 dependence of TLR4 endocytosis and TRIF signaling displays ligand specificity and is dissociable in endotoxin tolerance. *Proc. Natl. Acad. Sci. U. S. A.* **112**, 8391–8396 (2015).

19. Loh, S. H., Park, J.-Y., Cho, E. H., Nah, S.-Y. & Kang, Y.-S. Animal lectins: potential receptors for ginseng polysaccharides. *J. Ginseng Res.* **41**, 1–9 (2017).

20. Chemistry, I. U. of P. and A. IUPAC Gold Book - interfacial layer. doi:10.1351/goldbook.I03085

21. Junyaprasert, V. B. & Morakul, B. Nanocrystals for enhancement of oral bioavailability of poorly water-soluble drugs. *Asian J. Pharm. Sci.* **10**, 13–23 (2015).

22. Hu, J., Johnston, K. P. & Williams, R. O. Spray freezing into liquid (SFL) particle engineering technology to enhance dissolution of poorly water soluble drugs: organic solvent versus organic/aqueous co-solvent systems. *Eur. J. Pharm. Sci. Off. J. Eur. Fed. Pharm. Sci.* **20**, 295–303 (2003).

23. Elias, D. R., Poloukhtine, A., Popik, V. & Tsourkas, A. Effect of ligand density, receptor density, and nanoparticle size on cell targeting. *Nanomedicine Nanotechnol. Biol. Med.* **9**, 194–201 (2013).

24. Zhang, W. *et al.* Effect of Shape on Mesoporous Silica Nanoparticles for Oral Delivery of Indomethacin. *Pharmaceutics* **11**, 4 (2019).

25. Yokota, J. & Kyotani, S. Influence of nanoparticle size on the skin penetration, skin retention and anti-inflammatory activity of non-steroidal anti-inflammatory drugs. *J. Chin. Med. Assoc.* **81**, 511–519 (2018).

26. Chen, X., Young, T. J., Sarkari, M., Williams, R. O. & Johnston, K. P. Preparation of cyclosporine A nanoparticles by evaporative precipitation into aqueous solution. *Int. J. Pharm.* **242**, 3–14 (2002).

27. Akhter, K. F., Mumin, M. A., Lui, E. K. & Charpentier, P. A. Microfluidic Synthesis of Ginseng Polysaccharide Nanoparticles for Immunostimulating Action on Macrophage Cell Lines. *ACS Biomater. Sci. Eng.* **2**, 96–103 (2016).

28. Liang, Q. *et al.* Characterization of Sparstolonin B, a Chinese Herb-derived Compound, as a Selective Toll-like Receptor Antagonist with Potent Anti-inflammatory Properties. *J. Biol. Chem.* **286**, 26470–26479 (2011).

29. Jacobs, A. T. & Ignarro, L. J. Lipopolysaccharide-induced Expression of Interferon-β Mediates the Timing of Inducible Nitric-oxide Synthase Induction in RAW 264.7 Macrophages. *J. Biol. Chem.* **276**, 47950–47957 (2001).

30. He, W. & Frost, M. C. CellNO trap: Novel device for quantitative, real-time, direct measurement of nitric oxide from cultured RAW 267.4 macrophages. *Redox Biol.* **8**, 383–397 (2016).

31. Hao, N., Yang, H., Li, L., Li, L. & Tang, F. The shape effect of mesoporous silica nanoparticles on intracellular reactive oxygen species in A375 cells. *New J. Chem.* **38**, 4258–4266 (2014).

32. Jiang, L., Li, X., Liu, L. & Zhang, Q. Cellular uptake mechanism and intracellular fate of hydrophobically modified pullulan nanoparticles. *Int. J. Nanomedicine* **8**, 1825–1834 (2013).

33. Nam, H. Y. *et al.* Cellular uptake mechanism and intracellular fate of hydrophobically modified glycol chitosan nanoparticles. *J. Control. Release Off. J. Control. Release Soc.* **135**, 259–267 (2009).

34. Peng, Q., O'Loughlin, J. L. & Humphrey, M. B. DOK3 Negatively Regulates LPS Responses and Endotoxin Tolerance. *PLOS ONE* **7**, e39967 (2012).

35. Martins, P. R., de Campos Soares, Â. M. V., da Silva Pinto Domeneghini, A. V., Golim, M. A. & Kaneno, R. Agaricus brasiliensis polysaccharides stimulate human monocytes to capture Candida albicans, express toll-like receptors 2 and 4, and produce pro-inflammatory cytokines. *J. Venom. Anim. Toxins Trop. Dis.* **23**, (2017).

36. Nakaya, T.-A., Kita, M., Kuriyama, H., Iwakura, Y. & Imanishi, J. Panax ginseng induces production of proinflammatory cytokines via toll-like receptor. *J. Interferon Cytokine Res. Off. J. Int. Soc. Interferon Cytokine Res.* **24**, 93–100 (2004).

37. Baravalle, C. *et al.* Intramammary infusion of Panax ginseng extract in bovine mammary gland at cessation of milking induces changes in the expression of toll-like receptors, MyD88 and NF-kB during early involution. *Res. Vet. Sci.* **100**, 52–60 (2015).

38. Kitchens, R. L. & Munford, R. S. CD14-Dependent Internalization of Bacterial Lipopolysaccharide (LPS) Is Strongly Influenced by LPS Aggregation But Not by Cellular Responses to LPS. *J. Immunol.* **160**, 1920–1928 (1998).

39. Park, B. S. & Lee, J.-O. Recognition of lipopolysaccharide pattern by TLR4 complexes. *Exp. Mol. Med.* **45**, e66 (2013).

40. Kim, J.-I. *et al.* Crystal structure of CD14 and its implications for lipopolysaccharide signaling. *J. Biol. Chem.* **280**, 11347–11351 (2005).

41. Tobias, P. S., Soldau, K., Iovine, N. M., Elsbach, P. & Weiss, J. Lipopolysaccharide (LPS)-binding Proteins BPI and LBP Form Different Types of Complexes with LPS. *J. Biol. Chem.* **272**, 18682–18685 (1997).

42. Li, Q., Niu, Y., Xing, P. & Wang, C. Bioactive polysaccharides from natural resources including Chinese medicinal herbs on tissue repair. *Chin. Med.* **13**, (2018).

Chapter 4

Conclusions and Recommendations

4.1 Summary and conclusions

4.1.1 General objectives

In this project, two primary objectives have been addressed pertaining to the conversion of ginseng PS to their nanoparticle form by microfluidics: (1) modification of the existing microfluidics methodology for NPPS synthesis and characterization of their physicochemical and pharmacological properties; and (2) investigation of mechanism(s) underlying the immunostimulatory activity of nanoparticles to provide insight into the cellular action and target(s) of NPPS.

4.1.2 Modification of microfluidics methodology

Modification of the microfluidics procedure developed by Akhter et al. has provided information regarding its limitations and undefined variables (i.e., substrate concentration). The main limitations associated with the previously reported methodology are low total yield and susceptibility to poor sample recovery. Based on the physicochemical characterization data, we could conclude that the modified microfluidic methodology was able to produce NPPS from bulk PS with a reasonable yield of approximately 95 %, and a size distribution averaged around 19 nm. The NPPS exhibited monodispersed and spherical nanomorphology, which is characteristic of previously synthesized NPPS.

4.1.3 Biological and physicochemical characterization of NPPS

Biological characterization of the resulting NPPS revealed that microfluidic processing of bulk PS enhanced its immunostimulatory activity *in vitro*. Data from this experiment assisted in the development of a novel macrophage-based bioassay for PS and NPPS quantitation in order to address the lack of plant PS quantitation technology. Furthermore, coupling a keratinocyte monolayer model with the macrophage-based bioassay has provided a new *in vitro* system to assess bioavailability. By utilizing this system, we were able to study the transport of PS and NPPS across a cellular membrane barrier. Moreover, this approach reduces the number of experimental animals needed for initial screening purposes.

Using this novel technology, we have demonstrated that NPPS showed significant penetration across an established keratinocyte monolayer that acts as an effective barrier for bulk PS. These findings provided insight into the potential relationship between reduced particle size and enhanced permeability of ginseng NPPS.

While investigating the relationship between substrate molecular weight and the characteristics of NPPS, we were able to conclude that molecular size of the PS substrate influenced the physicochemical property and immunostimulatory potency of NPPS. However, findings revealed that nanosizing enhanced the potency of lower molecular weight bulk PS, which exhibited lower immunostimulatory potency relative to the higher molecular weight PS.

4.1.4 Mechanism of macrophage activation by NPPS

The mechanistic study of ginseng NPPS reported in Ch. 3 demonstrated reduced responsiveness of desensitized-macrophages to NPPS and impaired NPPS-induced response in macrophages treated together with an antagonist. Results from this study demonstrated the importance of TLR2/4 signaling in NPPS activation of macrophages and supports the conclusion that NPPS behave like ginseng PS. Taken together with the physicochemical prosperities of NPPS, these findings have allowed us to conclude that nanonization of bulk PS does not alter its ability to activate TLRs.

4.2 Challenges and solutions

The low sensitivity and specificity of the biological assay for PS and NPPS estimation of concentration is one of the major challenges associated with our study. To address this issue, we have proposed to develop a more sensitive and specific measurement of cellular marker for immunomodulation using new biotechnology such as cytokine gene expression. This would be advantageous for the detection of immunostimulatory responses to low concentrations of PS and NPPS, thereby allowing us to estimate sample concentration with higher sensitivity. Using labelled PS and NPPS is another alternative to measure PS and NPPS concentration.

Another major challenge is the lack of tools for PS and NPPS bioimaging. To address this, we propose the development of quantum-dot labelling-technology for ginseng PS that would allow for quantification, tracking and detection under *in vivo* and *in vitro* conditions. In addition, it would be beneficial to develop an innovative labelling methodology that is based on quantum dot technology.

4.3 Future studies

Looking at the project holistically, we suggest studying the structure-activity relationship between NPPS physicochemical characteristics and ginseng PS immunomodulatory effect to expand our understanding in this field. Elucidation of this relationship would offer helpful insight in determining why NPPS are more potent than bulk PS. In addition, it is important to investigate why NPPS exhibited higher immunostimulatory potency through more in-depth mechanistic studies.

We did not have the opportunity to investigate potential toxicity of NPPS *in vivo*, thus, further investigation on the disposition, pharmacology and safety of NPPS in a biological system is necessary. Furthermore, NPPS sub-cellular localization, translocation and transcription site in macrophages have not been defined. Detailed bioimaging would be very useful to define how NPPS exert their effect as well as their fate in macrophages. These follow-up studies would enable the development of innovative and safe nutraceuticals.

The interaction and fate of NPPS with keratinocytes have not been previously addressed. Keratinocytes were used as a model in this current study to assist in the physicochemical characterization of NPPS. Therefore, as a follow-up study, examining the response of keratinocytes following NPPS treatment would assist in developing a more specific biological assay and determining toxicity. In addition, using bioimaging would be helpful in addressing its transport and fate in keratinocytes. Alternatively, using fluorescent

markers for various proteins associated with endosomes would expand our understanding of the transport of these nanomaterials.

Other potential receptors of ginseng PS (e.g., animal lectins) have been identified in the literature; however, their implications have not been fully understood. Therefore, it would be helpful to determine alternative mechanisms of activation by ginseng PS and its nanoparticle counterpart. These findings would support or oppose the claim that nanoparticle synthesis does not alter or introduce new activation pathways of bulk PS.

Appendices

A.1. Bioassay standard curves.

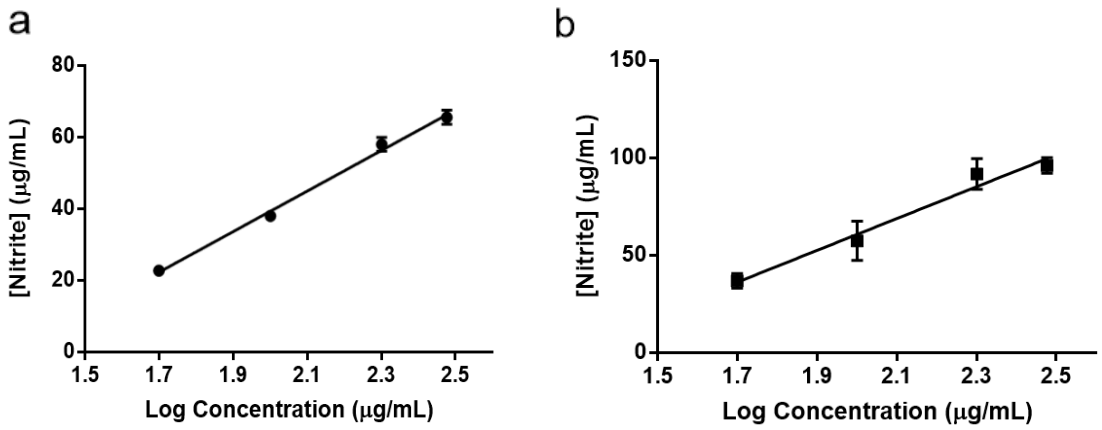

Figure A.1. Standard curve for biological assay of (a) ginseng PS and (b) NPPS. Twenty-four-hour macrophage stimulation of NO production with 50-300 µg/mL of ginseng PS and NPPS.

A.2. Copyrights.

Copyright Clearance Center RightsLink®

Home | Create Account | Help

ACS Publications
Most Trusted. Most Cited. Most Read.

Title: Microfluidic Synthesis of Ginseng Polysaccharide Nanoparticles for Immunostimulating Action on Macrophage Cell Lines

Author: Kazi Farida Akhter, Md Abdul Mumin, Edmond K. Lui, et al

Publication: ACS Biomaterials Science & Engineering

Publisher: American Chemical Society

Date: Jan 1, 2016

Copyright © 2016, American Chemical Society

LOGIN

If you're a copyright.com user, you can login to RightsLink using your copyright.com credentials.

Already **a RightsLink user** or want to learn more?

PERMISSION/LICENSE IS GRANTED FOR YOUR ORDER AT NO CHARGE

This type of permission/license, instead of the standard Terms & Conditions, is sent to you because no fee is being charged for your order. Please note the following:

- Permission is granted for your request in both print and electronic formats, and translations.
- If figures and/or tables were requested, they may be adapted or used in part.
- Please print this page for your records and send a copy of it to your publisher/graduate school.
- Appropriate credit for the requested material should be given as follows: "Reprinted (adapted) with permission from (COMPLETE REFERENCE CITATION). Copyright (YEAR) American Chemical Society." Insert appropriate information in place of the capitalized words.
- One-time permission is granted only for the use specified in your request. No additional uses are granted (such as derivative works or other editions). For any other uses, please submit a new request.

If credit is given to another source for the material you requested, permission must be obtained from that source.

BACK | CLOSE WINDOW

VITA

Name: Wai-Dun Vincent Lee

Post-secondary Education and Degrees:
The University of Western Ontario,
London, Ontario, Canada
2012-2016 B.A.

Honours and Awards:
Western Scholarship of Excellence, 2012
The University of Western Ontario,
London, Ontario, Canada

Related Work Experience:
Teaching Assistant
The University of Western Ontario
Sept 2016 – Dec 2016

Teaching Assistant
The University of Western Ontario
Jan 2018 – Apr 2018

Conferences Presentation:
W. V. Lee, K. F. Akhter, P. A. Charpentier, E. Lui, Nanosizing of ginseng polysaccharides enhanced cellular activity *in vitro* (poster presentation), 2018 London Health Research Day. (May 2018)

W. V. Lee, K. F. Akhter, P. A. Charpentier, E. Lui, Application of HaCaT keratinocyte monolayer culture to demonstrate enhanced bioavailability of ginseng polysaccharides nanoparticles (poster presentation), 15th Annual Conference of the Natural Health Product Research Society of Canada. (May 2018)